GEOLOGICA ULTRAIECTINA

Mededelingen van de
Faculteit Aardwetenschappen der
Rijksuniversiteit te Utrecht

No. 66

GEOCHEMISTRY OF HIGH-TEMPERATURE GRANULITIC SUPRACRUSTALS FROM ROGALAND, SW NORWAY

LUC C.G.M. BOL

GEOLOGICA ULTRAIECTINA

Mededelingen van de
Faculteit Aardwetenschappen der
Rijksuniversiteit te Utrecht

No. 66

GEOCHEMISTRY OF HIGH-TEMPERATURE GRANULITIC SUPRACRUSTALS FROM ROGALAND, SW NORWAY

CIP-DATA KONINKLIJKE BIBLIOTHEEK, DEN HAAG

Bol, Ludovicus Cornelis Gerardus Maria

Geochemistry of high-temperature granulitic supracrustals from Rogaland, SW Norway / Ludovicus Cornelis Gerardus Maria Bol. - [Utrecht : Instituut voor Aardwetenschappen der Rijksuniversiteit Utrecht]. - (Geologica Ultraiectina, ISSN 0072-1026 ; no. 66)
Thesis Utrecht. With ref. - With summary in Dutch.
ISBN 90-71577-19-8
SISO 562 UDC 549.6(043.3)
Subject headings: metamorphic petrology / stable isotopes

GEOCHEMISTRY OF HIGH-TEMPERATURE GRANULITIC SUPRACRUSTALS FROM ROGALAND, SW NORWAY

GEOCHEMIE VAN HOOG-TEMPERATUUR GRANULITISCHE SUPRACRUSTALEN UIT ROGALAND, ZW NOORWEGEN

(MET EEN SAMENVATTING IN HET NEDERLANDS)

PROEFSCHRIFT TER VERKRIJGING VAN DE GRAAD VAN DOCTOR
AAN DE RIJKSUNIVERSITEIT TE UTRECHT
OP GEZAG VAN DE RECTOR MAGNIFICUS, PROF. DR. J.A. VAN GINKEL,
INGEVOLGE HET BESLUIT VAN HET COLLEGE VAN DEKANEN
IN HET OPENBAAR TE VERDEDIGEN OP MAANDAG
11 JUNI 1990 DES NAMIDDAGS OM 12.45 UUR

DOOR

LUDOVICUS CORNELIS GERARDUS MARIA BOL
GEBOREN OP 12 FEBRUARI 1958, TE OISTERWIJK.

PROMOTOR: PROF. DR. R.D. SCHUILING
CO-PROMOTOR: DR. J.B.H. JANSEN

DIT PROEFSCHRIFT WERD MOGELIJK GEMAAKT MET FINANCIËLE STEUN VAN DE NEDERLANDSE ORGANISATIE VOOR WETENSCHAPPELIJK ONDERZOEK (NWO)

ter nagedachtenis aan mijn moeder
aan Geja

Metasediments near Nedrabö (by courtesy of F. Trappenburg).

VOORWOORD

De volgende personen hebben bijgedragen aan de totstandkoming van mijn proefschrift:

P. Anten, Prof. Dr. M. Barton, Dr. M. van Bergen, B.J. Bergenhenegouwen, Personeel Bibliotheek, Drs. R.J.P. Blok, W.J.H. Eussen, Prof. Dr. J.M. Ferry, Prof. Dr. W.E. Glassley, H.M.V.C. Govers, E. de Graaf, Prof. Dr. P. Hartman, Ir. G.E.A.M. Hermans, Prof. Dr. D.A. Hewitt, J.C. Jansen, Prof. Dr. B.H.W.S. de Jong, I. Kalt, Drs. G.J. Kippers, Dr. R. Kreulen, Drs. D.A. van de Kroef, M.H. Maarschalkerweerd, Drs. J.H.A.M. Meertens, J.A.N. Meesterburry, R.J. Meye, M.K. Moekoet-Kalikadien, Prof. Dr. N.W. Nessbitt, I.M. Santoe, Dr. P.C.C. Sauter, J.A. Schiet, P.G.G. Slaats, Personeel Slijpkamer, (Ex-) Studenten Petrologie, Dr. R.J.P. Poorter, F.J. Quint, Anonieme Reviewers (4), Prof. Dr. A.C. Tobi, F. Trappenburg, Drs. R.H. Verschure, Drs. C.F. Woensdregt.

Hartelijk bedankt allemaal, door Uw vakmanschap, vriendschap en hulp was dit onderzoek mogelijk.

De Nederlandse Organisatie voor Wetenschappelijk Onderzoek, c.q. de Stichting Aardwetenschappelijk Onderzoek Nederland, bedank ik voor financiële steun aan dit onderzoek (AWON project #751-353-016), en voor beurzen t.b.v. studie-reizen naar Noorwegen (2x), Groot Brittannië, en de Verenigde Staten (2x).

Voorts wil ik mijn promotor, Prof. Dr. R.D. Schuiling, bedanken voor het constructieve commentaar op de hoofdstuk manuscripten, en voor de onbureaucratische wijze waarop hij de voogdij over mijn onderzoek ter hand heeft genomen.

Drs. S.P. Vriend bedank ik voor zijn tolerante houding jegens inbreuken op zijn rust en privacy door frequent gebruik van afdruk-apparatuur op zijn studeerkamer.

Drs. R. Bakker, Dr. J.H.L. Voncken, G. Roy, Drs. A. Bos, en A.J.M. van der Eerden bedank ik voor bondgenootschap en gezelligheid gedurende de afgelopen jaren.

Dr. C. Maijer was door zijn unieke kennis van de geologie van Rogaland onmisbaar voor dit project. Bedankt Kees, ook voor een prima tijd in Noorwegen.

I am grateful to Prof. Dr. J.W. Valley for generously providing access to the stable isotope laboratory of the Department of Geology and Geophysics at the University of Wisconsin-Madison, and for stimulating and thoughtful discussions. I also want to thank K. Baker for his skillful instructions in the laboratory and for his good company. I would like to thank the students of 3rd floor of Weeks Hall for a great time in Wisconsin.

Dr. J.B.H. Jansen heeft op inspirerende wijze dit onderzoek begeleid. Beste Ben, bedankt voor het vertrouwen, het commentaar, en de discussie.

Tenslotte dank ik mijn ouders voor de onvoorwaardelijke steun die zij mij tijdens mijn opleiding hebben gegeven.

TABLE OF CONTENTS

Chapter II of this thesis is published in *The American Mineralogist*, volume 74, 1989, pages 439-447. Co-authors: A. Bos, P.C.C. Sauter, J.B.H. Jansen.

Chapter III of this thesis is published in *Contributions to Mineralogy and Petrology*, volume 103, 1989, pages 306-316. Co-authors: C. Maijer, J.B.H. Jansen.

Chapter IV of this thesis is intended for publication in an international journal. Co-authors: P.C.C. Sauter, J.B.H. Jansen, J.W. Valley

LIST OF FIGURES

LIST OF TABLES

SUMMARY

Were the granulite-facies metamorphic supracrustals of the Faurefjell Metasediment Formation in Rogaland, SW Norway, chemically open or closed systems? In order to assess differential element mobilities in response to pre-, syn- and post-metamorphic fluid fluxes through this formation, the mineralogy, crystal chemistry, bulk chemical composition, and mineral oxygen and carbon stable isotope composition is investigated in marbles and metavolcanics.

Chapter I of this thesis provides the reader with the geological background necessary to appreciate the importance of the problem. A review of the geology of the Rogaland high-temperature granulite terrane is given, and it is explained why the Faurefjell supracrustals are selected in this case study. At the end of the chapter the scope of this thesis is further refined.

The chemical occupancy of the hydroxyl-site in metamorphic micas potentially monitors compositions of coexisting metamorphic fluids. Therefore, the composition of phlogopites in the marbles is evaluated in **Chapter II**. It is inferred that, in Ba-Ti-rich phlogopites, an unnamed anhydrous Ba-Ti end-member composition ($BaMg_2TiSi_2Al_2O_{12}$) constitutes about 81 mole% of the solid solution.

In **Chapter III**, an extreme variation in bulk composition observed in metavolcanic layers of the Faurefjell Formation is related to premetamorphic chemical alteration processes. Composition-volume relations in one particular layer of these rocks support an origin involving Proterozoic weathering (lateritization) of a basaltic protolith. Some effects of syndiagenetic metasomatism are likely superimposed on these weathering trends. Subsequent high-grade metamorphic events merely enhanced preservation of the post-diagenetic bulk compositional characteristics.

Oxygen and carbon isotopic ratios in carbonate, silicate and oxide minerals of various lithological units of the Faurefjell Formation are discussed in **Chapter IV**. Calcites in the marbles show regionally a coupled $\delta^{18}O$-$\delta^{13}C$ trend. The magnitudes of the regional shifts in $\delta^{18}O$ (8.5 permil) and $\delta^{13}C$ (5 permil) cannot be explained by metamorphic volatilization reactions and isotopic exchange with external fluids is proposed. The $\delta^{18}O$ compositions of high-grade silicate minerals associated with the marbles are in accordance with the calcite isotopic compositions. Therefore, the fluid-rock interaction that caused the regional $\delta^{18}O$-$\delta^{13}C$ trend must have occurred before

formation of these silicates (ie, before the peak metamorphic conditions). Regional trends in $\delta^{18}O$ and $\delta^{13}C$ are not recorded in silicate minerals, oxides and graphites of other units within or adjacent to the Faurefjell Formation. Some late stage isotopic resetting is observed, mainly in feldspar and calcite but, generally, the metamorphic bulk isotopic compositions have been preserved. The possibility of preserving bulk isotopic trends, inherited from a Proterozoic weathering process, is ambiguous from the oxygen isotopic compositions of metamorphic minerals of the lateritized metavolcanics.

In **Chapter V**, it is concluded that, during and after the high-grade metamorphic conditions, the Faurefjell supracrustals were approximately closed for external fluid fluxes. However, considerable fluid-rock interaction must have occurred before exposure to high-grade metamorphic conditions. Hence, mobility of elements is mostly restricted to early episodes (sedimentation, diagenesis, low-grade metamorphism) in the formation of these rocks.

SAMENVATTING

Waren de granuliet-faciës metamorfe supracrustalen van de Faurefjell Metasediment Formatie uit Rogaland, ZW Noorwegen, chemisch open of gesloten systemen? Om differentiële element mobiliteiten ten gevolge van pre-, syn- en post-metamorfe vloeistof stromen door deze formatie te schatten, is onderzoek verricht naar de mineralogie en bulk-chemische samenstelling van marmers en metavulkanieten, en naar de stabiel isotopische samenstelling van zuurstof en koolstof en de kristal-chemie in afzonderlijke mineralen.

Hoofdstuk I van dit proefschrift informeert de lezer over de geologische achtergrond van het probleem. Een overzicht van de geologie van het hoog-temperatuur granuliet gebied in Rogaland wordt gegeven, en er wordt uitgelegd waarom juist de Faurefjell supracrustalen in het kader van de probleemstelling bestudeerd worden. Aan het eind van het hoofdstuk wordt de doelstelling van het proefschrift geformuleerd.

De anion bezetting van de hydroxyl plaats in metamorfe glimmers kan de samenstelling weerspiegelen van fluïde fasen die ten tijde van de metamorfose naast deze glimmers voorkwamen. Daarom wordt in **Hoofdstuk II** de samenstelling van phlogopiet in de marmer besproken. Er wordt afgeleid dat in barium- en titaan-rijke phlogopiet, 81 mol% van de vaste stof oplossing bestaat uit een watervrij Ba-Ti eindlid ($BaMg_2TiSi_2Al_2O_{12}$).

In **Hoofdstuk III** wordt de grote variatie, die waargenomen is in bulk samenstellingen van metavulkanieten van de Faurefjell Formatie, in verband gebracht met pre-metamorfe chemische alteratie. Samenstelling-volume relaties binnen een metavulkanietlaag wijzen op een vorming door Proterozoïsche verwering (laterietvorming) van een oorspronkelijk basaltisch substraat. Effecten van syn-diagenetische metasomatose zijn vermoedelijk gesuperponeerd op de verwering trends. De daaropvolgende metamorfe processen hebben voornamelijk conserverend gewerkt op bulk samenstellingen die al tijdens de diagenese zijn verworven.

Zuurstof en koolstof isotopen verhoudingen in carbonaten, silicaten en oxyden uit diverse gesteentesoorten in de Faurefjell Formatie worden besproken in **Hoofdstuk IV**. Calciet in de marmers vertoont regionaal een gekoppelde $\delta^{18}O$-$\delta^{13}C$ trend. De grootte van de regionale verschuiving in $\delta^{18}O$ (8.5 per mille) en $\delta^{13}C$ (5 per mille) kan niet veroorzaakt zijn door ontgassingsreacties. Vermoedelijk heeft

isotopische uitwisseling plaatsgevonden met externe vloeistoffen. De $\delta^{18}O$ waarden van hoog-gradig metamorfe silicaat mineralen in de marmers komen overeen met de isotopische samenstelling van de geassocieerde calciet. Daarom moet de gesteente-fluïde fase interactie, die de regionale $\delta^{18}O$-$\delta^{13}C$ heeft veroorzaakt, plaats hebben gevonden voordat deze silicaten gevormd zijn (d.w.z., voor het bereiken van de hoogste graad van metamorfose). Regionale trends in $\delta^{18}O$ en/of $\delta^{13}C$ zijn niet waargenomen in silicaten, carbonaten, oxyden en grafieten uit andere lithologische eenheden binnen (of grenzend aan) de Faurefjell Formatie. Isotopische aanpassing aan laat-metamorfe, laag-gradige omstandigheden wordt hier en daar waargenomen, (voornamelijk in calciet en veldspaat), maar in het algemeen zijn de bulk isotopische samenstellingen, zoals die waren ten tijde van de metamorfose, bewaard gebleven. De zuurstof isotopen samenstellingen in mineralen uit de gelateritizeerde metavulkanieten geven geen uitsluitsel over de vraag of bulk isotopische trends, veroorzaakt door Proterozoïsche verwering, bewaard zijn gebleven.

In **Hoofdstuk V** wordt geconcludeerd dat, gedurende en na de hoog-gradig metamorfe omstandigheden, de Faurefjell supracrustalen zo goed als gesloten waren voor externe fluïde fasen. Aanzienlijke gesteente-fluïde fase interactie heeft daarentegen plaatsgevonden voordat de hoog-gradig metamorfe condities ontstonden. De mobiliteit van de chemische elementen in de formatie is dus voornamelijk beperkt tot de eerste gedeelten van de petrologische geschiedenis (afzetting, diagenese, laag-gradige metamorfose).

CHAPTER I: GEOLOGICAL BACKGROUND AND SCOPE OF THIS THESIS

1.0 ABSTRACT

High-temperature granulite facies metamorphism in the Precambrian basement of Rogaland, SW Norway, is associated with the diapiric uprise and final emplacement of massif-type anorthosites during the Sveconorwegian orogenic period (1250-900 Ma). Fluid deficiency characterizes the high-grade metamorphic conditions and, hence, unique opportunities exist to reconstruct the thermal history of a Proterozoic lower crustal segment of the Baltic Shield. Especially metasediments are effective P-T-X_{fluid} sensors, due to small scale chemical contrast and the occurrence of sluggishly reacting Al-rich minerals adjacent to, or in the vicinity of, rapidly reacting Mg-rich minerals. Extensive isograd mapping during the past two decades has yielded excellent field control for metapelites, marbles and metavolcanics which are intercalated in migmatitic units. Therefore, in order to bracket mass transfer and fluid budgets at high-grade conditions, these rocks are selected as targets for further small scale and regional geochemical and stable isotope investigations.

1.1 INTRODUCTION

The scope of this thesis is to assess element mobilities in metasediments (the Faurefjell Metasediment Formation) of the Precambrian basement of Rogaland, SW Norway. The problem is: do the distinct rock types in this unit represent relatively open or relatively closed systems as function of time with regard to specific elements and/or isotopic ratios thereof?

This chapter provides a) geological information necessary to understand the importance of the problem, b) the rationale behind the selection of these particular metasediments in this case study and c) a compilation of what is already known about these rocks. The Faurefjell Metasediment Formation will be placed in a geological framework by zooming in from the Baltic shield to geological units of progressively smaller scale. *En passant*, an up to date (1990) section on the geology of Rogaland is given. At the end of this chapter, the scope of this thesis will be further refined.

While digesting this information, the reader should keep in mind that the complexity of the rocks studied, as displayed by the large textural, chemical and isotopic variation on small scale, is by no means typical for the Rogaland area. It is

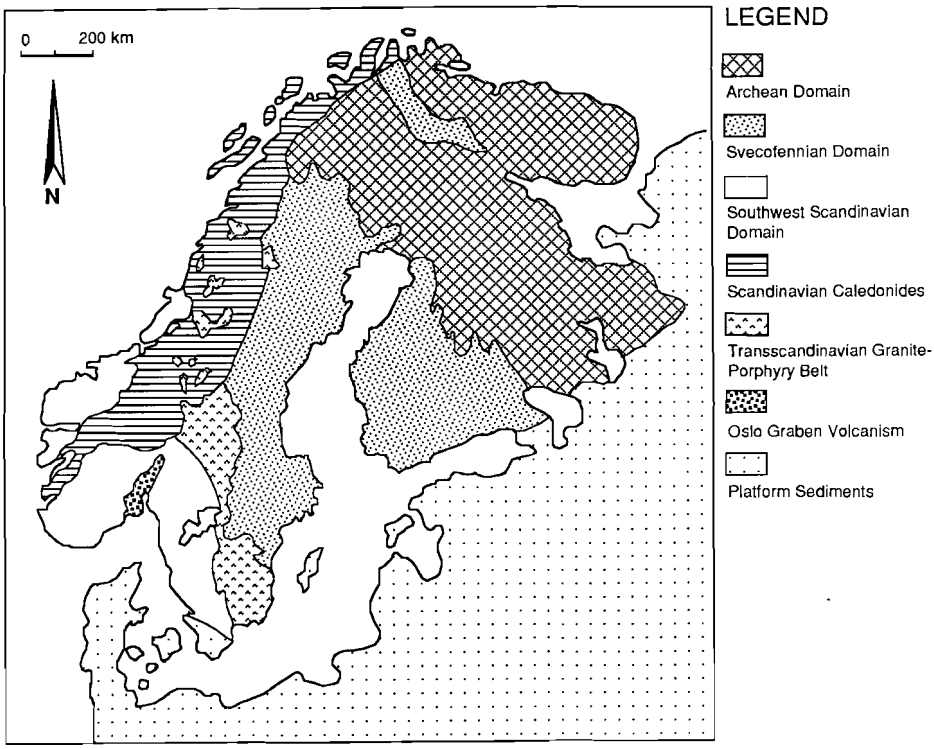

Fig. 1.1: Crustal Domains of the Baltic Shield (modified after: Verschure 1985; Gaàl and Gorbatschev 1987).

the preservation of evidence for such complexity that is typical for Rogaland.

1.2 STRUCTURE OF THE BALTIC SHIELD

On the basis of radiometric dating, tectonic style, metamorphic history and lithology, the Baltic Shield may be subdivided in three crustal domains, as shown in **Figure 1.1**. These domains were formed and reworked during distinct orogenic episodes, and reflect alternating accretion and rifting/dispersion regimes (Gaàl and Gorbatschev 1987; Gorbatschev 1990). The Archean Domain represents the oldest Baltic rocks, which are found in Karelia and on the Kola peninsula. They were cratonized predominantly during the Lopian orogenic period (2.9-2.6 Ga; see **Table 1.1**). The Svecofennian Domain, in the central and western part of the Shield, is proposed to have grown outward from this Archean nucleus, mainly during the

Table 1.1: Orogenic time-table

Era	Radiometric Age (Ga)		Event	Canadian Equivalent
Archean	Saamian	3.1 - 2.9	Orogenic	
	Lopian	2.9 - 2.6	Orogenic	Rebolian
Proterozoic	Karelian	2.45 - 2.0	Anorogenic	
	Svecofennian	2.0 - 1.77	Orogenic	Hudsonian
	Gothian	1.75 - 1.5	Orogenic	
	Hallandian	1.5 - 1.4	Anorogenic	
	Sveconorwegian	1.25 - 0.9	Orogenic	Grenvillian
Phanerozoic	Caledonian	0.6 - 0.4	Orogenic	

Svecofennian orogenic period (2.0-1.77 Ga; Lindh 1987). The Southwest Scandinavian Domain, the westernmost rim of the Baltic Shield, accreted during the middle Proterozoic. It is built up of Gothian rocks that were reworked during Hallandian (1.5-1.4 Ga), Sveconorwegian (1.25-0.9 Ga) and Caledonian (0.6-0.4 Ga) events. The geology of the Southwest Scandinavian Domain will be discussed in the next section. In general, the domains become progressively younger *and* more deformed from the northeast towards the southwestern part of the Shield. The northwestern edge of the Baltic Shield is fringed by the Scandinavian Caledonides, which represent nappe systems of remobilized Precambrian and early Phanerozoic crustal material.

1.3 DEVELOPMENT OF THE SOUTHWEST SCANDINAVIAN DOMAIN

The principal Sveconorwegian and pre-Sveconorwegian terranes in Scandinavia can be correlated with structural units in Canada, Greenland and Scotland (**Table 1.2**) indicating that they formed part of a major intercontinental pattern of proterozoic crustal accretion (Patchett et al. 1978; Gower 1985). The Southwest Scandinavian Domain is regarded as the European part of the vast North Atlantic Grenville province. It is separated from the Svecofennian platform by the Transscandinavian Granite-Porphyry Belt and the Protogine Zone (**Figs. 1.1; 1.2**) which are the Scandinavian equivalents of the Trans Labrador Batholith and the Grenville Front, respectively, in Canada.

The Protogine Zone is a paleomagnetic boundary that generally marks the eastern limit of Sveconorwegian deformations and ages (Gaål and Gorbatschev 1987),

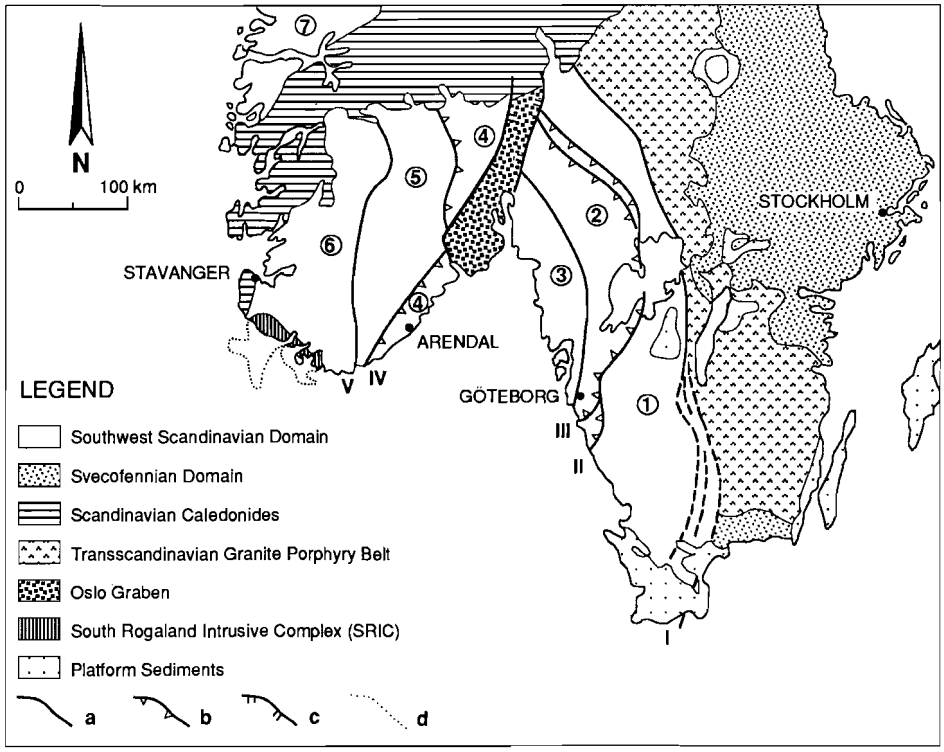

Fig. 1.2: Major tectonic zones in South Scandinavia. Modified after: Swanberg et al. 1974; Verschure 1985; Demaiffe and Michot 1985; Lindh 1987). Crustal Segments: **1** Eastern Segment; **2** Median Segment; **3** Western Segment; **4** Bamble/Kongsberg Segment; **5** Telemark Segment; **6** Rogaland/Vest-Agder Segment; **7** Western Gneiss Region. Major structural boundaries: **I** Protogine Zone; **II** Mylonite Zone; **III** Dalsland Boundary Thrust; **IV** Kristiansand-Bang Shear Zone; **V** Mandal-Ustaoset Line. Structural symbols: **a** fault in general; **b** thrust fault; **c** normal fault; **d** submarine extension of the South Rogaland Igneous Complex.

although some Sveconorwegian age resetting is observed in minerals within and directly east of the Transscandinavian Granite-Porphyry Belt (Verschure 1985). The Protogine Zone appears to be a deep-reaching listric feature which brings seismically two layered Sveconorwegian-reworked Gothian crust to override three-layered Svecofennian crust (Berthelsen 1990). It is inferred from paleomagnetic and structural data that 1190 - 1050 Ma ago, during the Sveconorwegian orogenic period, the Baltic shield rotated clockwise relative to the Canadian Shield (Poorter 1981, Stearn and Piper 1984, Gower 1985), which may explain the generally divergent orientation of major structural boundaries in the Baltic Shield.

Table 1.2: Synonyms and North Atlantic equivalents of Scandinavian structural units

Scandinavian Unit; (Synonym); "Canadian Equivalent"; {Greenland Equivalent};
Baltic Shield; (Fennoscandian Shield).
Svecofennian Domain; "Makkovic Province"; {Ketilidian Mobile Belt}.
Southwest Scandinavian Domain; (Sveconorwegian Province); Southwestern Gneiss Complex); "Grenville Province".
Protogine Zone; (Sveconorwegian Front); (Great Mylonite Zone); "Grenville Front".
Transscandinavian Granite-Porphyry Belt; (Småland-Värmland Granitoid Belt); "Trans-Labrador Batholith"
Eastern Segment; "Groswater Bay Terrane"
Median Segment; "Lake Melville Terrane"

Typical for the Southwest Scandinavian Domain is the occurrence of large zones of strained rocks, e.g. the Protogine Zone, the Mylonite Zone, the Kristiansand-Bang Shear Zone (**Fig. 1.2**). Together with the Permian Oslo Graben these zones define the boundaries of seven tectonic segments (**Fig. 1.2**) with distinct lithological, radiometric and metamorphic characteristics.

Several Gothian ages are reported for rocks east of the Oslo Graben and for the Bamble/Kongsberg Segment, but definitive Gothian ages are not known from the Telemark and Rogaland/Vest-Agder segments (Demaiffe and Michot 1985; Verschure 1985). This may be due to extensive metamorphic disturbance of U-Pb and Rb-Sr isotopic systems in the westernmost segments, as Sveconorwegian reworking increases westward (Falkum and Petersen 1980). In the Rogaland/Vest-Agder Segment, occasional dates between 1.4 and 1.5 Ga (Rb/Sr whole-rock, $^{207}Pb/^{206}Pb$ zircon, Pb/Pb whole-rock; Versteeve 1975; Pasteels and Michot 1975) indicate that part of the basement complex consists of at least 1.5 Ga old crust. Sm-Nd model ages of various basement gneisses in Rogaland indicate crustal residences between 1.5 and 1.9 Ga (Menuge 1988). Accretion of the present Southwest Scandinavian Domain was largely completed before the Sveconorwegian orogenic period, apart from the syn-kinematic intrusions which recur mainly in the Rogaland/Vest-Agder Segment. Sveconorwegian ages have been recorded throughout the Southwest Scandinavian Domain (Demaiffe and Michot 1985; Verschure 1985) and represent essentially a period of reworking previously formed crust (Gaål and Gorbatschev 1987; Lindh 1987).

The following gradients are observed from the Oslo Graben towards the North

Sea (Falkum 1985):

a)ages of deformation and intrusive activity become younger.

b)the volume of Sveconorwegian intrusions increases drastically.

These two features prompted Falkum (1985) to propose that the Rogaland/Vest-Agder Segment represents the core zone of an asymmetrical N-S running Sveconorwegian orogenic belt representing a true continental accretion zone with considerable crustal addition. The Telemark and Bamble/Kongsberg segments embody in this model the central orogenic zone where pre-orogenic gneisses were considerably reworked and mixed with numerous syn- and postkinematic intrusions. Finally, the region between the Oslo Graben and the Protogine Zone is seen as a peripheral zone, with less structural and metamorphic Sveconorwegian overprinting and with a mega-tectonic imbricate structure imposed from the west. The asymmetric character of such an orogen may be explained by a hypothetical, preexistent, proterozoic subduction zone to the present west of the South Scandinavian Domain (Berthelsen 1980; Falkum and Petersen 1980; Falkum 1985). For segments between the Oslo Graben and the Protogine Zone, subduction-type developments during the Gothian and Sveconorwegian orogenies seem also more consistent with the presently available data than, for example, continental collision-type developments (Lindh 1987; Åhäll and Daly 1989), although evidences for a subduction zone are not unequivocal (see below for alternative models in the Rogaland area).

1.4 SALIENT FEATURES OF THE ROGALAND HIGH-GRADE TERRANE

The geology in the Rogaland province (**Fig. 1.3**) is dominated by the vast (> 2000 km^2) anorthositic South Rogaland Intrusive Complex (SRIC) that produced a very high-grade metamorphic aureole in the pre-existing high-grade gneisses (Hermans et al. 1975; Tobi et al. 1985) during a multistage differentiation and emplacement history (1500(?)-900 Ma; Michot and Michot 1969; Demaiffe and Michot 1985; Duchesne et al. 1985).

1.4.1 lithology of the Rogaland Terrane

The SRIC is comprised of three large massif-type anorthosites (Egersund-Ogna, Håland-Helleren, and Åna-Sira), two smaller leuco-noritic bodies (Hidra and Garsaknatt), a mainly leuconoritic lopolith (Bjerkreim-Sokndal) and three large acidic

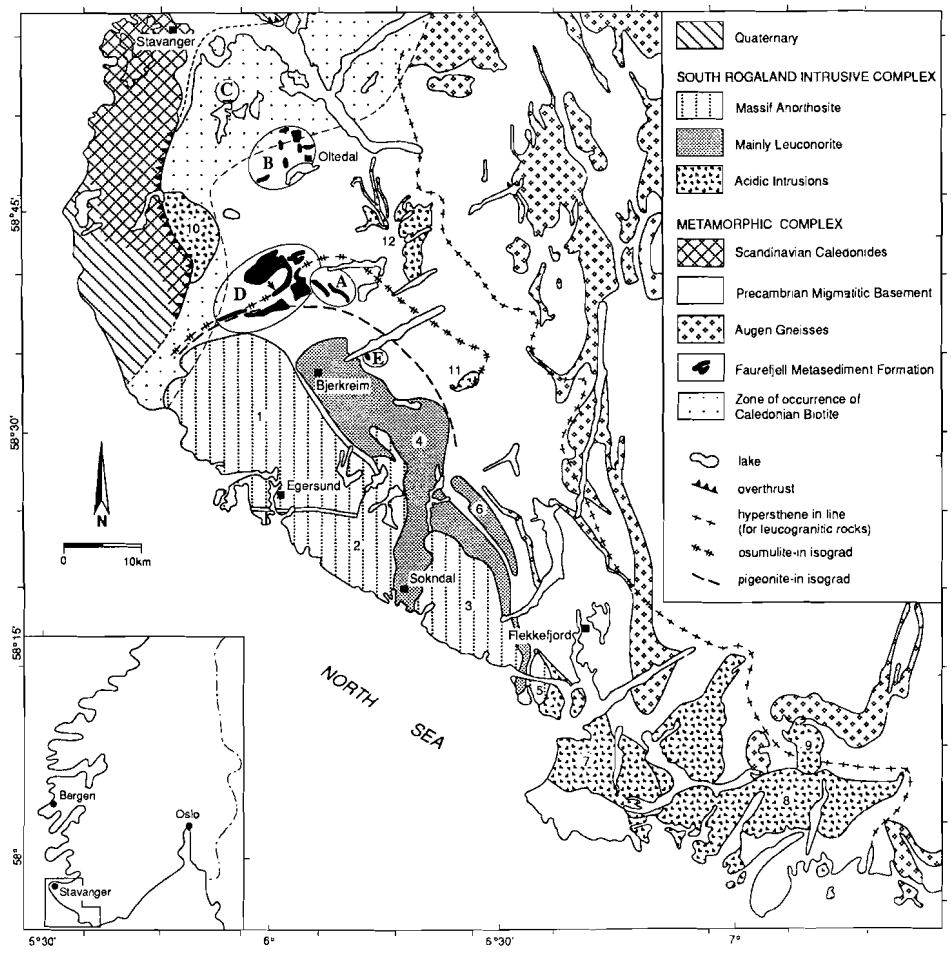

Fig. 1.3: Simplified geological sketch map of the Rogaland terrane. Magmatic bodies: **1** Egersund-Ogna; **2** Håland-Helleren; **3** Åna-Sira; **4** Bjerkreim-Sokndal; **5** Hidra; **6** Garsaknatt; **7** Farsund; **8** Lyngdal; **9** Kleivan; **10** Sjelset; **11** Botnavatnet; **12** Gloppurdi. **A-E**: Exposures of the Faurefjell Metasediment Formation.

plutons (the Farsund charnockite, the Lyngdal granodiorite and the Kleivan "granite"; Duchesne et al. 1985). The isolated Sjelset charnockite (Maijer et al. 1990) is possibly chemically and genetically linked to the post-kinematic acidic plutons in the SRIC (C. Maijer, personal communication). The Bjerkreim-Sokndal lopolith may be divided in a folded and layered anorthositic-leuconoritic lower part (1050 Ma) and a (quartz-) monzonitic upper part (930 Ma; Rietmeijer 1979; Wielens et al. 1980). An important part of the SRIC (about 75%) extends southwestward under the present North Sea

(Sellevoll and Aalstad 1971; see **Fig. 1.2**) and presumably also northward under the Caledonides (cf., Maijer 1990). Two major iron-rich syenitic to granitic sheet intrusions occur in Rogaland in addition to the SRIC (Botnavatnet and Gloppurdi; Rietmeijer 1979). These are petrographically very similar to the upper part of the Bjerkreim-Sokndal lopolith, but their intrusion (1200 Ma; Wielens et al. 1980; Rietmeijer 1979) predates final emplacement of the SRIC (1050-900 Ma; Demaiffe and Michot 1985).

The SRIC, Botnavatnet, Gloppurdi and Sjelset intrusions are surrounded by a Precambrian polymetamorphic complex of intensely folded Charnockitic and Granitic Migmatites (Hermans et al. 1975) with intercalations of augen gneisses (Bingen 1989) and metasupracrustal rocks. The latter are comprised of the Gyadal Garnetiferous Migmatites (mainly metapelites; Kars et al. 1980; Huijsmans et al. 1981) and the Faurefjell Metasediment Formation (marbles, quartzites, metavolcanics and reaction intermediates thereof; Sauter 1981, 1983; Bol et al. 1989a,b). The augen gneisses are structurally (Falkum 1985) and chemically (Bingen 1989) intrusive rocks, that were emplaced before or during the Sveconorwegian orogenic period (Menuge 1988).

1.4.2 magmatic evolution of the SRIC

Three features characterize the massif-type anorthosites of the SRIC: 1) foliated anorthosite inclusions; 2) giant (> 1m) Al-rich orthopyroxene crystals exhibiting plagioclase and spinel exsolutions; and 3) the presence of an anorthosito-leuconoritic complex. This so-called Egersund-Ogna trilogy is a manifestation of synemplacement deformation during diapiric uprise from great depth of crystal mushes lubricated by limited amounts of melt (Duchesne et al. 1985). Radiometric age dating of the anorthosites yields only minimum ages (1050 Ma) corresponding to the closing of isotopic systems upon cooling. The large variation in consolidation pressures inferred for the Egersund-Ogna body (4-12 kbar) indicates a prolonged evolution prior to final emplacement (Duchesne et al. 1985). The minimum age date combined with the variation in consolidation pressures suggest that magmatic evolution of the anorthosite parent magmas has started much earlier (1.5 Ga ago ?) in deep seated magma chambers at the base of a thickened crust (Duchesne et al. 1985; see also section on Proterozoic plate tectonic setting).

The conspicuous Fe enrichment in the mafic minerals of the rhythmically layered leuco-noritic phase (lower part) of the Bjerkreim-Sokndal lopolith is

attributed to closed system differentiation at dry conditions (Duchesne et al. 1985). The monzonitic top of the lopolith is interpreted as a flotation cumulate at the roof of a magma chamber, where also contamination with supracrustal material occurred (Duchesne et al. 1987).

On the base of U/Pb ratios and Pb, Nd, Sr and O isotopic evidence, the "anorthositic suite" in the SRIC (anorthosite, (leuco-)norite, monzonorite, (quartz-) monzonite, charnockite/granite) may be rationalized by invoking the presence of three distinct magma types (Duchesne et al. 1985, 1987, 1989): a) primarily basaltic, mantle derived magma generating massive anorthosite cumulates, b) monzonoritic magma with variable amounts of crustal contamination producing anorthositic-monzonitic cumulate suites such as found in the Bjerkreim-Sokndal lopolith and c) charnockitic magma resulting from fractionation of monzonoritic magma and/or partial melting of granulites creating the acidic intrusions. Alternatively, Nd and Sr isotope systematics may be taken to indicate that the anorthosites, leuconorites and at least some of the acidic intrusions are related by the same, mantle derived, picritic magma type, which was chemically and isotopically modified by assimilation of old crustal material at all stages (Menuge 1988).

1.4.3 metamorphic history of the basement complex

On the basis of mineral assemblages, four stages of metamorphism, **M1-M4** (Hermans et al. 1975; Jansen and Maijer 1980; Jansen et al. 1985; Maijer 1987), have been recognized in the metasupracrustal units and in their enveloping migmatitic complex (**Figs. 1.4a,b**; see also **Fig. 4.2**).

The **M1** phase (about 1200 Ma?; Wielens et al. 1980) has been assigned to an old regional upper amphibolite to granulite facies metamorphism (Wielens et al. 1980; Maijer and Padget 1987). Estimates of P-T conditions reached during this phase are scarce and range from P = 6-8 kbar and T = 550-850°C (Jansen et al. 1985). Garnet, sillimanite, sapphirine and possibly Al-rich orthopyroxene are observed as **M1** relics throughout the Precambrian basement in the Rogaland/Vest-Agder Segment. The **M1** phase predates all anorthositic and acidic intrusions and may have been a pre-Sveconorwegian event.

The granulitic high temperature-low pressure **M2** stage (1050 Ma; Wielens et al. 1980) is the main metamorphic event in Rogaland. It is essentially a thermal overprint induced by the intrusion of the anorthositic-leuconoritic phase (lower part)

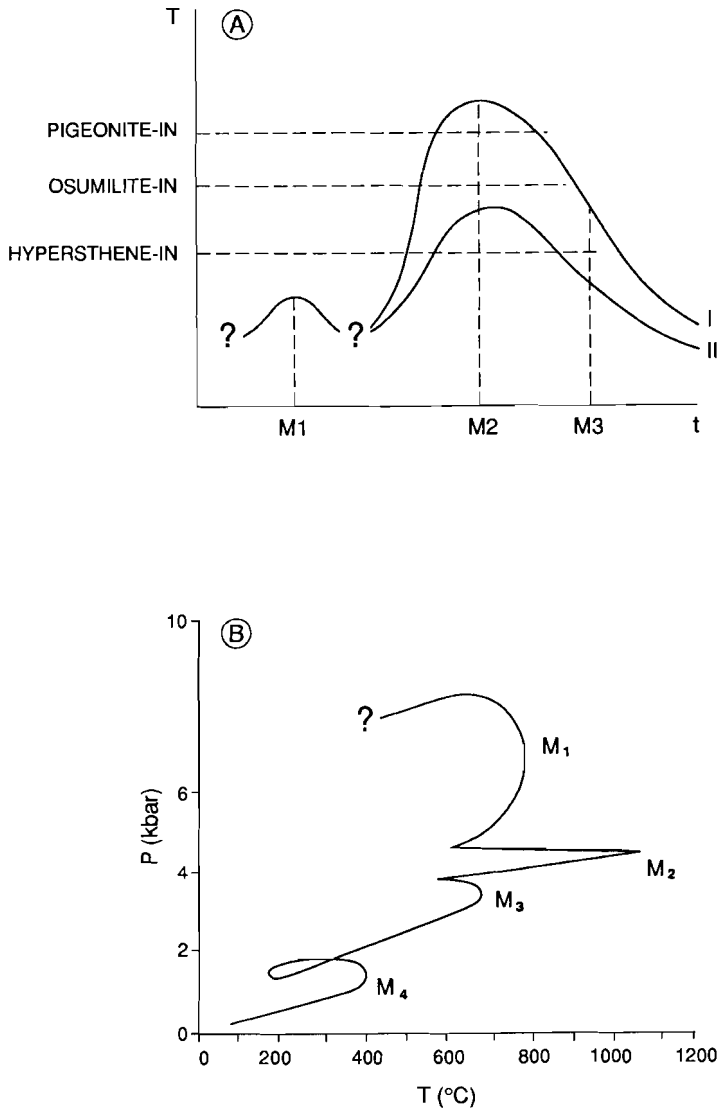

Fig. 1.4a,b: a) Schematic time (t) *vs.* temperature (T) diagram showing the temperature path in the high-grade metamorphic envelope of the SRIC during the Precambrian metamorphic events **M1-M3**, close to the Bjerkreim-Sokndal lopolith, within the pigeonite-in isograd (I) and further away, just outside the osumilite-in isograd (II; after Maijer 1987). b) Semi-quantitative P-T path for rocks within the pigeonite-in isograd (after Jansen and Maijer 1980).

of the Bjerkreim-Sokndal lopolith, superimposed on the diapiric rise of the massif-type anorthosites (Maijer et al. 1981; Maijer 1987). A 15-45 km wide metamorphic zoning pattern surrounding the SRIC (Tobi et al. 1985) is manifest by **a**) a pigeonite-in isograd (the metamorphic pigeonite is now inverted to orthopyroxene and clinopyroxene), **b**) an osumilite-in isograd, **c**) a garnet decomposition isograd, **d**) a (amphibole + quartz)-out isograd, and **e**) a hypersthene line (incoming of hypersthene in granitic rocks) (see **Fig. 1.3** for position of **a**, **b** and **e**). Geothermometric

calculations yield temperatures of about 1050°C between the pigeonite-in isograd and the igneous complex, decreasing to about 750°C near the hypersthene line (Jacques de Dixmude 1978; Jansen et al. 1985). Further to the east, amphibolite facies metamorphism is developed and a gradual regional change in chemical and optical properties of amphiboles and sillimanites related to distance to the intrusive complex is observed (Dekker 1978; Evers and Wevers 1984). Some of the metamorphic gradients and isograds, e.g. the hypersthene line, may in fact be of hybrid age and are presumably the composite results of various **M1-M2** events. Crystallization pressures inferred for **M2** assemblages are 4-5 kbar (Jansen et al. 1985) based on geobarometry and on the upper stability of **M2**-osumilite and the lower stability of **M1**-sapphirine + orthopyroxene assemblages. Wilmart and Duchesne (1987) arrive at slightly higher **M2** pressures considering late-magmatic crystallization pressures of post-tectonic intrusions of the SRIC. They inferred crystallization pressures ($Opx = Ol + Qtz$) for Hydra of >5 kbar and for the upper part of the Bjerkreim-Sokndal lopolith of 6-7.7 kbar (cf. Rietmeijer 1979: 5-7 kbar upper part; cf. Rietmeijer and Champness 1982: 9 kbar for the lower part). Possibly, these relatively high pressures reflect complex, polybaric, multistage crystallization/emplacement paths, such as inferred for the emplacement as a crystal mush of the Egersund-Ogna Anorthosite and other anorthositic bodies of the SRIC (Duchesne et al. 1985). The rocks between the hypersthene line and the SRIC would be classified as low-pressure granulites in the scheme of Green and Ringwood (1967) due to the combination of low or intermediate pressures and extremely high metamorphic temperatures. Indeed, kyanite is never reported from Rogaland whereas a few occurrences of andalusite (**M3**) are known (Jansen and Maijer 1980; Huijsmans et al. 1982).

The **M3**-stage of medium-grade metamorphism represents a period of retromorphism during slow, almost isobaric, post-**M2** regional cooling (Dekker 1978; Rietmeijer 1979; Swanenberg 1980; Kars et al. 1980; Sauter 1983; Kloprogge et al. 1989) that affected both the SRIC and its metamorphic envelope. The large temperature interval for **M3** conditions (400-750°C, see also **Fig. 4.2**) reflects the fact that various mineral pairs attain retrograde equilibrium compositions from different P-T conditions. **M3** features include the formation of exceptionally well developed exsolution textures in calcites, pyroxenes, and feldspars (Sauter 1983; Rietmeijer 1984; Maijer 1987), partial decomposition of typical **M2** minerals (e.g., osumilite, Al-rich orthopyroxene) into symplectites of lower grade minerals (Henry 1974; Kars et al. 1980; Tobi et al. 1985; Maijer 1987), formation of orthopyroxene poikiloblasts by

massive transformation of pigeonite (Rietmeijer and Dekker 1978), and formation of orthopyroxene/Fe-Ti oxide symplectites by overall re-equilibration of originally magmatic mineral assemblages (Barton and van Gaans 1988). Locally, renewed growth occurs of minerals which became unstable at **M2** conditions such as garnet, cordierite, sillimanite, and sapphirine (Maijer 1987). **M3** biotites and amphiboles may form rims around **M1** and **M2** minerals. Isotopic ages for osumilite (970 Ma (K-Ar; Rb-Sr), Maijer et al. 1981), hornblendes (950 Ma (K-Ar), Dekker 1978; Wielens et al. 1980), and brown biotite (870 Ma (K-Ar; Rb-Sr), Verschure et al. 1980) reflect passage through Rb-Sr and K-Ar closure temperatures during **M3** cooling. Current estimates for **M3** pressures are 3-4 kbar, locally 5 kbar (Jansen et al. 1985) or 3±0.5 kbar (Wilmart and Duchesne 1987). Previously, estimated pressures slightly in excess of 5 kbar were assigned to **M3** (Dekker 1978; Swanenberg 1980; Rietmeijer 1984).

Finally an **M4**-stage of low-grade (prehnite-pumpellyite to greenschist facies) metamorphism (400 Ma) is weak and omnipresent in the west and is attributed to the Caledonian orogenesis (Verschure et al. 1980). An isograd of Caledonian green biotite (Sauter et al. 1983) follows the front of the Caledonian nappe system at a distance of 5-15 km in the Precambrian basement (**Fig. 1.3**). Although often referred to as "Caledonian retrogression", the **M4**-assemblages in reality reflect partly a renewed stage of prograde metamorphism that is related to a reversed geothermal gradient caused by overthrusting of a pile of relatively hot Caledonian nappes (Maijer 1980; Jansen et al. 1985).

1.4.4 significance of metamorphic fluids

Low water pressures during high-grade metamorphic conditions are inferred from the stability of orthopyroxene in **M2**-**M3** assemblages in the metamorphic envelope of the SRIC (cf., Valley et al. 1983). Locally, orthopyroxene may have been stable in **M1** assemblages. The occurrence of **M2** osumilite in metasediments near the SRIC also supports low water pressures (Olesch and Seifert 1981). Highly variable mineral assemblages, complex textures and mineral zoning as well as element partitioning among relevant minerals indicate very local (mm-scale) equilibrium domains for **M2** assemblages. This chemical fixation points to restricted element transport due to generally very limited amounts of metamorphic fluids (Jansen and Maijer 1987). The subsolidus formation of orthopyroxene poikiloblasts (Rietmeijer and Dekker 1979) and orthopyroxene/Fe-Ti oxide symplectites (Barton and van Gaans 1988) indicates

an impediment for nucleation of orthopyroxene. The amount of undercooling needed to create the observed orthopyroxene textures was presumably reached by fluid deficiency during post-**M2** cooling (Rietmeijer 1979).

Fluid inclusion studies have, so far, not been successful in identifying peak metamorphic fluid compositions in Rogaland. The compositional ranges observed in fluid inclusions (dominantly H_2O, CO_2-H_2O, CO_2-N_2, N_2-CH_4, or CO_2-CH_4 respectively) are related to rock type rather than to metamorphic grade (Swanenberg 1980). For example, fluid inclusions in quartz nodules from marbles of the Faurefjell Metasediment Formation are CO_2-rich, whereas CH_4-rich inclusions are encountered in platy quartz of graphite bearing samples of the Gyadal Garnetiferous Migmatites. Swanenberg (1980) inferred, in general, high densities for CO_2-rich and N_2-rich fluid inclusions (especially in retrograde and/or intensely deformed rocks). Such densities are incompatible with current P-T estimates for the high-grade **M1**-**M3** conditions. He concluded that the fluid compositions of the inclusions were modified due to post-metamorphic re-equilibration towards higher densities, presumably during near-isobaric cooling of the complex, i.e. during **M3**. Van de Kerkhof et al. (in preparation) found that the superdense CO_2 inclusions of Swanenberg in fact represent metastable CO_2-CH_4 mixtures entrapped after peak metamorphic conditions. These authors argue that the observed compositional heterogeneity of fluid inclusions throughout the terrane supports the concept of fluid-deficient conditions during **M2**-**M3**. Oxygen fugacities reported to date (Henry 1974; Blok 1984; Jansen et al. 1985) are highly variable as well, again suggesting local fO_2 control during **M2**-**M3** by appropriate mineral assemblages (Bol et al. 1989a,b). Indeed, all results up till now are consistent with low amounts of fluid present at the high-grade metamorphic conditions, witch had compositions governed by local mineral assemblages. Large amounts of pervasive fluids (in contrast to channelized fluids), which were able to migrate over long distances, were apparently lacking (see also Chapter IV).

Late stage, low-grade metamorphic fluids were invariably water rich as indicated by the composition and low degree of filling of secondary fluid inclusions (Swanenberg 1980; Van de Kerkhof et al. in preparation) and by **M3**/**M4** mineral assemblages (Sauter 1983; Sauter et al. 1983).

1.4.5 structural evolution

The detailed relationship between magmatic, metamorphic and tectonic events is not completely resolved. North of the Egersund-Ogna anorthosite three deformational phases are recognized (Michot 1960) and five in the area near Flekkefjord, Vest-Agder (Falkum 1976). Structural analyses in Rogaland indicate at least four phases of deformation (Hermans et al 1975; Huijsmans et al 1981; Maijer 1987). The oldest recognizable phase produced isoclinal folding, which resulted in a transpositional foliation. The 2 (or 3: c.f., Falkum 1976) later phases of intense deformation produced large, tight to isoclinal, often recumbent folds. These folds are the major structures in the area and, generally, their axial planes curve concordantly around the SRIC. These deformations are reflected within the SRIC by the typical mantled dome structure of the Egersund-Ogna anorthosite, which is related to synemplacement deformation (Duchesne et al. 1985). The youngest phase of deformation produced large (km) scale open folds with steep E-W striking axial planes.

1.4.6 regional geochemistry

LILE depletion (e.g., Field et al. 1980; Weaver and Tarney 1981), ΣREE depletion (e.g., Pride and Muecke 1980; Field et al. 1980) and high K/Rb ratios (>500) are reported from many granulitic terranes. For the Rogaland terrane such a depleted, residual nature is not substantiated. Potassium bearing minerals, such as K-feldspar and (Mg-F-rich) biotite, are stable minerals in many **M2** assemblages within the **M2** granulite-facies area (C. Maijer, personal communication). The major element chemistry of Charnockitic and Granitic Migmatites also provides evidence against depletion in magmatophile elements of the granulite facies region (van Gaans et al. 1987). No systematic variation with metamorphic grade is found for K, Rb, Th and ΣREE contents in leucocratic rocks (Bergmans and Kuiperes 1986). K/Rb ratios are 129 ± 104 (2σ) in 76 samples of various leucocratic rocks (Bergmans and Kuiperes 1986), 120 ± 65 in 64 melanocratic rocks (Blok et al. in preparation) and 300 ± 74 in 45 augen gneisses (Bingen 1989), again without significant regional variation. No indication is found for differential mobilities or loss of REE as a result of the amphibolite-granulite facies transition in augen-gneisses (Bingen 1989) nor as a result of at least three high-grade metamorphic events in metabasites (Bol et al. 1989b).

1.4.7 Proterozoic plate tectonics

The MOHO discontinuity under SW Norway is presently situated at a depth of 28-30 km (Sellevoll 1973). Combining this depth with the recrystallization pressures of surficial rocks related to the main stage of granulite-facies metamorphism (4-8 kbar), Demaiffe and Michot (1985) inferred a proterozoic crustal thickness of 50-60 km. Gravimetric data indicate a thickness of 4-5 km for the Bjerkreim-Sokndal lopolith and at least 4-5 km for the Egersund-Ogna anorthosite body (Smithson and Ramberg 1979). Together with the low heat flow through the SRIC (0.4-0.5 HFU; Swanberg et al. 1974), these data suggest that there is still more than 20 km of low heat producing rocks (high-pressure, LILE depleted granulites?) below the SRIC. One problem, according to Demaiffe and Michot (1985), with an Andean-type model as discussed above arises from the juxtaposition in the Rogaland/Vest-Agder Segment of upper-crustal and lower-crustal magmatic bodies. Thus, Sr, Pb, Nd and O isotopic work on the anorthositic bodies of the SRIC suggests an origin in the upper mantel or in a LILE depleted lower crust, whereas initial Sr isotopic ratios and REE signatures of some syn-and post-kinematic acidic intrusions (e.g., the Farsund charnockite) point towards an origin by anatexis of upper-crust material (Demaiffe and Javoy 1980, Duchesne et al. 1985, Menuge 1988). Hence, the Rogaland/Vest-Agder Segment may, alternatively to an Andean-type model, be seen as a slice of lower crust obducted during a proterozoic plate collision and intruded by granitic melts derived from underlying upper-crustal material (Michot 1984; Demaiffe and Michot 1985). However, such model is not unique, as it is possible to reconcile the intrusion of acidic rocks in and along the border zone of the massif-type anorthosites with a multistage emplacement history of the SRIC, as reflected by the considerable spread in ages and consolidation pressures recorded by individual anorthositic bodies (cf., Duchesne et al. 1985).

Proterozoic crustal thickening may also result from lithospheric doubling (Vlaar 1985, 1988) introducing a gravitationally unstable, hot, young oceanic layer below a cool continent. Applying this model here would mean that anorthositic magmas, derived from the oceanic layer, rise diapirically to underplate the existing continental crust, with as result considerable crustal thickening (Vlaar 1985). The main drawback of any underplating model for the Rogaland terrane is the presence of clearly recognizable metasediments, that testify to an upper crustal residence, at least during part of the early evolution (ie, sometime between 1.5 and 1.9 Ga;

Menuge 1988) of the terrane.

1.5 THE FAUREFJELL METASEDIMENT FORMATION

In the past, the Faurefjell Metasediment Formation received a considerable amount of attention, both during petrological field practicals and in laboratory studies of the Utrecht Geochemistry Department (Hakstege 1973; Hermans et al. 1975; Teske 1977 a,b; Hilversum 1977; Sauter 1978, 1981, 1983; Swanenberg 1980; Venhuis 1982; Meertens 1983; Blok 1984; Koop 1988). Since these metasediments are the subject of this thesis, a summary of the petrology is given below, with emphasis on marbles and "heterogeneous basic layers" which are further discussed in Chapters II-V respectively.

Exposures of the Faurefjell Metasediment Formation are largely concentrated in five areas (A - E, **Fig. 1.3**) where it crops out as thin folded layers or boudinaged lenses with a total thickness varying from 10 to 50 meters. The contacts with the surrounding migmatites are usually concordant. Locally, in areas B and C, leucogranites intrude the metasediments discordantly. The joint occurrence of thick quartzite layers and impure dolomitic marbles is diagnostic for the Faurefjell Metasediment Formation. Generally, the Faurefjell Metasediment Formation is composed of various intercalations of quartz-diopside gneisses, diopside marbles, forsterite marbles, quartzites, quartz-K-feldspar rocks, diopside-K-feldspar rocks, K-feldspar rocks, diopside rocks, leuco-charnockites, and heterogeneous basic layers (lacking in area C) consisting of basic granulites and Fe-Al rich granofelses.

The marbles cover only a very small part of the total mapped area ($<0.01\%$). Most of them occur in areas A, B and C, usually as intercalations in quartz-diopside gneisses or, alternatively, in quartzo-feldspathic rocks. The marbles are generally separated from their host lithology by thick, almost monomineralic, diopside-layers. Marbles are subordinate in area E, and only one marble exposure is found in area D (see arrow in **Fig. 1.3**).

The principal marbles are **forsterite-marbles**, containing the mineral association *Fo-Phl-Cal±Dol±Di±Spl* (mineral abbreviations after Kretz (1983)). **Diopside-marbles** have generally a higher bulk silica content and have mainly the association *Di-Phl-Cal*. Chemically, the marbles are equivalents of impure siliceous dolomites, with Ca:Mg≈1 and variable silica content. **Diopside rocks** occur as layers or lenses within the marbles and at contacts between marbles and silica-rich rocks such as quartz-diopside gneisses, quartzites and pegmatites. Part of the fluctuation in *Di* content of

the marbles supposedly represents original (sedimentary) variations in silica content. However, the *Di*-rocks and many *Di*-rich parts in the marbles must reflect synmetamorphic mobility of silica. High-grade pegmatites in the marbles are invariably jacketed by *Di* and have margins depleted in silica and enriched in Al, K and Ba (Bol and Jansen, in preparation). Veins are often symmetrically rimmed by high-variant mineral assemblages. Typically, they have a core of *Kfs*±*Qtz* and, towards the *Fo*-marbles, they successively grade into *Kfs-Di* rocks, *Di*-rocks, *Di*-marbles ± *Fo* and *Fo*-marbles ± *Di*. The *Kfs* in pegmatites and in *Di*-rocks is often sanidine, partly converted to microcline.

Di grains in the marbles are occasionally strongly zoned, having Al-, Ti- and Fe^{3+}-rich cores and Mg- and Si-rich rims (Sauter 1983). Sometimes *Di* rims around *Fo* are interconnected to form large poikiloblastic crystals. In general, these phenomena are best explained by metasomatism at or before high-grade metamorphic conditions, involving migration of silica from silicate rocks to the marbles over a meter or more, and limited Al-K redistribution on the scale of a cm or less. **Diopside-nodules** (±*Cal*±*Kfs*) "floating" in the marbles are abundant in area A and may represent boudinaged veins or, alternatively, boudinaged remnants of silica-rich sedimentary intercalations. Phlogopite is frequently observed associated with *Di* in *Di*-rocks and in marbles or as separate monomineralic bands in *Di*-rocks, in marbles and in rims around *Spl-Di* veins. Mg-spinel is common in marbles and associated *Di*-rocks from area A and E, and rare in area B.

Several types of dolomite exsolution textures are discerned in the high-Mg calcites (Sauter 1983). These textures are related to a complex cooling history following **M2** and to serpentinization of olivines during **M4**. Exsolved *Dol* is abundant in areas B and C and rare in area A, where "primary" *Dol* (i.e., not intergrown with *Cal*) is conspicuously absent. The large variation in Mg/(Mg + Ca) (42-49 mole %) of the exsolved *Dol*, even within single *Cal* crystals, demonstrates that an overall re-equilibration at lower temperatures has not taken place. Barite is a common minor constituent in the marbles, and sphene and apatite in *Di*-bearing rocks. The barite, thought to be authigenic, may be associated with nearly anhydrous Ba-Ti oxy-phlogopite in area A (Bol et al. 1989a). This association, along with a general absence of graphite in the marbles, may be taken to indicate high fO_2/fH_2O (and thus low αH_2O) in the marbles at least during part of the metamorphic history.

The sequence of the Mg-bearing minerals with a decreasing Mg/(Mg + Mn + Fe), *Dol-Di-Phl* > *Fo* > *Cal-Spl* (Bol et al, 1989a) is similar to that found by Glassley

(1975) and Rice (1977a,1977b). Local attainment of equilibrium for the distribution of Fe, Mg and Mn is demonstrated for *Fo-Di-Phl* assemblages in marbles from areas A, B and C (Sauter 1981). In general, the K_D(Fe-Mg) variation reflects increasing peak-metamorphic temperatures towards the margin of the magmatic complex. The increase is also documented by minimum *Cal-Dol* exsolution temperatures estimated from integrated Mg-contents in calcites and primary dolomites from area C and B (Sauter 1983).

Basic granulites and **Fe-Al-rich granofelses** occur together in heterogeneous basic layers at several stratigraphic levels within the Faurefjell Metasediment Formation. They have transitional bulk chemical and mineralogical compositions which are related to premetamorphic weathering processes and syndiagenetic metasomatism of basaltic rocks (Bol and Jansen 1989; Bol et al. 1989b).

The **basic granulites** have a noritic to gabbroic mineralogy, *Pl* + *Opx* + Fe-Ti oxides ± *Cpx* ± *Bt* and accessory *Zrn, Ap* and *Spl*. The **Fe-Al-rich granofelses** contain *Pl, Crd*, Fe-Ti oxides, *Spl* (hercynite) and either *Sil* (often) or *Opx* (rare). Accessory minerals are: *Ap, Zrn, Mnz* and *Crn*.

In the metabasites, REE patterns and ratios of relatively immobile trace elements indicate sub-alkaline affinities of their volcanic precursors (Blok et al., in preparation). However, using published discriminant diagrams, the Proterozoic tectonic setting of the Faurefjell Metasediment Formation cannot conclusively be inferred from the chemical composition of the metabasites (Bol and Jansen 1989). The occurrence of metavolcanics together with quartzites and metadolomites suggest a shallow marine (back-arc basin?) setting.

1.6 SCOPE OF THIS STUDY

Considerable compositional contrast exists between various lithological units (marbles, metavolcanics, quartzites) within the Faurefjell Metasediment Formation and hence, extensive chemical interaction might be expected. Also, it might be anticipated that the various rock types within the formation would respond differently to changing metamorphic conditions and, therefore, monitor different parts of the crustal history of the formation. As a result of to extensive mapping in the past, virtually all exposed occurrences of the Faurefjell Metasediment Formation are known. Detailed petrographic, mineralogic work on the marbles has been performed (Sauter 1981, 1983) and (O,C) stable isotope work has been initiated (Sauter 1983).

Therefore, these metasediments are particularly conducive to mineralogical, geochemical and stable isotope investigations.

The scope of this thesis is to assess element mobilities in response to the depositional, diagenetic, metamorphic and post-metamorphic ambiance of the Faurefjell Metasediment Formation. The ultimate purpose is to bracket fluid budgets during the crustal history of quite distinct rock types and minerals, and hence, to shed light on the evolution of the crust during the Proterozoic. This information in turn is invaluable to gain further insight in Proterozoic plate tectonics and stabilization of the continental crust in general.

1.7 ACKNOWLEDGEMENTS

This chapter benefitted from discussions with, and comments of J.B.H. Jansen, B.H.W.S. de Jong, C. Maijer, G.J.L.M. de Haas, P.A. de Groot, B.P. Dam, G. Roy and R.D. Schuiling.

1.8 REFERENCES

Åhäll KI, Daly JS (1989) Age, Tectonic setting and Provenance of östfold-Marstrand Belt supracrustals: Westward Growth of the Baltic Shield at 1790 Ma. Precambrian Res 45:45-61

Barton M, Gaans C van (1988) Formation of orthopyroxene- Fe-Ti oxide symplectites in Precambrian intrusives, Rogaland, southwestern Norway. Am Mineral 73:1046-1059

Bergmans SHA, Kuiperes GTJ (1986) Migmatieten of een sedimentaire gelaagdheid?. Unpublished MSc thesis Utrecht, 74 pp

Berthelsen A (1980) Towards a palinspastic tectonic analysis of the Baltic Shield. Mém BRGM, 6th Coll Int Geol Cong, Paris 1980, 108:5-21

Berthelsen A (1990) The Baltic Shield: Tectonics and crustal structure (*abstr*). Geonytt 17:29

Bingen B (1989) Geochemistry of Sveconorwegian augen gneisses from SW Norway at the amphibolite-granulite facies transition. Norsk Geologisk Tidsskrift 69:177-189

Blok RJP (1984) Metamorphic norites from the Faurefjell Formation, Rogaland, SW Norway: Their chemistry and some thermometrical applications. Unpublished MSc thesis Utrecht, 92 pp

Blok RJP, Bol LCGM, Hermans GAEM, Tobi AC, Jansen JBH (in prep) Geochemical evidence for a sub-alkaline origin of metabasites and their lateritic derivates of the supracrustal Faurefjell Formation, Rogaland, SW Norway. Implications for the

Proterozoic Plate-tectonic setting.

Bol LCGM, Jansen JBH (1989) Proterozoic metasediments from the deep crust of Rogaland, SW Norway: Chemistry of metabasites and granofelses (*ext abstr*). In D Bridgwater (ed) Fluid movements-element transport and the composition of the deep crust, NATO Advanced Study Institute Series C vol 281, 111-113 pp

Bol LCGM, Jansen JBH (in preparation) REE distribution among minerals in marbles and pegmatites from the high-grade Precambrian, Rogaland, SW Norway

Bol LCGM, Bos A, Sauter PCC, Jansen JBH (1989a) Barium-titanium- rich phlogopites in marbles from Rogaland, southwest Norway (Chapter II, this thesis). Am Mineral 74:439-447

Bol LCGM, Maijer C, Jansen JBH (1989b) Premetamorphic lateritization in proterozoic metabasites of Rogaland, SW Norway (Chapter III, this thesis). Contrib Mineral Petrol 103:299-309

Bol LCGM, Maijer C, Jansen JBH, Valley JW (1990) Regional oxygen and carbon isotopic variation in granulite-facies metasediments from Rogaland, SW Norway (*abstr*). Geonytt 17:31

Dekker AGC (1978) Amphiboles and their host-rocks in the high-grade Precambrian of Rogaland, SW Norway. PhD Thesis, Geol Ultraiectina 17, 277 pp

Demaiffe D, Javoy M (1980) $^{18}O/^{16}O$ Ratios of anorthosites and related rocks from the Rogaland complex (SW Norway). Contrib Mineral Petrol 72:311-317

Demaiffe D, Michot J (1985) Isotope geochronology of the Proterozoic crustal segment of Southern Norway: A review. In: Tobi AC, Touret JLR (eds) The deep Proterozoic crust in the North Atlantic provinces, NATO ASI Series C Vol 158 Reidel, Dordrecht, 411-434 pp

Duchesne JC, Denoiseux B, Hertogen J (1987) The norite-mangerite relationships in the Bjerkreim-Sokndal layered lopolith (southwest Norway). Lithos 20:1-17

Duchesne JC, Maquil R, Demaiffe D (1985) The Rogaland Anorthosites: Facts and Speculations. In: Tobi AC, Touret JLR (eds) The deep Proterozoic crust in the North Atlantic provinces, NATO ASI Series C Vol 158 Reidel, Dordrecht, 449-476 pp

Duchesne JC, Wilmart E, Demaiffe D, Hertogen J (1989) Monzonorites from Rogaland (Southwest Norway): a series of rocks coeval but not comagmatic with massif-type anorthosites. Precambrian Res 45:111-128

Evers ThJJM, Wevers JMA (1984) The composition and related optical angle axis of sillimanites sampled from the high-grade metamorphic Precambrian of Rogaland, SW Norway. N Jb Miner Mh 2:49-60

Falkum T (1976) The structural geology of the Precambrian Homme granite and enveloping banded gneisses in the Flekkefjord area, Vest-Agder, Southern Norway. Nor Geol Unders 324:79-101

Falkum T (1985) Geotectonic evolution of southern Scandinavia in light of a late-Proterozoic plate-collision. In: Tobi AC, Touret JLR (eds) The deep Proterozoic crust in the North Atlantic provinces, NATO ASI Series C Vol 158 Reidel, Dordrecht, 309-322 pp

Falkum T, Petersen JS (1980) The Sveconorwegian orogenic Belt, a case of late-Proterozoic plate collision. Geol Rundsch 69:622-647

Field D, Drury SA, Cooper DC (1980) Rare-earth and LIL element fractionation in high-grade charnockitic gneisses, south Norway. Lithos 13:281-289

Gaâl G, Gorbatschev R (1987) An outline of the Precambrian evolution of the Baltic shield. Precambrian Res 35:15-52

Gaans PFM van, Schreurs JMCM, Vriend SP, Maijer C (1987) The petrogenesis of charnockitic and granitic migmatites of the high-grade Precambrian of Rogaland/Vest-Agder, SW Norway - A statistical interpretation of major element rock chemistry. Geol Mijnb 66:177-190

Glassley WE (1975) High grade regional metamorphism of some carbonate bodies: significance for the orthopyroxene isograd. Am J Sci 275:1133-1163

Gorbatschev R (1990) Alternating accretion and rifting/dispersion regimes in the Baltic Shield - a reflection of global geodynamics. Geonytt 17:50-51

Gower CF (1985) Correlations between the Grenville Province and Sveconorwegian orogenic belt - implications for proterozoic evolution of the southern margins of the Canadian and Baltic Shields. In: Tobi AC, Touret JLR (eds) The deep Proterozoic crust in the North Atlantic provinces, NATO ASI Series C Vol 158 Reidel, Dordrecht, 247-258 pp

Green DH, Ringwood AE (1967) An experimental investigation of the gabbro to eclogite transformation and its petrological applications. Geochim Cosmochim Acta 31:767-833

Hakstege, AL (1973) Verslag van een petrologisch veldwerk in het gebied begrensd door de meren Byrkjelandsvatnet, Austrumdalsvatnet en Orsdalvatnet; Rogaland, ZW Noorwegen. Unpublished MSc thesis Utrecht, 57 pp

Henry J (1974) Garnet-cordierite gneisses near the Egersund-Ogna anorthositic intrusion, SW Norway. Lithos 7:207-216

Hermans GAEM, Tobi AC, Poorter RPE, Maijer C (1975) The high- grade metamorphic Precambrian of the Sirdal-Ørsdal area, Rogaland/Vest-Agder, South-west Norway. Nor Geol Unders 318:51-74

Hilversum AH (1977) Thermometrie aan marmers uit de Faurefjell Formatie. Unpublished MSc thesis Utrecht, 18 pp

Huijsmans JPP, Barton M, Bergen, MJ van (1982) A pegmatite containing Fe-rich grandidierite, Ti-rich dumortierite and tourmaline from the Precambrian high-grade metamorphic complex of Rogaland, SW Norway. N Jb Miner Abh 143:249-261

Huijsmans JPP, Kabel ABET, Steenstra SE (1981) On the structure of a high-grade metamorphic Precambrian terrane in Rogaland, south Norway. Nor Geol Tidsskr 61:183-192

Jacques de Dixmude S (1978) Géothermometrie comparée de roches du faciès granulite du Rogaland (Norvège méridionale). Bull Minèralogique 101:57-65

Jansen JBH, Blok RJP, Bos A, Scheelings M (1985) Geothermometry and geobarometry in rogaland and preliminary results from the Bamble area, S Norway. In: Tobi AC, Touret JLR (eds) The deep Proterozoic crust in the North Atlantic provinces, NATO ASI Series C Vol 158 Reidel, Dordrecht, 499-516 pp

Jansen JBH, Maijer C (1980) Mineral relations in metapelites of SW Norway. In: Colloquium high-grade metamorphic Precambrian and its intrusive masses. Utrecht Dept of Petrology, Utrecht

Jansen JBH, Maijer C (1987) CO2 and preferent H2O depletion in fluid deficient local rock systems during granulite facies metamorphism related to anorthositic magmatism in the Precambrian of Rogaland, SW Norway (Abstr) Volume of abstracts of the NATO/ASI Conference: Fluid movements - element transport and the composition of the deep crust, May 18-24, 1987, Lindås, Norway

Kars H, Jansen JBH, Tobi AC, Poorter RPE (1980) The metapelitic rocks of the polymetamorphic Precambrian of Rogaland, SW Norway - Part 2. Mineral relations between cordierite, hercynite and magnetite within the osumilite-in isograd. Contrib Mineral Petrol 74:235-244

Kerkhof AM van den, Touret JLR, Maijer C, Jansen JBH (in preparation) Fluid inclusions in quartz veins from high-temperature granulites of Rogaland, SW Norway

Kloprogge JT, Roermund HLM van, Maijer C (1989) Complex exsolution microstructures in inverted pigeonites from the Sjelset Igneous Complex, Rogaland, SW Norway. Norsk Geologisk Tidsskrift 69:239-249

Koop K (1988) Oxygen and carbon isotopic compositions of carbonate phases in complex calcite and dolomite exsolution textures in the Faurefjell marbles. Unpublished MSc Thesis Utrecht, 27 pp

Kretz R (1983) Symbols for rock-forming minerals. Am Mineral 68:277-279

Lindh A (1987) Westward growth of the Baltic Shield. Precambrian Res 35:53-70

Maijer C (1980) Caledonian retromorphism of the Precambrian of Rogaland/Vest-Agder, SW Norway. In: Colloquium high-grade metamorphic Precambrian and its intrusive masses. Utrecht Dept of Petrology, Utrecht

Maijer C (1987) The metamorphic envelope of the Rogaland intrusive complex. In: Maijer C, Padget P (eds) The Geology of southernmost Norway. An excursion guide. Nor Geol Unders Spec Publ 1:68-73

Maijer C, Andriessen PAM, Hebeda EH, Jansen JBH, Verschure RH (1981)

Osumilite, an approximately 970 Ma old high-temperature index mineral of the granulite-facies metamorphism in Rogaland, SW Norway. Geol Mijnb 60:267-272

Maijer C, Padget P (eds) (1987) The Geology of southernmost Norway. An excursion guide. Nor Geol Unders Spec Publ 1, 109 pp

Maijer C, Jansen JBH, Verschure RH, Senior A (1990) Excursion log of the southernmost caledonian meta-eclogites and the westernmost Precambrian intrusives in Norway. 19th Nordic Geological Wintermeeting, Stavanger January 1990

Meertens JHAM (1983) Petrologie en oorsprong van enkele granofelsen uit de Faurefjell Formatie, ZW Noorwegen. Unpublished MSc thesis Utrecht, 68 pp

Menuge JF (1988) The petrogenesis of massif anorthosites: a Nd and Sr isotopic investigation of the Proterozoic of Rogaland/Vest-Agder, SW Norway. Contrib Mineral Petrol 98:363-373

Michot J (1984) The Rogaland segment: an obducted Precambrian mantle based crust. In: Galson DA, Mueller St (eds) Proceedings of the first workshop on the European geotraverse: the northern segment, Copenhague october 1983, European Science Foundation, 83-97 pp

Michot J, Michot P (1969) The problem of anorthosites: the South-Rogaland Igneous Complex, southwestern Norway. In: Isachsen YW (ed) New York State Museum and Sci Serv Mem 18:399-411

Michot P (1960) La géologie de la catazone: Le problème des anorthosites, la palingénèse basique et la tectonique catazonale dans le Rogaland méridional (Norvège méridionale). In: Dons A (ed) Norway, Guidebook g. Witussen & Jensen AJS, Oslo, 52 pp

Olesch M, Seifert F (1981) The restricted stability of osumilite under hydrous conditions in the system K_2O-MgO-Al_2O_3-SiO_2-H_2O. Contrib Mineral Petrol 76:362-367

Pasteels P, Michot J (1975) Geochronologic investigations of the metamorphic terrain of south-western Norway. Norsk Geologisk Tidsskrift 55:11-134

Patchett PJ, Bylund G, Upton BGJ (1978) Paleomagnetism and the Grenville orogeny: new Rb-Sr ages from dolerites in Canada and Greenland. Earth Plan Sci Lett 40:349-364

Poorter RPE (1981) Precambrian paleomagnetism of Europe and the position of the Balto-Russian Plate in relation to Laurentia. In: Kroner A (ed) Precambrian Plate Tectonics, Elsevier, Amsterdam, 599-622 pp

Pride and Muecke (1980) Rare earth geochemistry of the Scourian Complex NW Scotland - evidence for the granite-granulite link. Contrib Mineral Petrol 73:403-412

Rice JM (1977a) Progressive metamorphism of impure dolomitic limestone in the Marysville aureole, Montana. Am J Sci 277:1-24

Rice JM (1977b) Contact metamorphism of impure dolomitic limestone in the Boulder

aureole, Montana. Contrib Mineral Petrol 59:237-259

Rietmeijer FJM (1979) Pyroxenes from iron-rich igneous rocks in Rogaland, SW Norway. PhD thesis, Geol Ultraiectina 21, 341 pp

Rietmeijer FJM (1984) Pyroxene (re-)equilibration in the Precambrian terrain of SW Norway between 1030-990 Ma and reinterpretation of events during regional cooling (M3) stage. Norsk Geologisk Tidsskrift 64:7-20

Rietmeijer FJM, Champness PE (1982) Exsolution structures in calcic pyroxenes from the Bjerkreim-Sokndal lopolith, SW Norway. Min Mag 45:11-24

Rietmeijer FJM, Dekker AGC (1978) An extreme form of poikiloblastic texture in Rogaland/Vest-Agder, SW Norway. Norsk Geologisk Tidsskrift 58:191-198

Sauter PCC (1978) Metamorfose van silicieuze dolomieten en gerelateerde gesteenten in het granuliet-facies Precambrium van Rogaland, ZW Noorwegen. Unpublished MSc Thesis Utrecht, 92 pp

Sauter PCC (1981) Mineral relations in siliceous dolomites and related rocks in the high-grade metamorphic Precambrian of Rogaland, SW Norway. Nor Geol Tidsskr 61:35-45

Sauter PCC (1983) Metamorphism of siliceous dolomites in the high-grade Precambrian of Rogaland, SW Norway. PhD Thesis, Geol Ultraiectina 32, 143 pp

Sauter PCC, Hermans GAEM, Jansen JBH, Maijer C, Spits P, Wegelin A (1983) Polyphase Caledonian metamorphism in the Precambrian basement of Rogaland/Vest-Agder, Southwest Norway. Nor Geol Unders 380:7-22

Sellevoll MA (1973) Mohorovicic discontinuity beneath Fennoscandia and adjacent parts of the Norwegian and the North Sea. Tectonophys 20:359-366

Sellevoll MA, Aalstad I (1971) Magnetic measurements and seismic profiling in the Skagerak. Marine Geoph Res 1:284-302

Smithson SB, Ramberg IB (1979) Gravity interpretation of the Egersund anorthosite complex, Norway: its petrological and geothermal significance. Geol Soc Amer Bull 90:199-204

Stearn JEF, Piper JDA (1984) Paleomagnetism of the Sveconorwegian mobile belt of the Fennoscandian Field. Precambrian Res 23:201-246

Swanberg CA, Chessman MD, Simmons G and others (1974) Heat flow - heat generation studies in Norway. Tectonophysics 23:31-48

Swanenberg HEC (1980) Fluid inclusions in high-grade metamorphic rocks from SW Norway. PhD thesis, Geol Ultraiectina 25, 147 pp

Teske H (1977a) Geochemisch en petrologisch onderzoek aan de marmers in Rogaland. Unpublished MSc thesis Utrecht, 42 pp

Teske H (1977b) Petrografisch veldwerk verslag in het gebied Ålgård-Oltedal, Rogaland, SW Noorwegen. Unpublished MSc thesis Utrecht, 73 pp

Tobi AC, Hermans GAEM, Maijer C, Jansen JBH, (1985) Metamorphic zoning in the high-grade Proterozoic of Rogaland/Vest-Agder. In: Tobi AC, Touret JLR (eds) The deep Proterozoic crust in the North Atlantic provinces, NATO ASI Series C Vol 158 Reidel, Dordrecht, 477-497 pp

Valley JW, McLelland J, Essene EJ, Lamb W (1983) Metamorphic fluids in the deep crust: Evidence from the Adirondacks. Nature 301:226-228

Venhuis GJ (1982) Geologisch veldwerk verslag van de Faurefjell formatie ten noorden van Vikeså. Unpublished MSc thesis Utrecht 47 pp

Verschure RH (1985) Geochronological framework for the late-Proterozoic evolution of the Baltic shield in south Scandinavia. In: Tobi AC, Touret JLR (eds) The deep Proterozoic crust in the North Atlantic provinces, NATO ASI Series C Vol 158 Reidel, Dordrecht, 381-410 pp

Verschure RH, Andriessen PAM, Boelrijk NAIM, Hebeda EH, Maijer C, Priem HN, Verdurmen EA (1980) On the thermal stability of Rb-Sr and K-Ar biotite systems: Evidence from coexisting Sveconorwegian (ca 870 Ma) and Caledonian (ca 400 Ma) biotites in SW Norway. Contrib Mineral Petrol 74:245-252

Versteeve AJ (1975) Isotope geochronology in the high-grade metamorphic Precambrian of southwestern Norway. Norges Geol Unders 359:1-50

Vlaar NJ (1985) Precambrian geodynamical constrains. In: Tobi AC, Touret JLR (eds) The deep Proterozoic crust in the North Atlantic provinces, NATO ASI Series C Vol 158 Reidel, Dordrecht, 3-20 pp

Vlaar NJ (1988) Subduction of young lithosphere: lithospheric doubling, a possible scenario. In: Nolet G, Dost B (Eds) Proceedings of the fourth workshop on the European Geotraverse Project: The upper mantle. European Science Foundation, Utrecht, 5-12 pp

Weaver BL, Tarney J (1981) Chemical changes during dyke metamorphism in high-grade basement terrains. Nature 289:47-48

Wielens JBW, Andriessen PAM, Boelrijk NAIM, Hebeda EH, Priem HNA, Verdurmen EA, Verschure RH (1980) Isotope geochronology in the high-grade metamorphic Precambrian of southwestern Norway: new data and reinterpretations. Nor Geol Unders 359: 1-30

Wilmart E, Duchesne JC (1987) Geothermobarometry of igneous and metamorphic rocks around the Ana-Sira massif: implications for the depth of emplacement of the South Norwegian anorthosites. Norsk Geologisk Tidsskrift 67:185-196

CHAPTER II: BARIUM-TITANIUM-RICH PHLOGOPITES IN MARBLES FROM ROGALAND, SOUTHWEST NORWAY

2.0 ABSTRACT

Phlogopites in forsterite-bearing marbles of the metasedimentary Faurefjell Formation in the high-grade Precambrian rocks of Rogaland, southwest Norway contain up to 24.6 wt% BaO and 13.9 wt% TiO_2. The very high TiO_2 content and the low cation sums (Σcations < 16 and Si + Al < 8 per 22 oxygens) could be taken to indicate incorporation of tetrahedral Ti and/or Ti-vacancy substitutions. However, combinations of Ti-oxy and Ti-vacancy substitution schemes explain the analytical data better. Structural formulae of the solid-solution trend have been expressed as approximately linear combinations of pure phlogopite and a Ba-Ti component $BaMg_2TiSi_2Al_2O_{12}$, with small contributions of "eastonite" and Ti-vacancy end-member. The structural formula of the most Ba- rich mica is:

$$(K_{0.14}Na_{0.05}Ba_{0.81})(Mg_{1.61}Fe_{0.45}Ti_{0.84}Al_{0.06}[\ ]_{0.03})Si_{2.13}Al_{1.88}O_{10}(OH_{0.38}O_{1.62}),$$

indicating that the unnamed anhydrous Ba-Ti end-member composition constitutes about 81 mol% of the solid solution.

2.1 INTRODUCTION

The Precambrian basement of southwest Norway (**Fig. 2.1**) consists of massif-type anorthosites, the layered anorthositic to mangeritic lopolith of Bjerkreim-Sokndal (Duchesne et al. 1985) and surrounding high-grade metamorphic migmatites containing intercalations of garnetiferous migmatites, augen gneisses, and rocks of the supracrustal Faurefjell Formation (Hermans et al. 1975; Maijer and Padget 1987).

On the basis of mineral assemblages in the garnetiferous migmatites, four main stages of metamorphism (**M1-M4**) have been recognized (Kars et al. 1980; Jansen and Maijer 1980; Maijer et al. 1981; Tobi et al. 1985). The **M1** phase is assigned ages of around 1200 Ma (Wielens et al. 1981). This phase is overprinted by the **M2** phase, which essentially was developed in a thermal aureole associated with intrusion of the magmatic complex. The **M2** phase is dated at about 1050 to 1000 Ma (Verschure 1985). Peak metamorphic temperatures were reached during the **M2** stage of metamorphism and are calculated to be 800°C near Oltedal, increasing to 1000°C

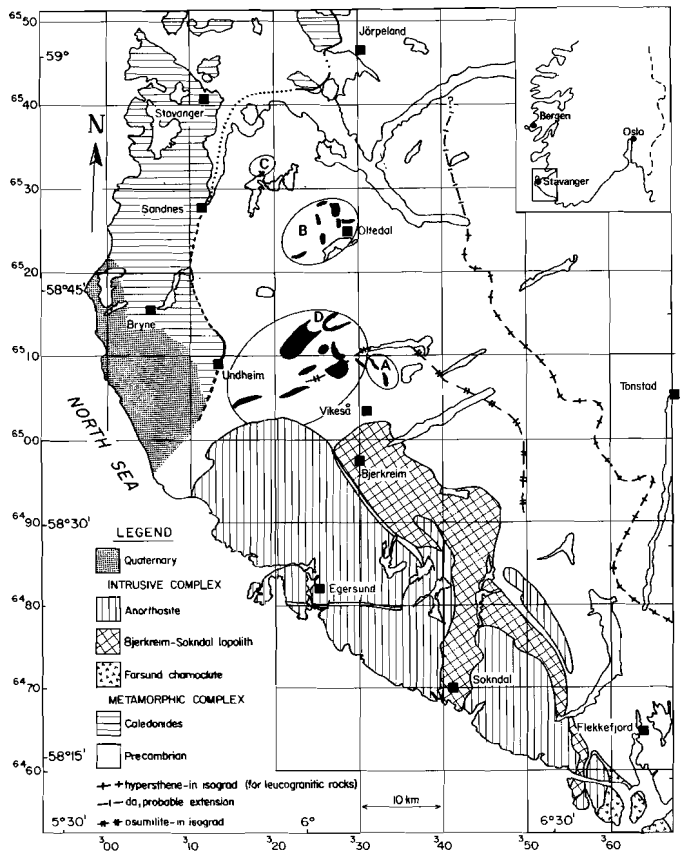

Fig. 2.1: Geologic sketch-map of southwest Norway. Outcrops of the Faurefjell Formation, at locations A, B, C and D, are indicated in black (after Bol and Jansen 1989).

near the lopolith at pressures of maximally 4 to 5 kbar (Jansen et al. 1985). The **M3** phase of metamorphism is correlated with granitic injections during the post-**M2** cooling history. **M3** minerals reveal ages between 970 and 870 Ma (Maijer et al. 1981; Maijer and Padget 1987). The **M4** phase resulted from incipient burial metamorphism of early Paleozoic age and of very low-grade metamorphism assigned to Caledonian overthrusting (Verschure et al. 1980; Sauter et al. 1983).

The Faurefjell Formation consists of metasedimentary rocks, most notably marbles and calc-silicate rocks with intercalations of metavolcanics. The major

outcrops, denoted A, B, C, and D, are indicated in **Figure 2.1**. Details of the locations and related rock types are given by Sauter (1983).

Analyses of phlogopites in siliceous dolomites of the Faurefjell Formation revealed high to very high BaO contents. The BaO contents of phlogopites in sample C480 are the highest described to date for natural phlogopite (cf. Wendlandt 1977; Mansker et al. 1979; Gaspar and Wyllie 1982; Solie and Su 1987). The TiO_2 contents are also high and show a strong positive correlation with BaO contents. The purpose of this paper is to discuss the mineral chemistry of the Rogaland phlogopites and to evaluate appropriate substitution schemes that involve Ba and Ti.

2.2 PETROLOGY AND PETROGRAPHY

Phlogopite is a common constituent in the forsterite- and diopside-bearing marbles. The phlogopites can be subdivided into two groups on the basis of their BaO content and paragenesis. One group is relatively low in BaO (0 to 4.8 wt%) and occurs in diopside-bearing rocks and forsterite-bearing marbles. In the diopside-marbles the phlogopite is associated with diopside + calcite ± dolomite, and in the diopside-bearing calc-silicate rocks, it is associated with diopside ± calcite ± spinel. In forsterite-marbles it is accompanied by forsterite, calcite, dolomite ± diopside ± spinel and occasionally by barite. The other group, with high BaO contents (around 20 wt%), occurs exclusively in forsterite-bearing marbles.

Commonly, the low-Ba phlogopites are developed as subhedral platelets with a maximum grain size of about 2 mm (**Fig. 2.2**) and they exhibit no preferred orientation. In spinel- and forsterite-bearing marbles the low-Ba phlogopite is entirely enclosed by forsterite crystals and some high-Ba phlogopites are also present as large discrete grains (**Fig. 2.3**). In forsterite + spinel marble C480 the high-Ba phlogopite has a dark brown pleochroic colour (O = red-brown, E = light-brown), in contrast to the very pale-brown pleochroic colors regularly observed in phlogopites of siliceous dolomites. Especially in samples from retrograde metamorphic exposures in location B, chloritization of the phlogopites is evident and occurred during the Caledonian low-grade metamorphic overprint (Sauter et al. 1983).

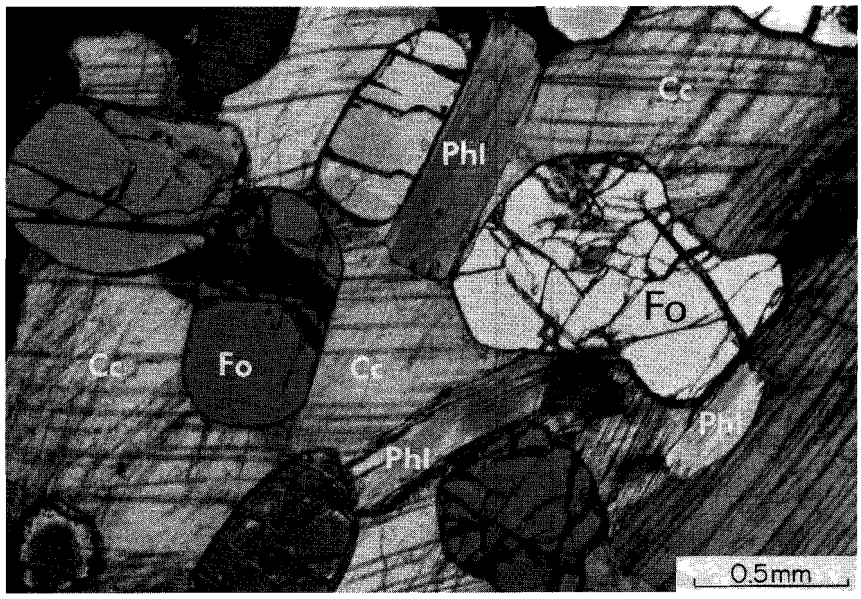

Fig. 2.2: Forsterite-phlogopite marble. Photomicrograph, A122, crossed nicols. Fo = forsterite; Phl = phlogopite; Cc = calcite; Sp = spinel.

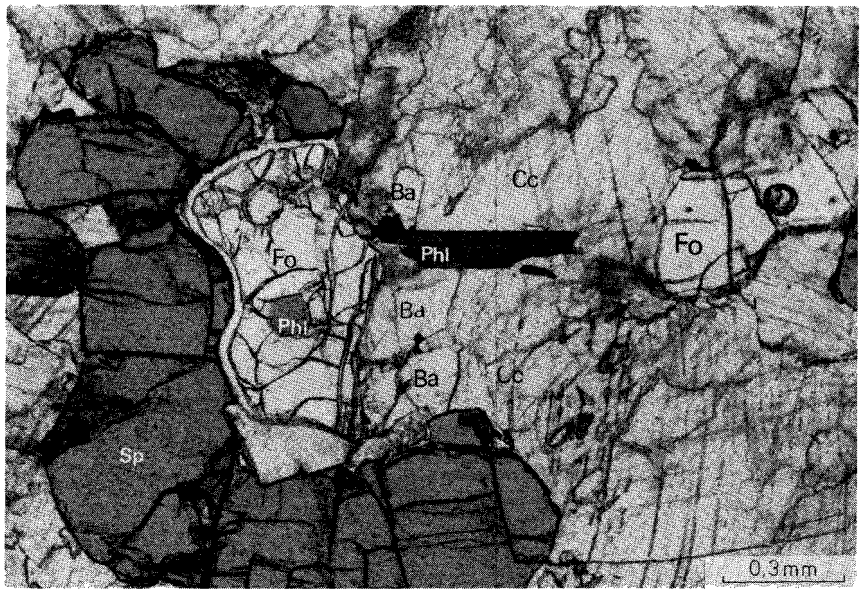

Fig. 2.3: Phlogopite as small inclusion in forsterite and as large grain of Ba-rich phlogopite (center). The Ba-rich phlogopite is in contact with barite (= Ba). Photomicrograph, C480, plane-polarized light.

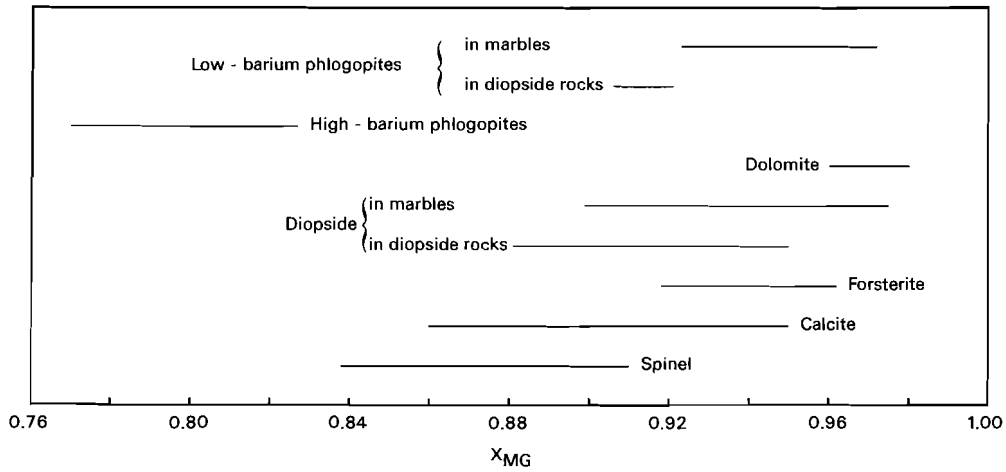

Fig. 2.4: Range of X_{Mg} (=Mg/Mg+Mn+Fe)of minerals in marbles and in diopside-bearing rocks. X_{Mg} calculated with total Fe as Fe^{2+}, except for spinel, which was corrected for magnetite.

2.3 ANALYTICAL METHODS

Electron-microprobe analyses of the phlogopites are given in **Table 2.1**. Most analyses were performed with a Cambridge Scientific Instruments Geoscan and a Microscan M-9 at the Free University of Amsterdam using wave-length dispersive techniques. Operating conditions were 20-kV accelerating voltage and 25-nA beam current. Various natural and synthetic oxide and silicate minerals were used as standards. Data were corrected with the M-9 correction program (Z-A-F). Some analyses were done on a TPD electron microprobe at the Institute for Earth Sciences of the University of Utrecht also using wave-length dispersive techniques. Operating conditions were 15-kV and 40-nA sample current for a periclase standard. Data were corrected with the Springer correction program (Z-A-F). Interference of Ba and Ti peaks during the measurements proved to be negligible.

TABLE 1. Representative microprobe analyses of the Rogaland phlogopites

Sample:	C165		BE24		C480		Q75		A164	
No.:	B032		B111		B021		B043		B135	
SiO_2	40.31		37.25		36.37		40.74		38.21	
Al_2O_3	14.05		18.57		17.06		13.92		16.87	
TiO_2	0.41		0.64		2.70		0.49		0.50	
FeO_T	2.61		1.36		3.18		1.32		2.46	
MnO	bd		0.06		bd		bd		0.05	
MgO	26.67		24.87		22.40		26.31		24.69	
BaO	0.05		3.83		1.44		0.13		1.68	
Na_2O	0.16		0.12		0.12		0.24		0.06	
K_2O	10.50		9.43		10.25		10.84		9.98	
F	0.9		0.5		na		3.1		0.5	
Total*	95.28		96.42		93.52		95.78		94.79	
					Formula proportions**					
Si	5.726	5.694	5.315	5.328	5.326	5.385	5.807	5.830	5.495	5.497
$^{[4]}Al$	2.274	2.306	2.685	2.672	2.674	2.615	2.193	2.170	2.505	2.503
$^{[6]}Al$	0.079	0.034	0.439	0.459	0.271	0.363	0.146	0.178	0.355	0.357
Ti	0.044	0.044	0.069	0.069	0.297	0.301	0.053	0.053	0.054	0.054
Fe	0.310	0.308	0.162	0.163	0.389	0.394	0.157	0.158	0.296	0.269
Mn			0.007	0.007			0.006	0.006		
Mg	5.646	5.614	5.289	5.302	4.889	4.943	5.589	5.611	5.292	5.291
Σ	14.079	14.000	13.966	14.000	13.846	14.000	13.951	14.000	13.997	14.000
Ba	0.003	0.003	0.214	0.215	0.083	0.084	0.007	0.007	0.095	0.095
Na	0.044	0.044	0.033	0.033	0.034	0.034	0.066	0.067	0.017	0.017
K	1.903	1.892	1.717	1.721	1.915	1.936	1.971	1.979	1.831	1.831
Σ	1.950	1.937	1.964	1.969	2.032	2.054	1.055	2.053	1.943	1.942
+Charge†		43.756		44.109		44.487		44.174		43.992

TABLE 1.—*Continued*

Sample	C480		C480		C480		C480		C480	
No.	B502		B512		B036		B046		B056	
SiO_2	27.88		27.55		24.31		24.34		24.31	
Al_2O_3	17.74		18.33		18.05		18.87		18.85	
TiO_2	10.32		11.89		13.94		13.16		13.00	
FeO_T	5.44		5.96		6.33		6.07		6.21	
MnO	bd		bd		bd		bd		bd	
MgO	14.60		14.17		12.47		11.98		12.35	
BaO	17.79		19.61		21.25		24.67		23.94	
Na_2O	0.37		0.37		0.34		0.58		0.39	
K_2O	3.65		3.06		1.24		1.34		1.57	
F	bd		bd		bd		bd		bd	
Total*	97.79		100.94		97.93		100.96		100.62	
					Formula proportions					
Si	4.425	4.710	4.284	4.581	3.967	4.257	3.942	4.291	3.936	4.259
$^{[4]}Al$	3.319	3.290	3.360	3.419	3.472	3.743	3.603	3.709	3.598	3.741
$^{[6]}Al$		0.243		0.179		0.017		0.213		0.152
Ti	1.232	1.311	1.390	1.487	1.711	1.836	1.603	1.745	1.583	1.713
Fe	0.722	0.769	0.775	0.829	0.864	0.927	0.822	0.895	0.841	0.910
Mn										
Mg	3.453	3.676	3.283	3.511	3.032	3.254	2.892	3.148	2.980	3.225
Σ	13.151	14.000	13.092	14.000	13.046	14.000	12.899	14.000	12.938	14.000
Ba	1.106	1.178	1.195	1.278	1.359	1.458	1.562	1.701	1.519	1.643
Na	0.114	0.121	0.112	0.119	0.108	0.115	0.182	0.198	0.122	0.132
K	0.739	0.787	0.607	0.649	0.258	0.277	0.277	0.301	0.324	0.351
Σ	1.959	2.086	1.914	2.046	1.725	1.850	2.021	2.200	1.965	2.126
+Charge†		46.840		47.051		47.220		47.894		47.608

Note: Samples: Low-Ba phlogopites—C165, diopside- and phlogopite-bearing rock (location C); BE24, forsterite- and spinel-bearing marble (location A); C480, forsterite- and spinel-bearing marble (location A); Q75, forsterite-bearing marble (location B); A164, forsterite-bearing marble (location A). High-Ba phlogopites—C480, Forsterite- and spinel-bearing marble (location A). bd = below detection limit. na = not analyzed.

* Less oxygen ≡ F.

** Based on 22 oxygens (1st column) and Σcations − (Na + K + Ba) = 14 (2nd column of each pair).

† Calculated positive charge per formula unit based on the 14-cation normalization procedure.

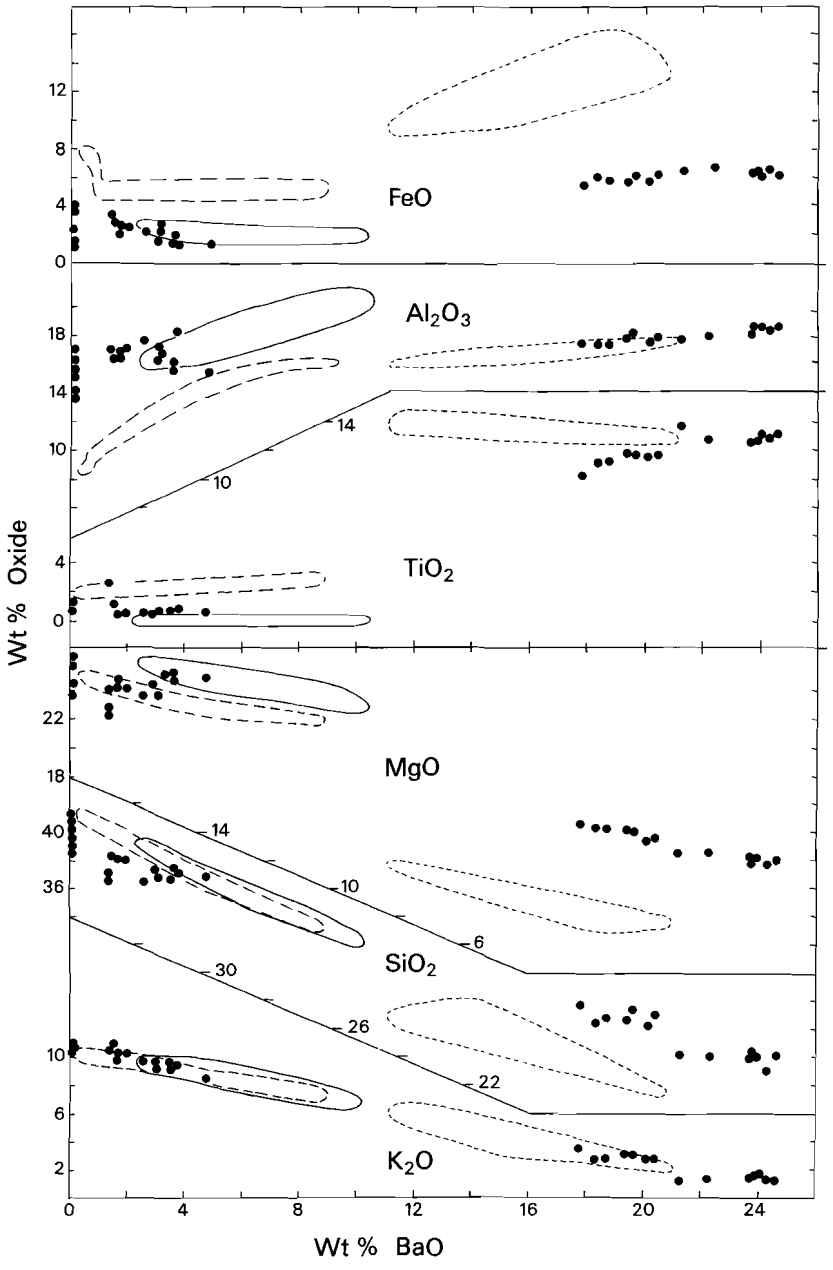

Fig. 2.5: Chemical variation in phlogopites in wt% oxides. Dots: Rogaland phlogopites, this work; Stippled line: Mansker et al. (1979); Solid line: Gaspar and Wyllie (1982); Broken line: Wendlandt (1977).

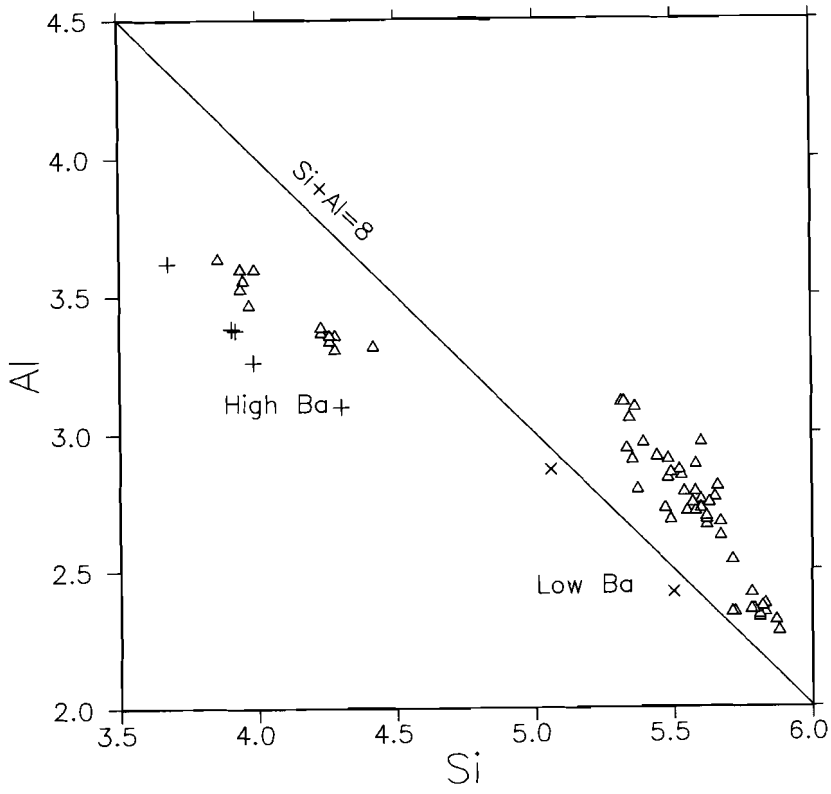

Fig. 2.6: Atoms of Si *vs.* Al diagram for phlogopites. Triangles: Rogaland phlogopites of this work; Plus signs: data of Mansker et al.; Crosses: data of Wendlandt. All formula proportions are based on the 22 oxygen normalization procedure.

2.4 MINERAL CHEMISTRY

The X_{MG} of the phlogopites varies between 0.95 and 0.91 in diopside-bearing rocks, from 0.97 to 0.93 in forsterite-bearing marbles and between 0.83 and 0.76 for the high Ba-phlogopites in sample C480 (**Fig. 2.4**). The X_{Mg} is not corrected for trivalent Fe. Wet-chemical analyses for Fe^{2+} of separated fractions of phlogopites yield Fe^{2+}/Fe^{3+}-ratios of approximately 4, use of which would increase the X_{MG}-ratio to only slightly higher values.

The most remarkable feature of the phlogopites is the variation in BaO-content. Phlogopites in barite-bearing marbles contain several percent BaO. The BaO-content

of the low-Ba phlogopites varies from 0 to 4.8 wt%. In the discrete coarse phlogopites, which are not enclosed in forsterite, the BaO contents range from 17.8 to 24.6 wt%. These phlogopites also have significantly low K_2O and SiO_2 contents, 1.2 and 23.3 wt% respectively. The TiO_2-content of the phlogopites generally is low in diopside-bearing rocks (0.4 to 0.8 wt%), but low-Ba phlogopites enclosed in forsterite crystals in the spinel- and forsterite-bearing marbles contain up to 2.7 wt% TiO_2 (e.g., sample C480, spot B021). The high-Ba phlogopites have extremely high TiO_2 contents, up to 13.9 wt%. Low-Ba phlogopites contain up to 18.6 wt% Al_2O_3 whereas high-Ba phlogopites are uniformly high in Al_2O_3, the contents of which range from 17.7 to 18.9 wt%. In all micas Na_2O and MnO are minor components and CaO was not detected.

F concentrations range up to 3.3 wt% in low-Ba phlogopite of the forsterite-bearing marbles, corresponding to a F/(F+OH) ratio (X_F) of 0.37 assuming that the rest of the hydroxyl-sites is occupied by OH. This can be compared with an X_F of 0.42 to 0.56 for coexisting clinohumite. The F contents in the high Ba-phlogopites are below the detection limit, and Cl was not detected in any mica.

The oxide totals of the high-Ba phlogopites generally are very high. In combination with the low F content this is believed to reflect a low OH, and therefore presumably a high oxygen, occupancy of the hydroxyl sites.

A detailed description of the accompanying main mineral phases is available upon request.

2.5 PETROGENESIS

The formation of phlogopite in impure siliceous dolomites usually takes place by the reaction of dolomite with alkali feldspar (Rice 1977). The equilibrium reaction commences at relatively low grade metamorphic conditions. Unfortunately, in the marbles of Rogaland no specific reaction can be described for the phlogopite production. The rocks contain the assemblage (Phlog+Cc±Fo±Dol)which is stable above 700°C at P_{total} of about 5 kbar (Sauter 1983). The coexistence of Fo+Cc+Spis an additional indication of high-temperature metamorphism and is consistent with the inferred regional metamorphic gradient of the **M2** phase. In the spinel- and forsterite-bearing marble C480, the low-Ba phlogopites are enclosed in forsterite, whereas the high-Ba phlogopites are developed as large separate grains, pointing to a later growth stage. The low-Ba phlogopites are apparently relics that survived the

prograde spinel-forming reaction at high temperature, as proposed by Glassley (1975) for analogous environments:

$$6\text{Phlog} + 7\text{Cc} \;<\!\!-\!\!>\; 7\text{Di} + 4\text{Fo} + 3\text{Sp} + 7\text{CO}_2 + 6\text{H}_2\text{O} + 3\text{K}_2\text{O} \qquad (1)$$

The BaO-content of the Rogaland marbles is fairly constant at all investigated locations and varies between 0.2 and 0.8 wt% as it is reflected by the occurrence of accessory barite. Ba mobility is traditionally considered to be negligible during regional metamorphism (Barbey and Cuney 1982), and an authigenic provenance for most of the barite is favored. **M2** pegmatites at location B contain BaO up to 6.4 wt%. Preliminary results of a chemical study along profiles across a pegmatite-marble contact reveal that local enrichment of Ba in the pegmatite margin is related to progressive desilification. On the other hand, Ti seems to have been introduced to the marbles as indicated by volume-composition relations in the vicinity of the marble-pegmatite contact.

The high-Ba phlogopites have, to date, only been observed in the southernmost part of area A which is the closest occurrence of marble to the lopolith (**Fig. 2.1**). Peak metamorphic temperatures may have approached 900°C, suggesting that relatively high temperature may be an important factor in the formation of these micas.

2.6 DISCUSSION

The chemical composition of 33 selected phlogopites from Rogaland, SW Norway, is plotted in **Figure 2.5**. Chemical compositions of Ba-bearing phlogopites reported by Wendlandt (1977), Mansker et al. (1979) and Gaspar and Wyllie (1982) are shown for comparison. Comparing the high-Ba phlogopites to the low-Ba phlogopites described in this study, K_2O, SiO_2 and MgO decrease with increasing BaO, whereas TiO_2 and FeO increase. Compositions of the high-Ba phlogopites show minor scatter about definite trends. The data for the low-Ba phlogopites show much more scatter than those for the high-Ba phlogopites and seem to define different trends (**Fig. 2.5**) for FeO and for MgO.

The composition of the low-Ba phlogopites is similar to that in other high-grade impure siliceous dolomite occurrences investigated by Glassley (1975), Rice (1977),

Kretz (1980) and Bucher-Nurminen (1982). Ba-bearing phlogopites from peridotite and turjaite (Wendlandt 1977) have compositions close to those of the low-Ba phlogopites from Rogaland with respect to K_2O, SiO_2 and MgO, although the Al_2O_3 contents are somewhat higher, and the FeO and TiO_2 contents are lower. The Ba-bearing phlogopite from the Jacupiranga carbonatite (Gaspar and Wyllie 1982) has a slightly lower TiO_2-content. Brown Ba-rich micas from the Alaska Range (not plotted) are much lower in TiO_2 (Solie and Su 1987). The high-Ba phlogopites have a composition resembling the high Ba-biotites from Hawaiian nephelinites (Mansker et al. 1979) with respect to SiO_2, Al_2O_3, TiO_2 and K_2O, but have higher Mg/Fe-ratios.

2.6.1 Substitution schemes for Ba-bearing phlogopite

For complex micas it is generally impossible to derive a unique set exchange vectors for components (Thompson 1982) that correspond to crystallochemically valid substitutions. Even if Fe_2O_3 and H_2O are known, several equivalent sets of exchange components can be adopted to describe a single phase (Hewitt and Abrecht 1986). Therefore, some knowledge of inter-atomic correlations is necessary to identify set(s) of exchange components and hence valid substitutions.

The negative correlation between K and Ba (cf., **Fig. 2.5**) reflects Ba substitution on the interlayer site of the phlogopites. In contrast to A-site substitution of the univalent cations Rb^+, Cs^+ (Hazen and Wones 1972) and NH_4^+ (Bos et al. 1988), the charge balance for Ba^{2+} is maintained by simultaneous substitution of Al^{3+} for Si^{4+} on the tetrahedral site, according to the scheme proposed by Wendlandt (1977):

$$K^+(A) + Si^{4+}(IV) <--> Ba^{2+}(A) + Al^{3+}(IV) \quad (2).$$

In the Rogaland phlogopites, the amount of $Al^{3+}(IV)$ is more than sufficient to achieve charge balance for Ba^{2+} (Ba < (Al(IV)-2)) in all of the phlogopites (see **Table 2.1**). However, the high-Ba phlogopites show an apparent deficiency in tetrahedral cations ($Si^{4+}(IV) + Al^{3+}(IV) < 8$ per 22 oxygens), whereas the low-Ba phlogopites do not (**Table 2.1, Fig. 2.6**), suggesting that the two groups obey distinct substitution schemes. Ti-substitutions will be discussed only for the high-Ba phlogopites.

It is suggested that Ti contents of biotite commonly increases with increasing metamorphic grade (Kwak 1968), and this is supported by experimental results (Robert 1976). The high-Ba, high-Ti phlogopites of Rogaland have probably indeed crystallized at high-grade conditions. However, Ti-contents far exceed the 0.7 atoms Ti per 20 oxygens that was found experimentally at 1000°C and 1 kbar by Robert (1976). The presence of Fe^{2+} seems to enhance Ti-substitution (Czamanske and Wones 1973), but this effect must be negligible for the Rogaland phlogopites given their high Mg/Fe ratios. Assuming that pressure does not have a large effect on Ti solubility the presence of other cations must therefore enhance Ti contents.

Substitution schemes that involve titanium were reviewed by Dymek (1983):

Ti-Tschermak's: $R^{2+}(VI) + 2Si^{4+}(IV) <--> Ti^{4+}(VI) + 2Al^{3+}(IV)$ (3)

Ti-vacancy: $2R^{2+}(VI) <--> Ti^{4+}(VI) + [\,](VI)$ (4)

Ti-oxy: $R^{2+}(VI) + 2OH^{-} <--> Ti^{4+}(VI) + 2O^{2-} + H_2$ (5)

Additionally, substitutions involving tetrahedral Ti might be considered. The possibility of Ti(IV) in silicates is controversial (Hartman 1969). Synthetic high-Ti OH-phlogopites do not contain tetrahedral Ti (Robert 1976), whereas Kovalenko et al. (1968) report Ti(IV) in synthetic F-phlogopites. Farmer and Boettcher (1981) invoked the occurrence of tetrahedral Ti as well as tetrahedral Fe^{3+} in phlogopites in South African kimberlites. The high Ti content of the high-Ba biotites of Mansker et al. (1979) and Wendlandt (1977) and in those from Rogaland together with the low tetrahedral cation sums ($Si + Al < 8$ per 22 oxygens, **Fig. 2.6**) seems to support the existence of tetrahedral Ti. In this respect, it is interesting to note that all of these micas have formed in silica- and alumina-undersaturated environments. Crystallochemically, however, tetrahedral Ti in high-Ba biotites is unlikely. The electrostatic repulsion between Ba^{2+} and Ti^{4+} increases the lattice energy and octahedral positions for Ti are strongly favored over the tetrahedral positions, since the latter are more closer to the interlayer sites. Therefore, vacancy- or oxy-substitutions must be involved. Formula proportions normalized to a fixed anion-frame are not affected by vacancies (Dymek 1983). Low cation-sums in the first column of the formula-proportions in **Table 2.1** may be attributed to the Ti-vacancy

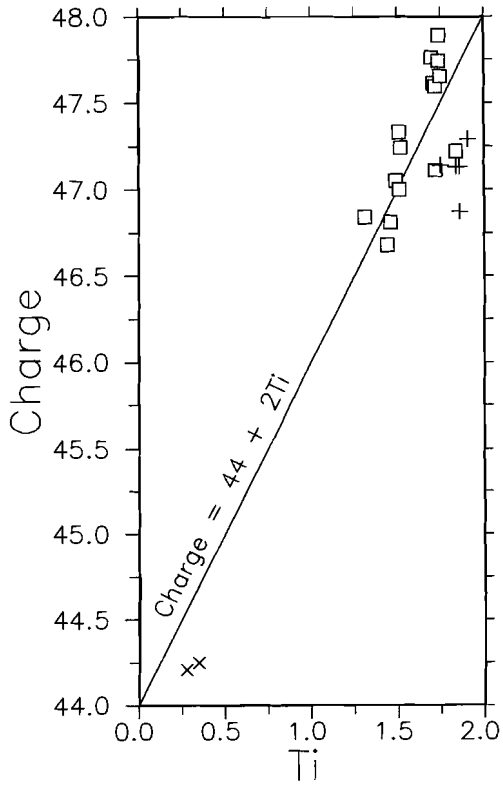

Fig. 2.7: Atoms of Ti *vs.* total cation charge for the high-Ba phlogopites from Rogaland (squares), Mansker et al. (plusses) and Wendlandt (crosses). All formula proportions based on the 14 cation normalization procedure.

substitution (4). Normalization procedures that assume complete occupancy of the tetrahedral and octahedral sites are indifferent to variations in H_2O content (second column of the formula proportions in **Table 2.1**), and they may be used to calculate the total cation charge, which ideally equals 44 assuming an anion-frame of 20 oxygens and 4 (OH + F + Cl). Charge calculations considering all iron as Fe^{2+} yield minimum values for the total charge (**Table 2.1**). The high Ba-phlogopites have a large excess charge that correlates well with 2Ti (**Fig. 2.7**) which points to substitutions (4) and (5) and rules out (3) as a dominant substitution.

A plot of Ti versus (Fe + Mg) per 22 oxygens (**Fig. 2.8**) yields a trend with a slope between -2 and -1 that is not conclusive evidence in favor of either substitution (4) or (5). When normalized to 14 cations the data plot close to the line predicted by (5), but some combination of (4) and (5) is probably necessary to explain the substitution of Ti. The high oxide-totals of the high Ba-phlogopites and the extremely dry granulite-facies conditions of formation supports the concept of substitution schemes involving dehydrogenation reactions. Furthermore, if a dominant role for the Ti-oxy substitution is accepted there is no need to invoke tetrahedral Ti, since on the basis of 14 cations (Si + Al) exceeds 8 for all phlogopites.

The strong covariation of Ti and Ba in the Rogaland phlogopites suggests that

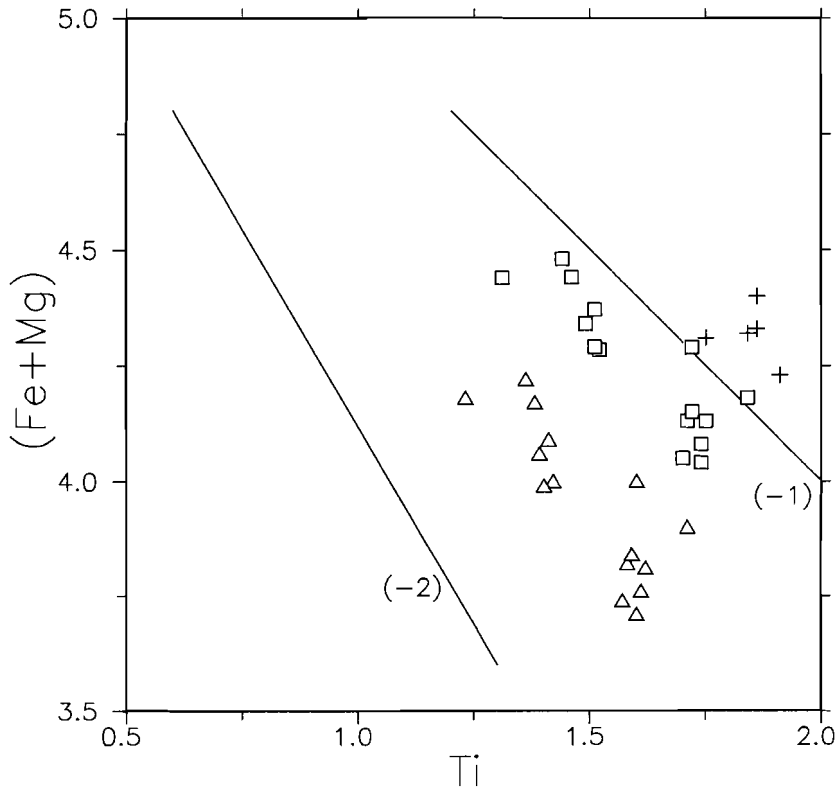

Fig. 2.8: Atoms Ti *vs.* (Fe + Mg) for the high-Ba phlogopites. Lines have inclinations -1 and -2 and correspond to Ti-oxy and Ti-vacancy substitutions respectively (Squares: based on the 14-cation normalization procedure; Triangles: based on the 22-oxygen normalization procedure). Plus signs represent data from Mansker et al. normalized on 14 cations.

combinations of substitutions (2) with Ti-oxy substitution (5) and, to a lesser extent, Ti-vacancy substitution (4) play a significant role. Adding (2) and (5) yields an overall substitution,

$$K^{+}(A) + Si^{4+}(IV) + R^{2+}(VI) + 2OH^{-} <--> Ba^{2+}(A) + Al^{3+}(IV) + Ti^{4+}(VI) + 2O^{2-} + H_2 \quad (6)$$

which ultimately leads to an anhydrous Ba-Ti end-member $BaMg_2TiSi_2Al_2O_{12}$.

The very small differences between Ahrens ionic radii of Ba^{2+}(1.33Å) and

K^+(1.34Å) on the one hand and Ti^{4+}(0.66Å) and Mg^{2+}(0.68Å) on the other do not indicate the necessity of an exact 1:1 covariation of Ba and Ti. The composition of the phlogopites is probably controlled by localized buffering of Ba and Ti activities in fluids in grain-boundary films and in nearby minerals, and no unique overall substitution scheme is thought to control the chemical variation within the high-Ba phlogopites.

Least squares mixing calculations are performed in order to recast the cation formula proportions of the high-Ba phlogopites into linear combinations of $KMg_3Si_3AlO_{10}(OH)_2$ (phlogopite), $KMg_2AlSi_2Al_2O_{10}(OH)_2$ ("eastonite"), $KMgTiSi_3AlO_{10}(OH)_2$ (Ti-vacancy) and $BaMg_2TiSi_2Al_2O_{12}$ (6). All iron was assumed to be Fe^{2+} and was added to Mg and all Na was added to K. Ideally, the squared sum of residuals (SSR) should be less than 1.0% since the analytical error is believed to be of this order of magnitude. In **Table 2.2**, results of the mixing calculations are given. SSR-values exceed 1.0 in two cases owing to neglect of other minor substitution components, such as anandite ($BaFe_3Si_3FeO_{10}(OH)S$) and kinoshitalite ($BaMg_3Si_2Al_2O_{10}(OH)_2$). The proposed anhydrous Ba-Ti end-member constitutes up to about 81 mol% in the phlogopite solid-solution of analysis B056. Using the end-member proportions in **Table 2.2** the inferred structural formula for B056 is:

TABLE 2. Substitution of $BaMg_2TiSi_2Al_2O_{12}$ in the high-Ba phlogopites

Spot:	B502	B512	B036	B046	B056
Phlogopite	26.61	20.80	9.79	5.97	8.45
$BaMg_2TiSi_2Al_2O_{12}$	57.94	63.50	74.85	82.95	81.14
"Eastonite"	9.20	8.19	6.86	6.45	6.93
Ti-vacancy	6.26	7.51	8.50	4.63	3.49
SSR	0.48	0.07	1.90	1.64	0.41

$$(K_{0.14}Na_{0.05}Ba_{0.81})(Mg_{1.61}Fe_{0.45}Ti_{0.84}Al_{0.06}[\ ]_{0.03})Si_{2.13}Al_{1.88}O_{10}(OH_{0.38}O_{1.62})$$

Mansker et al. (1979) suggest the following substitution scheme as a 1:1:1 combination of (2), (3) and (4):

$$K^+(A) + 3R^{2+}(VI) + 3Si^{4+}(IV) <--> Ba^{2+}(A) + 2Ti^{4+}(VI) + [\ ](VI) + 3Al^{3+}(IV) \quad (7).$$

However, the Ti-Tschermak's substitution (3) is not strictly valid for the Hawaiian biotites (**Fig. 2.7**). Both Mansker et al (1979) and Wendlandt (1977) report tetrahedral deficiencies (**Fig. 2.6**). Mansker et al. assumed contributions of large amounts of Fe^{3+}(IV); Wendlandt assigned part of the Ti content to the tetrahedral sites. It is notable that these data may be explained by substitution schemes involving

Ti-oxy contributions (**Figs. 2.7** and **2.8**), without invoking the existence of Ti^{4+}(IV).

Detailed investigations of the structure and physical properties of anhydrous Ba-Ti phlogopite end-member are in progress.

2.7 CONCLUSIONS

1) At least 75% of the K on the interlayer sites of phlogopites from Rogaland is replaced by Ba.

2) Analytical data for Ba-micas are best explained by assuming various amounts of Ti-oxy substitution, without invoking the presence of Ti on tetrahedral sites.

3) $BaMg_2TiSi_2Al_2O_{12}$ constitutes about 80 mol% of the natural biotite solid solutions from Rogaland.

4) The Ti content of the high-Ba phlogopites has been influenced by parameters other than temperature or Fe-activity. The actual parameters cannot be identified from existing data.

5) The approximately 1:1 Ba-Ti coordination in the Rogaland high-Ba phlogopites is not crystal-chemically controlled but reflects local availability Ba and Ti.

2.8 ACKNOWLEDGEMENTS

Profs. P. Hartman, W.E. Glassley, R.D. Schuiling, A. Senior, M. Barton and especially D.A. Hewitt are acknowledged for critical comments on the text. Drs. R.J.P. Poorter and M. van Bergen are thanked for their assistance with the microprobe analyses at the Institute for Earth Sciences of the University of Utrecht, and C. Kieft and W.J. Lustenhouwer for their assistance with the microprobe analyses at the Free University of Amsterdam. This investigation was supported financially by N.W.O, with A.W.O.N. grants 18-21-06 and 751- 353-016. Microprobe facilities were provided by W.A.C.O.M., subsidized by N.W.O.

Barbey P, Cuney M (1982) K, Rb, Sr, Ba, and Th geochemistry of the Lapland granulites (Fennoscandia). LILE fractionation controlling factors. Contrib Mineral Petrol 81:304-316

Bol LCGM, Jansen JBH (1989) Proterozoic metasediments from the deep crust of Rogaland, SW Norway: Chemistry of metabasites and granofelses (ext. abstr.). In: D Bridgwater (Ed) Fluid movements- element transport and the composition of the deep crust, NATO ASI Series C vol 281 Reidel, Dordrecht, 111-113 pp

Bos A, Duit W, van der Eerden A, Jansen JBH (1988) Nitrogen storage in biotite: An Experimental study of the ammonium and potassium partitioning between 1M-phlogopite and vapor at 1 kb. Geochim Cosmochim Acta 52:1275-1283

Bucher-Nurminen K (1982) Mechanism of mineral reactions inferred from textures of impure dolomitic marbles from East Greenland. J Petrol 23:325-343

Czamanske GK, Wones DR (1973) Oxidation during magmatic differentiation, Finnmarka Complex, Oslo area, Norway - Part 2: The mafic silicates. J Petrol 14:349-380

Duchesne JC, Maquil R, Demaiffe D (1985) The Rogaland anorthosites: Facts and speculations. In: AC Tobi and JLR Touret (Eds) The Deep Proterozoic Crust in the North Atlantic Provinces. NATO ASI Series C Vol 158 Reidel, Dordrecht, 411-434 pp

Dymek RF (1983) Titanium, aluminium and interlayer cation substitutions in biotite from high-grade gneisses, West Greenland. Am Mineral 68:880-899

Farmer GL, Boettcher AL (1981) Petrologic and crystal-chemical significance of some deep-seated phlogopites. Am Mineral 66:1154-1163

Gaspar JC, Wyllie PJ (1982) Barium phlogopite from the Jacupiranga carbonatite, Brazil. Am Mineral 67:997-1000

Glassley WE (1975) High grade regional metamorphism of some carbonate bodies: significance for the orthopyroxene isograd. Am J Sci 275:1133-1163

Hartman P (1969) Can Ti^{4+} replace Si^{4+} in silicates? Mineral Mag 37:366-369

Hazen RM, Wones DR (1972) The effect of cation substitutions on the physical properties of trioctahedral micas. Am Mineral 57:103-129

Hermans GAEM, Tobi AC, Poorter RPE, Maijer C (1975) The high-grade metamorphic Precambrian of the Sirdal-Ørsdal area, Rogaland/Vest-Agder, South-west Norway. Norg Geol Unders 318:51-74

Hewitt DA, Abrecht J (1986) Limitations on the interpretation of biotite substitutions from chemical analyses of natural samples. Am Mineral 71:1126-1128

Jansen JBH, Maijer C (1980) Mineral relations in metapelites of SW Norway.

Colloquium high-grade metamorphic Precambrian and its intrusive masses, Institute for Earth Sciences, State University of Utrecht, 8-9 May 1980

Jansen JBH, Blok RJP, Bos A, Scheelings M (1985) Geothermometry and geobarometry in Rogaland and preliminary results from the Bamble area, South Norway. In: AC Tobi, JLR Touret (Eds) The Deep Proterozoic Crust in the North Atlantic Provinces. NATO ASI Series C Vol 158, Reidel, Dordrecht 499-516 pp

Kars H, Jansen JBH, Tobi AC, Poorter RPE (1980) The metapelitic rocks of the polymetamorphic Precambrian of Rogaland, SW Norway. Part II. Mineral relations between cordierite, hercynite and magnetite within the osumilite-in isograd. Contrib Mineral Petrol 74:235-244

Kovalenko NI, Kashayev AA, Znamenskiy YeB, Zhuravleva RM (1968) Entry of titanium into micas (experimental studies). Geochemistry International 5:1099-1107

Kretz R (1980) Occurrence, mineral chemistry and metamorphism of Precambrian carbonate rocks in a portion of the Grenville province. J Petrol 21:573-620

Kwak TAP (1968) Ti in biotite and muscovite as an indication of metamorphic grade in almandine amphibolite facies rocks from Sudbury, Ontario. Geochim Cosmochim Acta 32:1222-1229

Maijer C, Padget P (Eds) (1987) The geology of southernmost Norway: an excursion guide. Nor Geol Unders Spec Publ 1, 109 pp

Maijer C, Jansen JBH, Hebeda EH, Verschure RH, Andriessen PAM (1981) Osumilite, an approximately 970 Ma old high- temperature index mineral of the granulite facies metamorphism in Rogaland, SW Norway. Geol Mijnb 60:267-272

Mansker WL, Ewing RC, Keil K (1979) Barian-titanian biotites in nephelinites from Oahu, Hawaii. Am Mineral 64:156-159

Rice JM (1977) Progressive metamorphism of impure dolomitic limestone in the Marysvill Aureole, Montana. Am J Sci 277:1-24

Robert JL (1976) Titanium solubility in synthetic phlogopite solid solutions. Chem Geol 17:213-227

Sauter PCC (1983) Metamorphism of siliceous dolomites in the high-grade Precambrian of Rogaland, SW Norway. PhD Thesis, Geol Ultraiectina 32, 143 pp

Sauter PCC, Hermans GAEM, Jansen JBH, Maijer C, Spits P, Wegelin A (1983) Polyphase Caledonian metamorphism in the Precambrian basement of Rogaland/Vest-Agder, South-west Norway. Norg Geol Unders 380:7-22

Solie DN, Su SC (1987) An occurrence of Ba-rich micas from the Alaska Range. Am Mineral 72:995-999

Thompson JB, Jr (1982) Composition space: An algebraic and geometric approach. MSA Reviews in Mineralogy 10:1-32

Tobi AC, Hermans GAEM, Maijer C, Jansen JBH (1985) Metamorphic zoning in the high-grade proterozoic of Rogaland-Vest Agder, SW Norway. In: AC Tobi, JLR Touret (Eds) The Deep Proterozoic Crust in the North Atlantic Provinces NATO ASI Series C Vol 158 Reidel, Dordrecht, 477-497 pp

Verschure RH (1985) Geochronological framework for the late-Proterozoic evolution of the Baltic shield in South Scandinavia. In: AC Tobi, JLR Touret (Eds) The Deep Proterozoic Crust in the North Atlantic Provinces. NATO ASI Series C, Vol 158 Reidel, Dordrecht 381-410 pp

Verschure RH, Andriessen PAM, Boelrijk NAIM, Hebeda EH, Maijer C, Priem HNA, Verdurmen EATh (1980) On the thermal stability of Rb-Sr and K-AR biotite systems: Evidence from coexisting Sveconorvegian (ca 870 Ma) and Caledonian (ca 400 Ma) biotites from SW Norway. Contrib Mineral Petrol 74:245-252

Wendlandt RF (1977) Barium-phlogopite from Haystack Butte, Highwood Mountains, Montana. Carnegie Institution of Washington Year Book 76:534-539

Wielens JBW, Andriessen PAM, Boelrijk NAIM, Hebeda EH, Priem HNA, Verdurmen EATh, Verschure RH (1981) Isotope geochronology in the high-grade metamorphic Precambrian of Southwestern Norway: New data and reinterpretations. Norg Geol Unders, 359:1-30

CHAPTER III: PREMETAMORPHIC LATERITISATION IN PROTEROZOIC METABASITES OF ROGALAND, SW NORWAY

3.0 ABSTRACT

Heterogeneous layers of granulite facies metamorphic basites of the Proterozoic supracrustal Faurefjell Formation in Rogaland, S.W. Norway, display an extreme chemical variation. Within a single layer the bulk chemical composition gradually changes from approximately basaltic in basic granulites to alumina-iron-rich in granofelses. Component-ratios and composition-volume relations indicate open-system chemical reactions mainly involving the extraction of silica. Apparent enrichment in Fe, Ti, P, Al, Zr, Ni, Co, Zn, Y, Nb, Hf and REE and variations in resulting metamorphic mineral assemblages are related to premetamorphic progressive lateritisation of a basaltic protolith. The weathering generated a continuous chemical suite from $SiO_2 = 48$ wt%, $Fe_2O_3 = 10$ wt% and $Al_2O_3 = 19$ wt% in the basic granulites to 14 wt%, 40 wt% and 25 wt% in the Fe-Al granofelses. Metasomatism during diagenesis and during (very) high-grade metamorphism (1200-900 Ma) further perturbed the concentrations of relatively mobile elements Ca, Mg, K, Rb, Sr, Ba, Na and Li in the laterites without affecting the transition metal ratios. In particular, the REE did not fractionate differentially during the supracrustal and metasomatic alteration.

3.1 INTRODUCTION

Residual products of surficial geochemical processes in the past are potentially economic resources of metals (Button and Tyler 1981; Wilson 1983). In particular, ancient weathering horizons (paleosols) may be valuable indicators of paleoenvironment (atmosphere, climate, groundwater, topography, local circumstances) and they may be used successfully as marker horizons in unravelling tectonically complex terrains (Gay and Grandstaff 1980; Schau and Henderson 1983; Valeton 1983; Holland 1984; Retallack 1986; Reinhardt and Sigleo 1988; Golani 1989). Many *in situ* laterite and bauxite deposits are the result of geochemical (as opposed to biochemical) weathering and their formation is not necessarily restricted to Phanerozoic times (e.g., Valeton 1972; Bardossy 1982).

Despite its obvious economic and scientific importance, the study of paleosols in Precambrian terrains is still in its infancy. This is partly due to the fact that most Precambrian rocks have been subjected to at least some degree of strain and recrystallisation such that preexisting weathering profiles are not readily identified and their investigation by conventional pedological techniques is seriously hampered. Precambrian weathering horizons may be modified before burial, during diagenesis, during one or more cycles of prograde and retrograde metamorphism, and during post-metamorphic weathering. Modifications may include erosion and redeposition, mechanical addition of material, collapse of the weathering column, folding, metasomatism, dehydration, formation of dense minerals, fracturing, changes in oxygen content related to the oxidation state of iron and melting. Besides being a complicating factor, metamorphism also reduces the water rock ratio, the water flux, and, hence, the mobility of many elements. Therefore, metamorphism is expected to enhance the preservation of post-diagenetic bulk compositional characteristics (Schau and Henderson 1983).

High-grade metamorphic equivalents of bauxites and laterites may have unusual Al-excess mineralogies (e.g. emeries) that provide unique insight in metamorphic conditions (Jansen and Schuiling 1976; Feenstra 1985). Comparison in granulite facies terrains of such dense, impermeable, residua lithologies with rock types that are more susceptible to reaction with metamorphic fluids such as impure marbles is a promising field of future research (Bol et al. in preparation), specially since the association of carbonate rocks and residual deposits, once recognized, may prove to be quite common in (meta)sediments of all ages (Bardossy 1982; Reimer 1986).

The purpose of this geochemical study is 1) to establish the basaltic affinity of heterogeneous basic layers in a granulite facies metasedimentary unit from the Proterozoic shield in Rogaland, SW Norway, 2) to identify premetamorphic lateritisation as the main process that effected the bulk chemical variation, and 3) to evaluate the extent of metamorphic mass transfer. Major, trace and rare earth element abundances in samples from one specific layer are used in combination with their bulk densities in order to assess volume-composition relations resulting from chemical alteration during weathering, diagenesis and metamorphism.

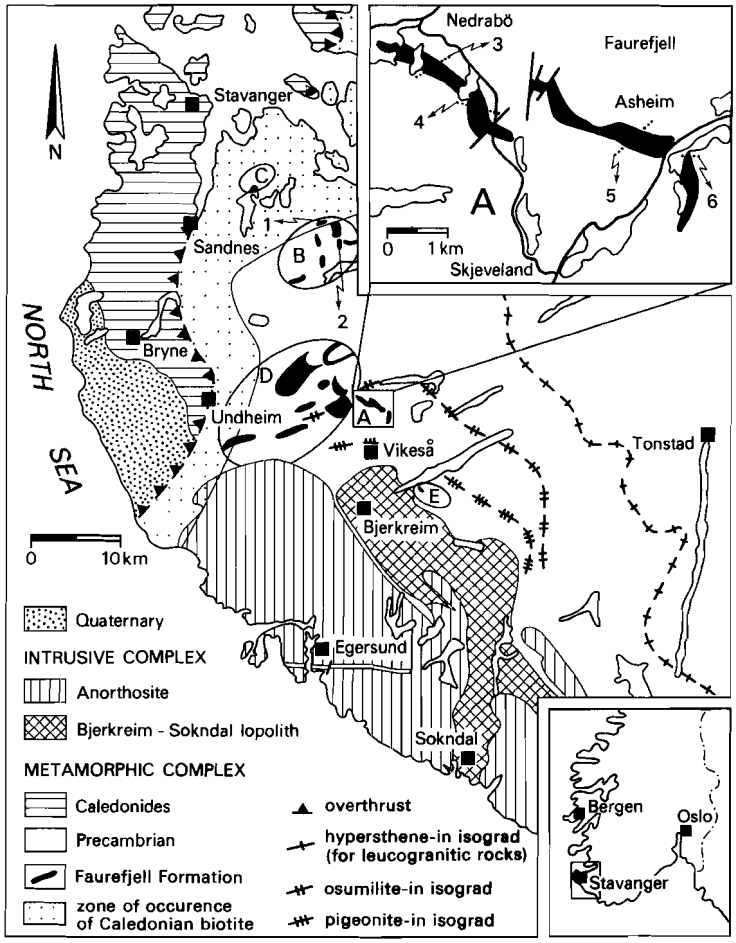

Fig. 3.1: Simplified geological map of SW Norway. The inset shows outcrop of the **FF** in area A and locations of the sampling profiles.

3.2 GEOLOGICAL SETTING

Massif-type anorthosites and the folded anorthositic to mangeritic Bjerkreim-Sokndal lopolith are exposed in the western part of the Precambrian basement in S.W. Norway (**Fig. 3.1**) (Duchesne et al. 1985). These intrusive units are surrounded by a Precambrian polymetamorphic complex of charnockitic and granitic migmatites with intercalations of augen gneisses and metasupracrustal rocks (Hermans et al. 1975).

The latter are comprised of the Gyadal Garnetifereous Migmatites (Huijsmans et al. 1981) and the Faurefjell Metasediment Formation (**FF**) (Sauter 1981).

On the basis of mineral assemblages, four stages of metamorphism (**M1-M4**) have been recognized in the metasupracrustal units and in their enveloping migmatitic complex (**Fig. 3.2**). The **M1** phase (about 1200 Ma) has been related to an old upper amphibolite to granulite facies metamorphism (Wielens et al. 1980; Maijer and Padget 1987). The granulitic high temperature-intermediate pressure **M2** stage (1050 Ma) is essentially a thermal overprint induced by the intrusion of the leuconoritic phase of the Bjerkreim-Sokndal lopolith (Maijer et al. 1981). Metamorphic zoning related to the **M2** stage (Tobi et al. 1985) is manifest by a) a pigeonite-in isograd (the metamorphic pigeonite is now inverted to orthopyroxene), b) an osumilite-in isograd, c) a garnet decomposition isograd, d) a (amphibole + quartz)-out isograd, and e) a hypersthene line (incoming of hypersthene in granitic rocks) (see **Fig. 3.1** for position of a, b and e). Geothermometric calculations yield temperatures of about 1050°C between the pigeonite-in isograd and the igneous complex, decreasing to about 750°C near the hypersthene line (Jacques de Dixmude 1978; Jansen et al. 1985). Further to the east, the amphibolite facies is developed and a gradual regional change in chemical and optical properties of amphiboles related to distance to the intrusive complex is observed (Dekker 1978). The **M3**-stage of medium-grade metamorphism represents a period of retromorphism during slow, almost isobaric, post-**M2** regional cooling (Kars et al. 1980). **M3** features include exceptionally well developed exsolution phenomena and partial decomposition of typical **M2** minerals (e.g., osumilite, Al-rich orthopyroxene) into symplectites of lower grade minerals. In the vicinity of pegmatites and granites, **M3** mica and amphibole may form rims around **M1** and **M2** minerals. Isotopic ages for osumilite (970 Ma (K-Ar; Rb-Sr), Maijer et al. 1981), hornblendes

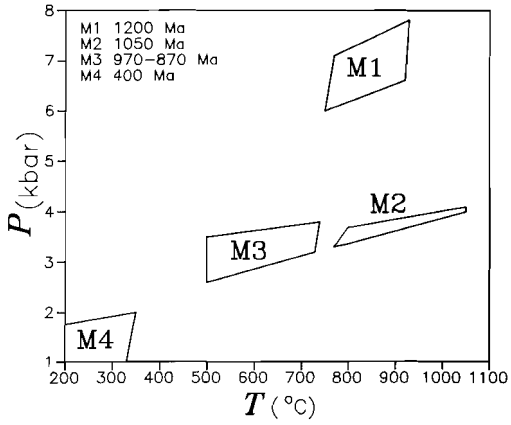

Fig. 3.2: Compilation of P-T-t estimates for **M1-M4** (see text) (after: Jansen et al. 1985; Maijer and Padget 1987).

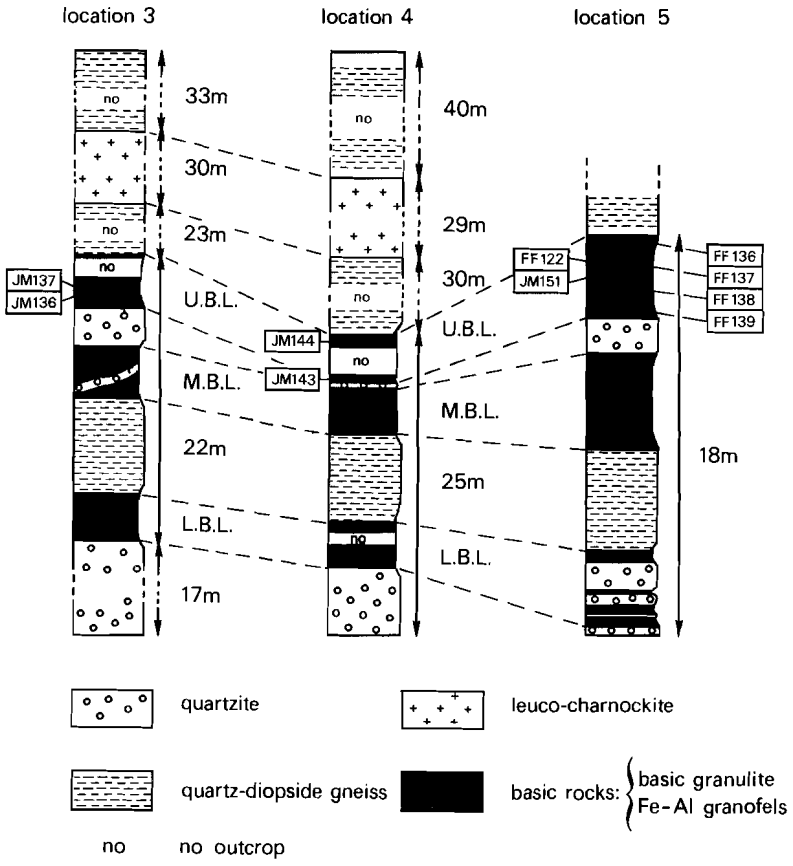

Fig. 3.3: Lithostratigraphic columns at locations 3, 4 and 5 (see inset **Fig. 3.1**). Positions of the 10 samples of **Table 3.1** are labeled.

(950 Ma (K-Ar), Dekker 1978; Wielens et al. 1980), and brown biotite (870 Ma (K-Ar; Rb-Sr), Verschure et al. 1980) reflect passage through Rb-Sr and K-Ar closure temperatures during **M3** cooling. Finally an **M4**-stage of retrograde prehnite-pumpellyite to greenschist facies metamorphism (400 Ma) is weak and omnipresent in the west and is attributed to the Caledonian orogenesis (Verschure et al. 1980). An isograd of Caledonian green biotite follows the Caledonian front at a distance of 5-15 km in the Precambrian basement (**Fig. 3.1**) and is related to Caledonian overthrusting (Sauter et al. 1983).

Exposures of the **FF** are largely concentrated in five areas (A - E, **Fig. 3.1**) where it crops out as thin folded layers or boudinaged lenses with a total thickness varying from 10 to 50 meters. The contacts with the surrounding migmatites are usually concordant. Locally, in areas B and C, leucogranites intrude the metasediments discordantly. The **FF** is composed of various intercalations of quartz-diopside gneisses, diopside marbles, forsterite marbles, quartzites, quartz-alkali feldspar rocks, diopside-alkali feldspar rocks, alkali feldspar rocks, diopside rocks and heterogeneous basic layers consisting of basic granulites and Fe-Al rich granofelses. In areas A, B and D, Al-Fe-rich granofelses are arbitrarily discriminated from basic granulites by the presence of cordierite in the former (**Table 3.1**). At locations 3, 4 and 5 (**Fig. 3.1**) in area A three heterogeneous basic layers are correlated in schematic profiles (**Fig. 3.3**). Of the three layers the Upper Basic Layer (**UBL**) shows the widest compositional variation, both chemically and mineralogically and it was selected for sampling, both parallel and perpendicular to strike.

3.3 PETROGRAPHY

The **UBL**-basic granulites (massive hypersthene-plagioclase granolites according the nomenclature of Winkler (1979)) are medium-grained inequigranular granoblastic rocks with coarser grained lenticular aggregates of ferromagnesian minerals that define a weak foliation. They have a noritic to gabbroic mineralogy, plagioclase (An_{35}-An_{55}) + orthopyroxene + iron-titanium oxides ± clinopyroxene ± biotite and accessory zircon and apatite (**Table 3.1**). Magnetite grains occasionally enclose spinel. Orthopyroxene crystals are large and have moderate to strong pleochroism related to changes in alumina contents (up to 12 wt% Al_2O_3, R.J.P. Blok personal communication 1987). Fine-grained orthopyroxene-garnet symplectites are occasionally associated with orthopyroxene.

The **UBL**-granofelses (spinel-cordierite-sillimanite granoblastites) have textures similar to those of the basic granulites and are generally coarse-grained. They contain plagioclase (An_{30}-An_{60}), cordierite, Fe-Ti oxides, spinel (hercynite) and either sillimanite (often) or orthopyroxene (seldom). Accessory minerals are: apatite, zircon, monazite and corundum. Sillimanite-bearing rocks locally contain complex intergrowths of magnetite, spinel, sillimanite and cordierite. Sillimanite and the intergrowths define a weak foliation. The most iron and alumina-rich granofelses have

Table 1. Whole-rock analyses of 10 representative UBL samples with relevant petrographic data

Sample	(2σ)	FF139	FF138	FF136	FF137	JM144	FF122	JM143	JM136	JM151	JM137
Type		Grano	Grano	Grano	Grano	Grano	Grano	Grano	Grano	BGranu	BGranu
SiO_2	(0.7)	13.4	19.4	22.8	24.4	29.1	32.3	33.0	37.7	42.1	45.5
Al_2O_3	(0.5)	25.4	30.7	34.6	34.0	27.0	27.7	28.1	23.8	19.7	19.6
TiO_2	(0.04)	6.53	5.50	5.66	5.24	4.77	4.85	4.87	3.77	3.24	2.89
Fe_2O_3*	(0.3)	43.1	32.8	29.4	28.4	23.3	23.9	23.0	19.2	14.9	13.2
MnO	(0.02)	0.48	0.42	0.27	0.25	0.40	0.24	0.32	0.27	0.31	0.29
MgO	(0.3)	3.49	4.39	1.09	1.00	7.84	4.68	5.95	6.52	7.40	6.04
CaO	(0.3)	4.65	4.18	3.54	3.83	4.26	4.04	2.45	3.07	8.55	7.29
Na_2O	(0.4)	1.30	0.70	0.80	0.96	0.99	1.81	0.12	2.22	1.44	2.80
K_2O	(0.08)	0.19	0.10	0.10	0.12	0.48	0.66	0.13	1.70	0.26	0.92
P_2O_5	(0.04)	2.1	2.5	1.9	1.8	1.2	1.4	1.3	0.9	1.0	0.9
Total		100.67	100.63	100.23	100.07	99.33	101.68	99.18	99.14	98.93	99.47
LOI	(0.04)	−0.76	−0.43	−0.57	−0.25	0.15	1.18	−0.80	0.41	−0.13	0.41
Ba	(40)	383	165	186	250	960	740	652	2093	1976	389
Sr	(21)	216	201	227	287	190	226	196	232	566	297
Rb	(3)	5	5	4	4	11	16	9	36	18	28
Ni	(4)	415	281	135	127	99	151	87	74	68	53
Zn	(3)	419	292	98	96	151	158	127	129	100	94
Zr	(10)	759	611	628	596	504	426	558	438	324	333
Y	(2)	108	109	81	75	11	72	9	36	18	28
Nb	(3)	22	20	21	16	16	15	18	14	8	9
Sc	(1)	43	39	43	34	38	34	37	34	25	21
Co	(3)	390	245	165	155	107	123	95	80	63	48
Hf	(0.6)	23.35	14.75	14.47	14.10	11.29	14.81	11.59	10.09	9.83	7.59
Be	(0.1)	0.33	1.51	0.17	0.08	2.36	0.26	0.90	0.17	1.00	3.51
Li	(2)	35	54	35	30	31	169	60	21	40	12
La	(3)	41.3	41.2	46.1	56.2	43.5	34.9	29.0	34.5	23.1	22.9
Ce	(2)	101.7	104.2	110.4	121.6	107.6	79.6	78.0	83.7	52.5	55.8
Sm	(1.2)	17.4	17.9	16.7	16.6	15.6	13.5	15.3	14.6	10.5	9.5
Eu	(0.6)	5.04	5.53	4.79	4.61	4.74	3.75	4.29	3.92	2.71	2.61
Tb	(0.3)	2.75	3.16	2.52	2.25	1.80	2.03	2.00	2.00	1.39	1.39
Yb	(0.7)	8.84	8.33	5.77	5.85	6.11	5.58	5.94	6.61	3.90	2.99
B.D.	(0.03)	3.85	3.72	3.53	3.47	3.35	3.26	3.26	3.25	3.07	3.02
Plagioclase		X	X	X	X	X	X	X	X	X	X
Orthopyroxene		O	O	O	O	X	O	O	X	X	X
Opaque		X	X	X	X	X	X	X	X	X	X
Spinel		X	X	X	X	X	X	X	X	A	A
Cordierite		X	X	X	X	X	X	X	X	O	O
Biotite		O	O	O	O	X	O	X	O	X	X
K-Feldspar		O	O	O	O	X	O	O	X	X	O
Sillimanite		O	X	X	X	O	A	X	O	O	O
Zircon		A	A	A	A	A	A	A	A	A	A
Apatite		A	A	A	A	A	A	O	O	A	A
Monazite		A	A	A	O	O	O	O	O	O	O
Sphene		O	O	O	O	O	O	A	O	O	O

In parentheses estimated 2σ values: for major element oxides and LOI in wt%, for other elements in ppm, for bulk density (*B.D.*) in g/cm^3. Fe_2O_3*: Total iron reported as Fe_2O_3; *LOI*: Loss on ignition. Petrographic data: *X* = present, *O* = absent, *A* = accessory; *Grano* = Fe − Al Granofels, *BGranu* = Basic granulite

Table 2. Average ratios of some elements in ten UBL rocks and in modern basalts and modern andesites from various tectonic settings[a]

			Basalts				Andesites	
	UBL	(σ)	MORB	arc	calc-alk.	cont. rift	arc	calc-alk.
$(La/Yb)_N$	4.3	(1.0)	1.2	2	8	10	1.1	6.3
Eu/Eu*	0.84	(0.04)	0.92	1.2	1.0	0.85	1.09	0.86
Ni/Co	1.0	(0.1)	3	1.3	1.3	2.5	0.75	0.75
Ti/Zr	55	(5)	90	83	60	66	39	38
Ti/P	3.5	(0.6)	8.0	4.9	5.3	14.6	–	–
Zr/Hf	40	(6)	37	34	32	–	–	–

[a] Basalt and andesite data after Condie (1976) and Pearce (1982). Subscript *N* refers to chondrite normalised values. $Eu/Eu^* = (Eu_N/[Sm_N - 0.333*(Sm_N - Tb_N)]$

both apatite and monazite as accessory phosphate phases. Occasionally corundum grains are included in magnetite and spinel. Both the basic granulites and the Fe-Al granofelses may contain some perthitic K-feldspar.

The **UBL** rocks have granulite facies mineral associations. Premetamorphic textures or structures are not preserved. Relict **M1** minerals or replacement textures thereof are not identified in this particular layer. Spinel-magnetite exsolution textures and the orthopyroxene-garnet symplectites presumably are formed during the **M3** metamorphism. Typical **M4** minerals (pumpellyite, prehnite, green biotite) are not observed and there is no textural evidence for a retrograde origin of the brown biotite that occurs in some of the samples. Partial saussuritization of plagioclase and partial pinitization of cordierite are volumetrically insignificant and are either **M4** alterations or very low-grade Recent alterations.

Fig. 3.4A-L: Whole-rock chemical variation diagrams for 15 samples of the Upper Basic Layer (**UBL**). Diagrams F, G and I contain 13 data points due to incomplete chemical analyses of some samples. Open squares: Fe-Al Granofelses; Closed squares: Basic granulites.

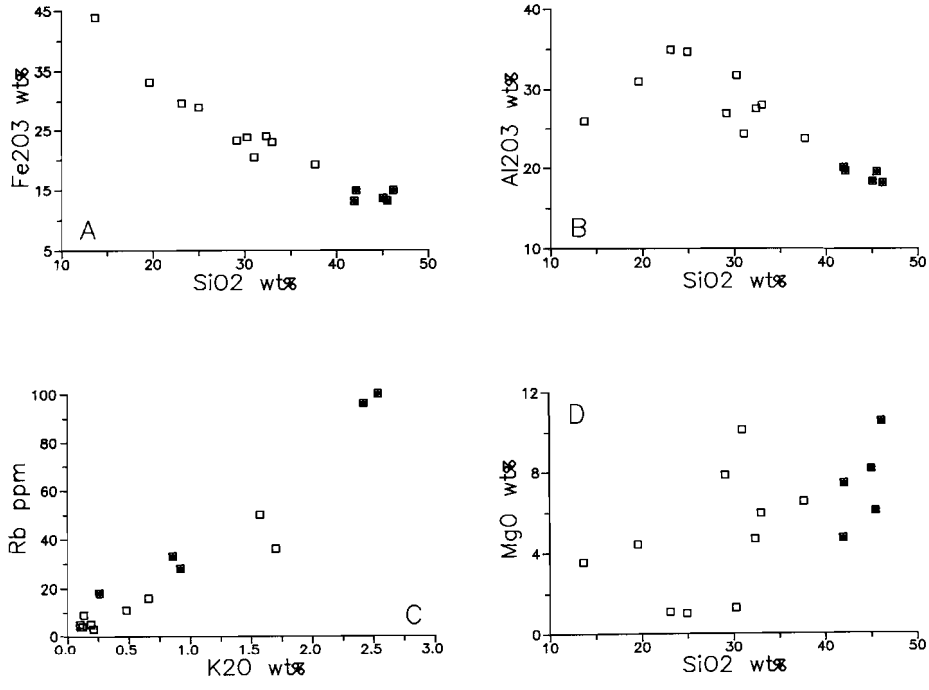

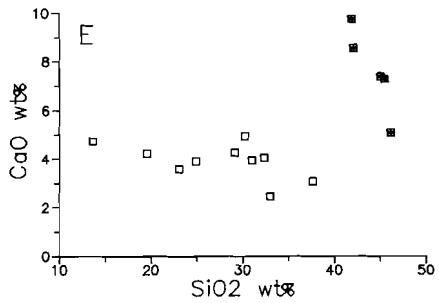
E
CaO wt%
SiO2 wt%

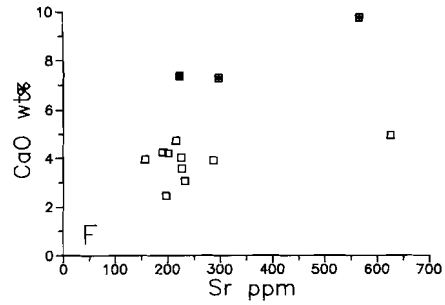
F
CaO wt%
Sr ppm

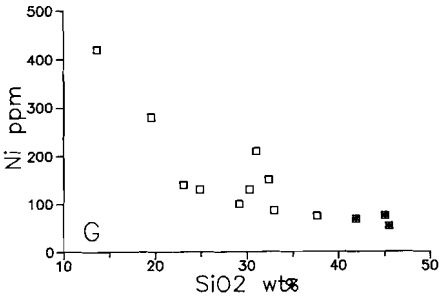
G
Ni ppm
SiO2 wt%

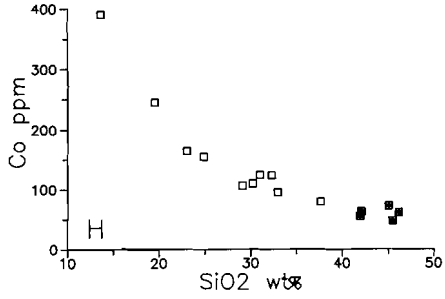
H
Co ppm
SiO2 wt%

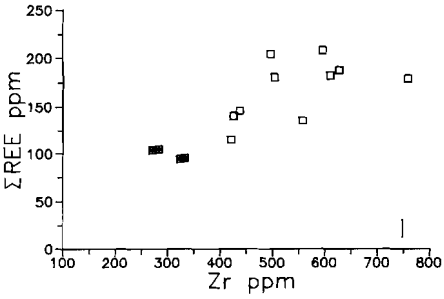
I
ΣREE ppm
Zr ppm

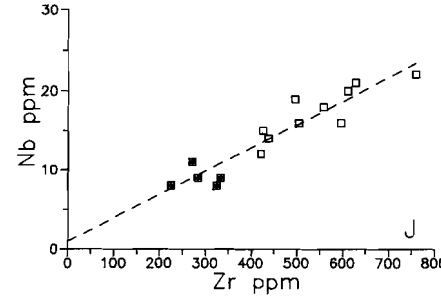
J
Nb ppm
Zr ppm

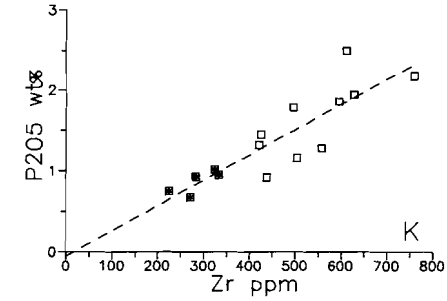
K
P205 wt%
Zr ppm

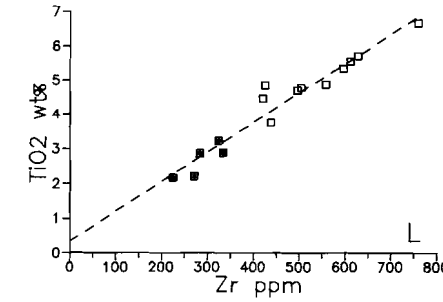
L
TiO2 wt%
Zr ppm

3.4 ANALYTICAL PROCEDURES

Whole-rock major element and Ba, Sr, Rb, Ni, Zr, Zn, Nb, and Y contents were determined by standard XRF techniques using an automated Philips PW1400 Spectrometer. Ignited splits of rock powder were mixed with $LiBO_2/LiB_4O_7$ (66/33) Spectroflux in a ratio of 1:10 and fused at 1000°C in a Herzog HAG 1200 automated furnace to obtain glass beads for major element analyses. Pressed powders cemented with Elvacite were used to determine trace element abundances. REE (La, Ce, Sm, Eu, Tb, Yb) and Sc, Co and Hf contents were determined at IRI, Delft, by INAA using established techniques (de Bruin 1983). Li and Be were analyzed by ICP-AES using the sample decomposition method described by Voncken et al. (1986). For most elements precision-values at the 95% confidence level for the concentration range of interest were calculated from replicate analyses (Huijsmans 1985) and included in **Table 3.1.** A variety of well-characterized standards were included in each batch for analyses. Accuracy is better than 1% (relative) for all major element oxides except MnO and P_2O_5 (both better than 5%) and better than 10% for the trace elements except La, Tb, (better than 15%) and Nb (better than 20%).

3.5 RESULTS

Bulk chemical compositions of sixty samples of heterogeneous layers in areas A, B and D, including fifteen **UBL** samples from area A, were analyzed. Ten representative **UBL** rocks were selected for model calculations and analytical results for these are reported with relevant petrographic data in **Table 3.1.** Contents of major element oxides are not corrected for H_2O since LOI values are small and occasionally even negative due to low water content and iron oxidation during calcination. In this study all calculations are performed with water free analyses normalised to 100%.

The basic granulites fall within a range of 42 to 47 wt% SiO_2. Granofelses contain more Fe_2O_3, TiO_2, Al_2O_3, P_2O_5, Zr, Nb, Ni, Co, REE (and Zn, Hf, Y, Sc and MnO, not shown) and less SiO_2, CaO, MgO (and Be, not shown) (**Fig. 3.4**). Li, Ba, Sr and Na_2O contents are erratic and not related to rock-type. The **UBL**-rocks generally define curvi-linear trends with SiO_2 on variation diagrams (**Fig. 3.4A,B,G,H**), except for the alkali and alkaline earth elements (**Fig. 3.4E,D**). For the entire suite sampled, K_2O correlates significantly with Rb (**Fig. 3.4C**) and Ba, but typically not with SiO_2 or

Zr. Couples of CaO, MgO and Sr contents scatter widely on variation diagrams (**Fig. 3.4D,E,F**) and yield weak positive correlations. Li, Be and Na contents do not correlate significantly with any of the other elements. In contrast, strong positive correlations are observed for couples of transition metals (and phosphorous) (**Fig. 3.4I,J,K,L**).

There is no simple relation between composition and lateral or vertical position within the **UBL**. For example, samples FF136 to FF139 (**Fig. 3.3**) were obtained along a traverse from bottom to top of the exposure at location 5 and all are Fe-Al rich granofelses. Sample JM151 is a basic granulite that occurred approximately 10 meters to the west near the stratigraphic center of the **UBL**. FF139 (13.3 wt% SiO_2) and JM137 (45.7 wt% SiO_2) are both from the top of the **UBL** and represent compositional extremes within the layer.

In the **UBL**-samples the continuous chemical variation is reflected in mineral chemistry and mode (**Table 3.1**). Low-silica granofelses are high in P_2O_5 and contain monazite in addition to apatite. Modal contents of spinel, magnetite and zircon increase with increasing Fe_2O_3, Al_2O_3, TiO_2 and Zr content. The whole-rock Al_2O_3 content relates generally to the Al_2O_3 content of orthopyroxene (R.J.P. Blok personal communication 1987) and the presence or absence of sillimanite. The **UBL**-granofels with the lowest silica content (FF139) has no sillimanite and an anomalously low Al_2O_3 content (**Fig. 3.4B**). Basic granulites and Fe-Al granofelses can be sampled within a few meters of each other and for both rock types the P-T conditions were virtually the same during the high-grade metamorphisms. Therefore, the mineralogical variation must be the result of premetamorphic and/or metasomatically acquired differences in bulk chemistry.

Rare earth patterns are normalised to the average chondritic values after Haskin et al. (1968) (**Fig. 3.5**). Generally, a good positive correlation exists between REE and the transition metals (e.g. Zr vs. ΣREE in **Fig. 3.4I**). Granofelses have REE-abundances 20 (Yb) to 170 (La) * chondritic values. Basic granulites yield abundances 15 - 85 * chondritic values. The REE-patterns are rather flat with a slight enrichment of the LREE, $(La/Yb)_N$-ratios = 3 - 6. No systematic relation between the small variation in $(La/Yb)_N$ and any of the elemental abundances is observed. A small negative Eu-anomaly is obvious. Basic granulites and Fe-Al granofelses from the **UBL** display closely similar REE-patterns, varying mainly in total REE abundances.

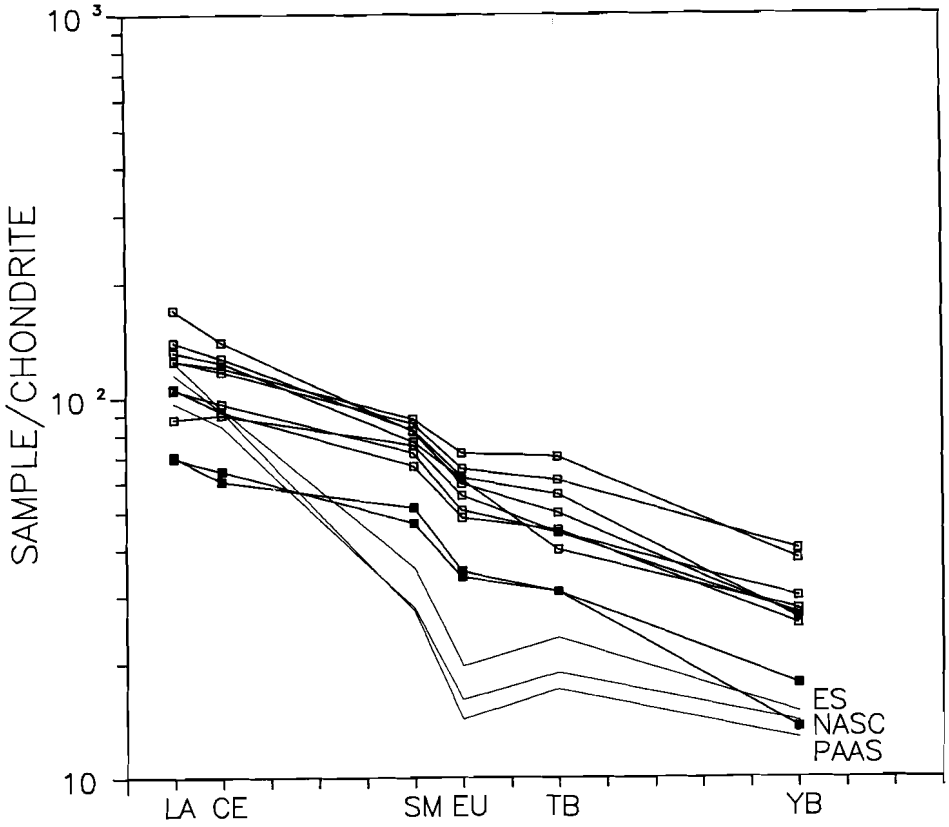

Fig. 3.5: Chondrite normalised REE-patterns for the **UBL**-samples from **Table 3.1**. Patterns of three shale-composites (ES, NASC and PAAS) are included. Symbols as in **Fig. 3.4**.

3.6 DISCUSSION

Previously, the Fe-Al granofelses of the **FF** were thought to represent metapelites (Michot 1960). However, REE evidence presented in this study does not support that hypothesis. Nance and Taylor (1977) estimated that average REE abundances are enriched in LREE ($(La/Yb)_N = 7\text{-}12$) for Post-Archean Australian Shales (PAAS, **Fig. 3.5**). The Paleozoic North-American and European shale composites (NASC, ES) are enriched in LREE as well (Haskin and Haskin 1966; Haskin 1979). NASC, PAAS and ES have a marked negative Eu-anomaly ($Eu/Eu^* = 0.66\text{-}0.70$). Basic granulites

and Fe-Al rich granofelses of the **UBL** exhibit less fractionated REE-patterns with smaller Eu-anomalies (**Table 3.2**). Hence, a pelitic origin is unlikely and an alternative precursor must be sought.

Linear mixing of a basaltic composition and an aluminous metasediment such as a shale could produce the semi-linear element-element covariations of transition-elements and phosphorous. However, shales generally have REE signatures different from those of basalts and progressive admixture of one component to the other is likely to result in a systematic rotation of REE patterns, which is not observed. Furthermore, linear best fits for **UBL** datapoints on orthogonal plots of two *relatively* immobile constituents, (that is, constituents with a high positive correlation coefficient), intersect the axes approximately at the origin (e.g. **Fig. 3.4J,K,L**). This does not support a mixing concept, since it is unlikely (albeit not impossible) that the basalt and shale endmembers involved had exactly the same Nb/Zr, TiO_2/Zr and P_2O_5/Zr ratios. The REE, Ti, P, Zr and Nb data rather point at selective extraction or addition of one or more other constituents.

Possible precursors of the **UBL** are **magmatic rocks**. Transition elements, especially those from groups IIIB, IVB and VB of the periodic table, are believed to be *relatively* immobile during metamorphic and secondary alteration processes (e.g. Winchester and Floyd 1977; Floyd and Winchester 1978). Indeed, systematic analysis of component ratios in the **UBL** yields fairly constant values for E/Zr some of which are shown in **Fig. 3.6A,B** (E is one of: Al_2O_3, Fe_2O_3, TiO_2, P_2O_5, Ni, Zn, Y, Nb, Sc, Co, Hf, REE; similar conclusions as below can be reached by using any E other than Zr as denominator). In particular, the REE are not fractionated notably with respect to themselves or to Zr (**Figs. 3.5, 3.6B**), or to TiO_2, P_2O_5, Hf, Y and Nb (not shown). In granofelses with $SiO_2 < 25$ wt% the ratios Fe_2O_3/Zr, Ni/Zr, Co/Zr, Hf/Zr and Zn/Zr show a slight net increase with decreasing wt% SiO_2 whereas Al_2O_3/Zr, P_2O_5/Zr and REE/Zr show a slight net decrease. The small peaks near 32 wt% SiO_2 result from the anomalously low Zr content of sample FF122. In the basic granulites and the Fe-Al granofelses Zr/Hf, Zr/TiO_2, P_2O_5/TiO_2, Ni/Co ratios are nearly constant for various silica contents and have typical basaltic values (**Table 3.2**). Moreover, $(La/Yb)_N$ and Eu/Eu* values of all **UBL** samples are very similar and underline their basaltic affinity (**Table 3.2**). The constancy and the values of transition element ratios and the REE signatures indicate that, in terms of these elements, the **UBL**-rocks had a common progenitor that was rather homogeneous and had a basaltic composition.

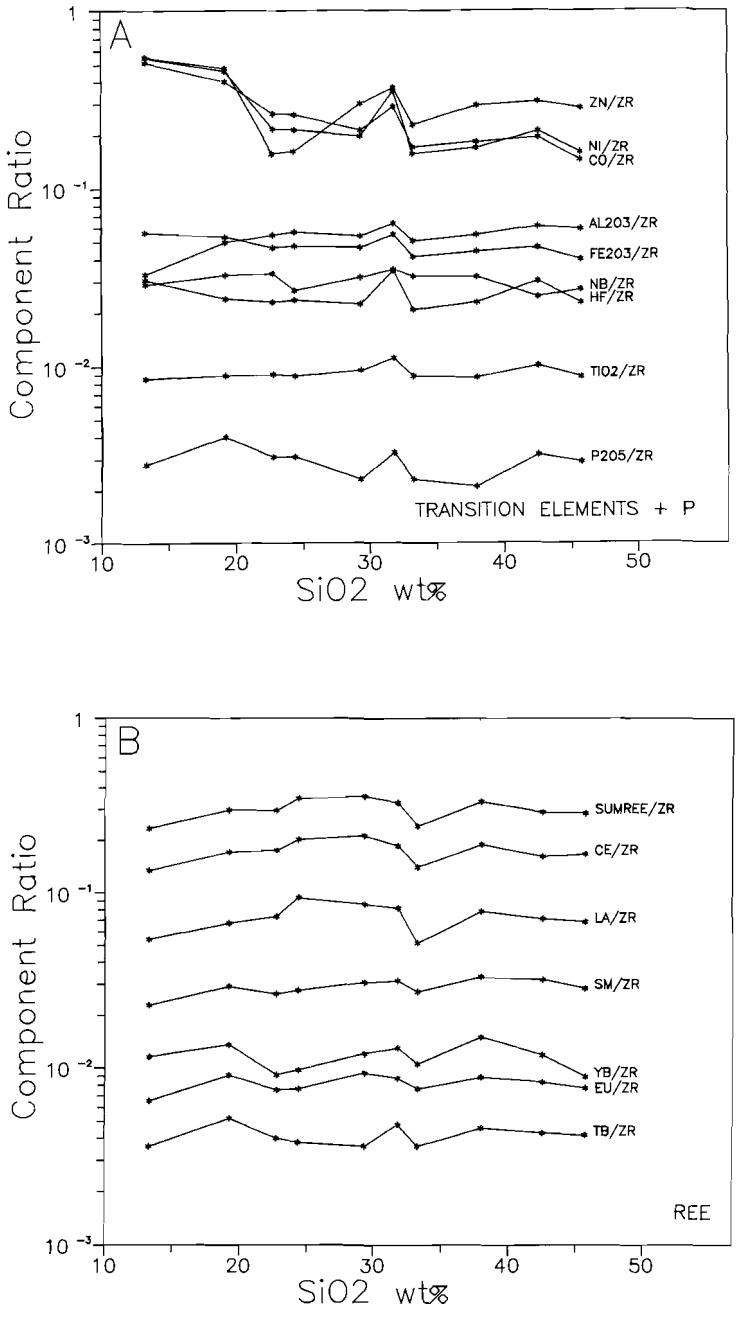

Fig. 3.6A-B: Component-ratios versus wt% SiO_2 for the **UBL** samples. A) Transition metals; B) Rare earth elements.

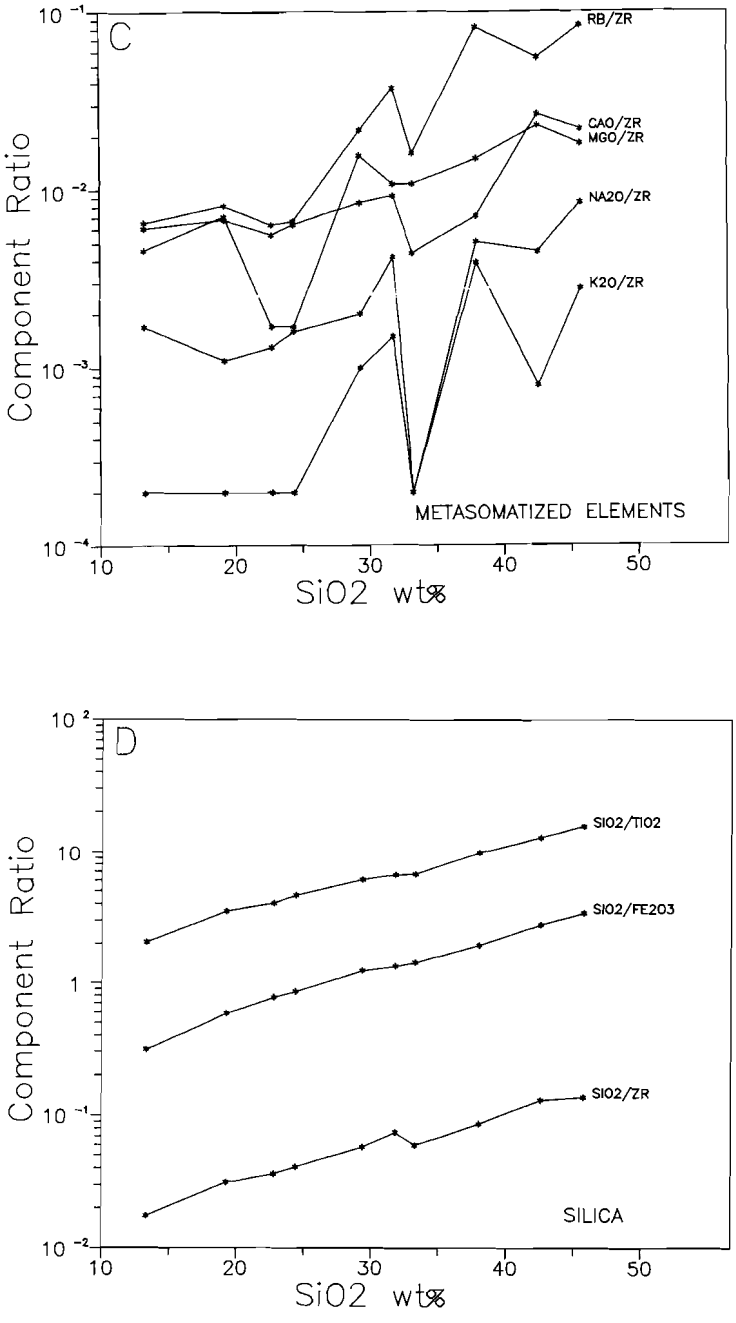

Fig. 3.6C-D: Component-ratios versus wt% SiO_2 for the **UBL** samples. C) Alkali and alkaline earth elements; D) Silica.

Basalts, basaltic andesites and first-cycle sediments derived from them are plausible precursors and in the ensuing discussion the composition of the protolith will be referred to as "basaltic".

The diagram of SiO_2/Zr, SiO_2/TiO_2 and SiO_2/Fe_2O_3 vs. wt% SiO_2 yields near-linear trends with positive slopes (**Fig. 3.6D**) indicating that the granofelses are depleted in SiO_2 relative to the transition metals. Similar net depletions, although less systematic, are observed for MgO, CaO, K_2O, Na_2O, and Rb (**Fig. 3.6C**) and for Ba and Sr (not shown). Any process invoked to explain the chemical variation in the **UBL**-suite must account for a considerable loss of silica and alkali and alkaline earth elements and concomitant fixation of the transition metals.

3.6.1 lateritisation

In terms of bulk Fe_2O_3, Al_2O_3 and SiO_2 content, the granofelses are very similar to laterites *sensu stricto* (**Table 3.3**). Many element variations in the **UBL** could be well explained by an incipient **lateritisation** (ferallitisation) of an originally homogeneous basaltic protolith. Such a process would have operated before metamorphism and before burial by other sediments since similar apparent enrichments in transition metals, though less extensive, are found in the other heterogeneous layers in area A (**MBL** and **LBL, Fig. 3.3**), but not in the quartzites, marbles and diopside-gneisses

Table 3.3: Selection of bulk chemical analyses of modern laterites in comparison with the granofelses from this study. Data normalised to 100% on a water free basis

Location	wt% SiO_2	Fe_2O_3	Al_2O_3
Kumba, West Cameroon[a)]	25.2	29.2	24.8
Libreville, Gabon[a)]	10.0	46.3	27.1
Nairobi, Kenya[a)]	11.4	25.3	14.6
Cape of Good Hope, RSA[a)]	25.7	34.5	19.0
Tira, Uganda[b)]	22.5	37.3	25.5
Kauai, Hawaii[c)]	4.7	39.4	25.9
East Maui, Hawaii[c)]	6.6	31.4	33.4
FF139, Rogaland	13.3	42.8	25.3
FF136, Rogaland	22.8	29.3	34.6

a) Persons (1970)
b) McFarlane (1983)
c) Patterson (1971)

that directly overly the **UBL** nor in metabasites of the basement that envelops the **FF**. Leaching of silica would increase immobile element contents of the residue, creating compositions similar to those of the Fe-Al granofelses. Concomitant leaching of Ca, Mg and the alkali elements is expected during lateritisation (Patterson 1971; Golightly 1981; Esson 1983). Indeed, these elements are generally less abundant in the granofelses (e.g. **Fig. 3.4D,E**) although original lateritic covariations with silica, if any, are supposedly blurred now due to superimposed metasomatic effects (see below).

3.6.2 metasomatism

Quartzofeldspathic pegmatites intruded the siliceous metadolomites of the **FF** at various locations before the granulite facies **M2** metamorphism. Generally, these pegmatites are progressively depleted in silica towards their rims and they are symmetrically enclosed by high-variance mineral assemblages (Bol et al. 1989). In the marbles the mode of diopside may vary from $<2\%$ in forsterite marbles, to $>95\%$ in diopside rocks near contacts with quartz-bearing rocks (quartzites, quartz nodules, diopside gneisses). These phenomena are related to **synmetamorphic silica metasomatism** (Hermans et al. 1975; Sauter 1981, 1983), and are exclusively observed within the marbles.

Systematic bulk-compositional variations at contacts with quartzites are not found in the **UBL**. Contacts of **UBL** rocks with marbles are not exposed. Some Ca-rich specimens of the **MBL** are near to marble lenses and locally contain hedenbergite and andradite. Others contain sapphirine and have conspicuously high Mg contents. Although rocks with such mineralogies do not occur in the **UBL** they demonstrate that the Ca and Mg contents in the **UBL** may have been variably contaminated by Ca and Mg from nearby dolomitic marbles.

The **UBL**-granofelses have mineral associations that resemble those of corundum-bearing rocks (emeries) from the Cortland Complex, New York. The latter are regarded as the highly aluminous residua produced by the interaction (desilification by fractional fusion and mass transfer) of pelitic schist xenoliths with mafic magma (Tracy and Thompson 1979). No evidence for partial melting was observed in the three heterogeneous basic layers, nor textures that suggest extraction of silica towards adjacent rocks. Textural or compositional indications for silica transfer from the contacting quartzites and diopside gneisses (**Fig. 3.3**) to the **UBL** are

also absent (c.f. Tracy and McLellan 1985, for distinct textural, structural and compositional evidence from the Cortland emeries).

The contents of K and Rb in the **UBL** have a strong positive correlation (**Fig. 3.4C**) and vary erratically with transition element contents indicating that K-metasomatism affected the **UBL** (Bol and Jansen 1989). In general, Li, K, Rb, Ba contents in the **UBL** vary irregularly by a factor ten or more. Regarding the fairly constant transition element ratios in the **UBL** this variation presumably cannot solely be attributed to original inhomogeneity of a basaltic protolith. Burial of weathering profiles that have been depleted in alkali and alkaline earth elements often leads to *addition* of these elements by **syn-diagenetic metasomatism** (Gay and Grandstaff 1980; Grandstaff et al. 1986; Kimberley and Grandstaff 1986; Nesbitt and Young 1989) depending on the availability and nature of ground waters.

Therefore, the lack of systematic relations between contents of transition metals and those of the alkali and alkaline earth elements (e.g. **Fig. 3.6C**) is probably caused by the syn-diagenetic and syn-metamorphic mobility of the latter. In contrast, SiO_2 yields smooth, near-linear trends in **Fig. 3.6D** indicating that metasomatic processes in the **UBL** had negligible influence on SiO_2/E. The effects of silica and alkaline (earth) metasomatism upon the bulk content of Si, P, REE and the transition elements must have been small compared to the effects of silica and alkaline (earth) leaching during lateritisation.

3.6.3 gains and losses

Various calculation schemes exist to estimate net gains and losses or enrichment-factors of constituents in present-day laterite profiles. The procedures have in common that the weathering horizon must be examined *in situ* in order to evaluate the validity of the assumptions underlying the calculations, to identify and characterize the protolith, and to assess the relative importance of lateral movement, differential losses from the profile by mechanical means and addition of extraneous material. Calculations are greatly facilitated when an index constituent has been quantitatively retained in the residue (e.g., Esson 1983) or when undeformed protolith textures have been preserved and the weathering was essentially isovolumetric (e.g., Millot and Bonifas 1955). One-dimensional mass-balance equations (Brimhall and Dietrich 1987) that interrelate chemical composition, volume, density, porosity and

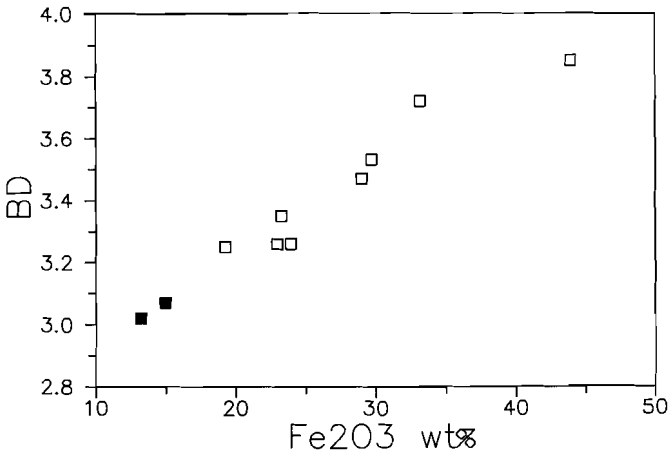

Fig. 3.7: Bulk density vs wt% Fe_2O_3 for the **UBL**-samples from **Table 3.1**. Symbols as in **Fig. 3.4**.

strain in protolith, enriched zone and leached zone may be used when the original weathering stratification is still present (or can be reconstructed) and when lateral fluxes of constituents can be neglected.

None of these methods can be applied to the **UBL** since it is recrystallized and deformed during at least three high-grade metamorphisms. Gresens (1967) provided a more general mathematical formalism to model volume-composition relations resulting from chemical alteration processes irrespective of whether these were accompanied by recrystallisation, volume change or disruption of alteration stratification. In his equations the volumes V_A and V_B of a reactant rock A and a product rock B are related by a volume-factor

$$f_V = V_A/V_B = (g_A*x_i)/(100*g_B*c_i(B)) + (c_i(A)*g_A)/(c_i(B)*g_B) \quad (1)$$

where g is the bulk density, c_i is the wt% of element i and x_i represents net gains and losses (grams per 100 gram A) of element i during open system chemical reactions. Bulk densities of the **UBL**-samples were obtained from their buoyancy in water (**Table 3.1**). They correlate well with the whole-rock Fe_2O_3 content (**Fig. 3.7**) and show a considerable range ($>>2\sigma$)demonstrating the amenability of the **UBL** for assessing premetamorphic weathering by volume-composition calculations. For the **UBL** rocks the f_v values reflect the "net volume" effect of the alterations, after dehydration and compaction due to diagenesis and metamorphism. There is no reason to assume that the operating processes were isovolumetric ($f_v = 1$). Conservation of one or more

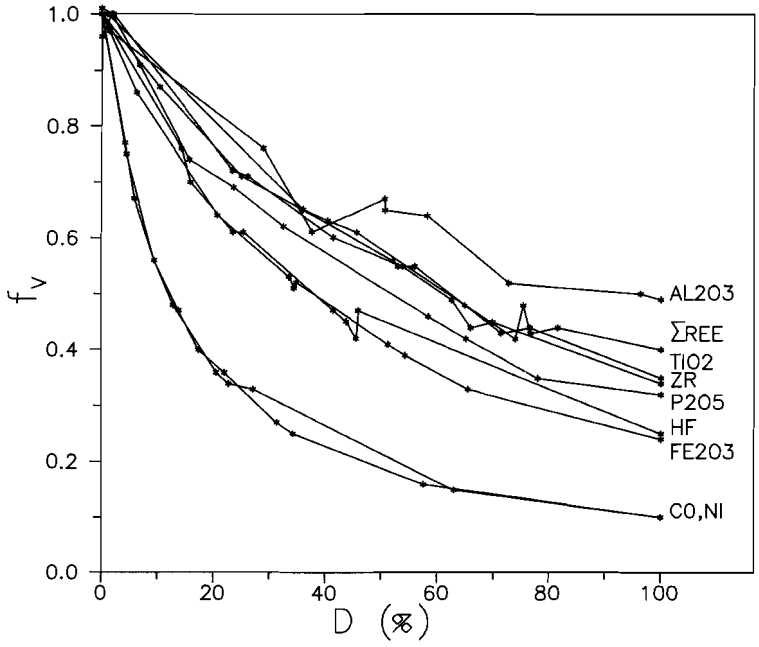

Fig. 3.8: Hypothetical f_v versus D_i curves assuming isochemical behaviour for the involved elements and element oxides (see text).

elements ($x_i = 0$) cannot be assumed *a priori*. If an element i was immobile during the reactions the degree of lateritisation (D) of sample S can be expressed as:

$$D_i(S) = ((c_i - c_i^{MIN})/(c_i^{MAX} - c_i^{MIN}))*100\% \quad (2)$$

where c_i^{MIN} and c_i^{MAX} refer to the minimum and maximum concentrations of element i observed in the **UBL**. If, for example, Fe was immobile during the lateritisation, D_{Fe}(FF139) is 100%. Alternatively, if P behaved conservatively, D_P(FF139) is 73%. The D_i-values are relative to the concentration range of element i in the sample set and D_{Ni}(JM137) = 0% does not necessarily imply that sample JM137 represents an unaltered rock. Assuming conservation for element i ($x_i = 0$) and taking the sample with $D_i = 0$ as the first reactant composition (A), a hypothetical volume-factor can be calculated for the product rock B (being the sample with the next D-value in the set). In turn, B serves as reactant in order to calculate f_v for the sample with the next D-value, et cetera. Eventually, a curve can be constructed for i on a D_i vs f_v diagram. This is done for various elements and element-oxides in the **UBL**, merely in order to assess their relative mobilities during the premetamorphic alterations (**Fig. 3.8**). The diagram suggests that the degree of mobility increases in the order:

$$M_{Ni,Co} < M_{Fe,Hf} < M_{Ti,Zr,P,REE} < M_{Al}.$$

If Ni (or Co) was immobile during the alteration reactions, then Al_2O_3, P_2O_5, TiO_2, Fe_2O_3, Zr and REE were lost. In the most Ni-rich granofelses the net rock volume would have been reduced by about 90%. Alternatively, if Ti (or Zr,P,REE) was immobile Co, Ni, Hf and Fe_2O_3 should have been *added* to the system and Al_2O_3 should have been lost. Ultimately, the net rock volume would be reduced by 65%. Model-calculations that account for progressive leaching of silica and Ca, Mg, Na and K from a starting rock composition of sample JM137 yield slightly concave curves on diagrams of D_i vs f_v. Minimum f_v values achieved in "subtraction-only" models are about 40%. These values are reached when the rock is depleted in silica and (earth-) alkaline elements to the same extent as FF139. The strongly concave curvatures and low f_v values for Co, Ni, Hf and Fe_2O_3 in **Fig. 3.8** and the negative slopes for these elements in the low silica part of **Fig. 3.6A** suggest that *addition* of mass played a significant role in reaching the bulk compositions of Fe-Al granofelses with <25 wt% SiO_2.

From (1) net gains and losses of the major element oxides relative to 100g of starting composition (JM137) can be calculated for the ten **UBL**-rocks. This was done for SiO_2, Fe_2O_3, TiO_2, Al_2O_3 and P_2O_5 assuming zero mobility for Ni, Fe_2O_3, TiO_2 and Al_2O_3 respectively (**Fig. 3.9A-D**). Conservative behaviour of Fe or Ni (**Fig. 3.9A,B**) implies a significant loss of Al and other constituents (e.g. Zr, REE, Ti, P) that are often found to be relatively immobile during weathering processes. Alumina conservation (**Fig. 3.9D**) requires significant *addition* Fe_2O_3 (and Ni, Co and Hf) in the most Fe-rich rocks. Brimhall et al. (1988) reported metal enrichment (Fe, Al, Zr, Ti, Cr and Mo) by deposition of chemically mature aeolean dust in bauxites from Western Australia. Infiltration of detritus from external sources cannot be excluded for the **UBL**. However, in typical modern laterite profiles Fe is often internally inhomogeneously redistributed leading to the formation of "cuirasses" or ferruginous crusts. The Fe is normally liberated by the breakdown of Fe-bearing substances and may be redeposited *in situ* or in Fe-enrichment horizons elsewhere in the weathering horizon, depending mainly on pH and drainage characteristics. Zones of net depletion and net enrichment (i.e., supergene enrichment superimposed upon residual enrichment) can thus be defined for Fe, Ni and Co (Golightly 1981; Brimhall and Dietrich 1987). Aluminium and titanium migrate less easily and as a result several types of alteration banding may develop (Maignien 1966). Similar processes may have

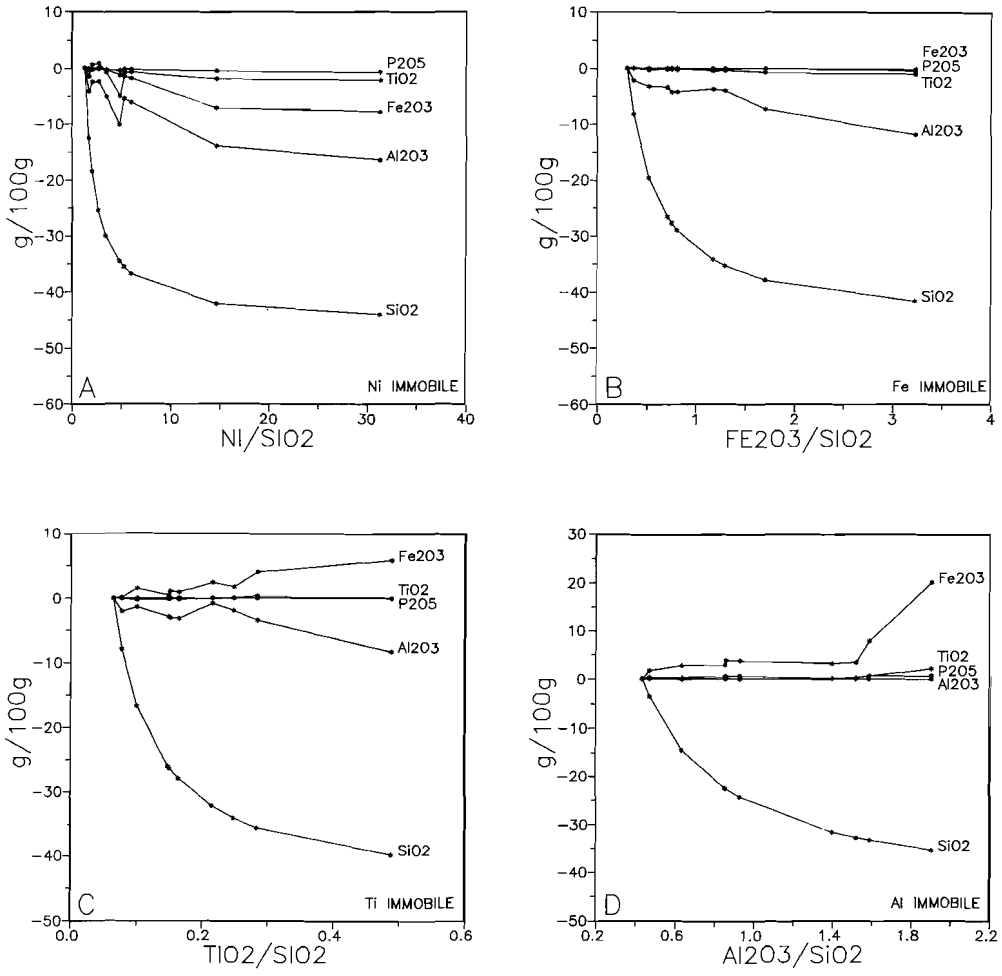

Fig. 3.9A-D: Net gains and losses of the major element oxides SiO_2, Al_2O_3, TiO_2 and P_2O_5 during lateritisation assuming isochemical behaviour of Ni (A), Fe_2O_3 (B), TiO_2 (C) and Al_2O_3 (D).

operated upon the **UBL** protolith, and **Fig. 3.9C** and **D** mimic modern lateritization processes more accurately than **Fig. 3.9A** and **B**.

If bulk chemical systematics of modern laterites can indeed be used as templates against which the chemical histories of ancient lateritic profiles can be read (cf. Nesbitt and Young 1989), it is conceivable that isochemical behaviour was most

closely approached by Al, Ti and the REE. A D-f_v curve of a truly immobile element would plot near the curves for TiO_2 and Al_2O_3 in **Fig. 3.8** and the net volume of the **UBL** protolith would be reduced by at least 50% in the Fe-Al granofelses.

Net depletion of REE (Kronberg et al. 1979) or REE fractionation (Duddy 1980; Nesbitt 1979) are reported for extreme weathering processes. Differential mobilities of the REE resulting from supracrustal and metasomatic alterations is not observed in the **UBL** and significant net depletion of the REE cannot be substantiated from our data (**Figs. 3.4L, 3.5, 3.6B**) suggesting that the bulk of the REE initially present in the **UBL**-protolith was accommodated in minerals resistant to weathering.

3.7 CONCLUSIONS

1) Basic granulites and high Fe-Al granofelses from the upper basic layer of the Faurefjell Formation have a common progenitor with basaltic affinities.

2) Premetamorphic processes that mainly involved the extraction of silica and the alkali and alkaline earth elements have shifted their original basaltic composition toward higher Fe, Al, Ti, P, Ni, Co, Zn, Zr, Nb, Y, Hf and REE contents and lower Si, Ca and Mg contents.

3) The bulk compositions of the Fe-Al granofelses compare well with those of modern laterites and the transition element variations in the **UBL** are best explained by premetamorphic weathering.

4) Metasomatism during diagenesis and during repeated high grade metamorphism blurred lateritic variations of K, Rb, Na, Ba, Ca and Mg and had negligible effects on ratios among Si, Fe, Al, Ti, P, Ni, Co, Zn, Zr, Nb, Y, Hf and REE.

5) Extreme premetamorphic alteration of the protolith of the **UBL** and superimposed chemical alterations during diagenesis and during three high-grade Proterozoic metamorphisms did not result in differential mobilities of REE. Net depletion of REE is not suggested by our data but cannot be ruled out.

6) Despite the high grade and long duration of the metamorphism, Gresens formula (1) could be applied successfully to assess relative mobilities of elements during premetamorphic open-system geochemical processes. This is due to: a) Si, P, REE and the other transition metals were *relatively* immobile during metamorphism, and b) the premetamorphic alteration resulted in a considerable range of specific gravities in the **UBL** rocks.

3.8 ACKNOWLEDGMENTS

We are indebted to R.J.P. Blok and J.H.A.M. Meertens for providing us their unpublished data. T. van Zessen, P. Anten, and W.J.H. Eussen are kindly thanked for analytical assistance. Constructive reviews by H.W. Nesbitt, R.D. Schuiling, J.M. Ferry, A.C. Tobi, S.P. Vriend and an anonymous reviewer are greatly appreciated. Financial support from NWO-grant 751-353-016 (LCGMB) is gratefully acknowledged.

3.9 REFERENCES

Bardossy G (1982) Karst bauxites: Bauxite deposits on Carbonate rocks. Elsevier, Amsterdam, 441 pp

Bol LCGM, Jansen JBH (1989) Proterozoic metasediments from the deep crust of Rogaland, SW Norway: Chemistry of metabasites and granofelses (ext. abstr.). In: D Bridgwater (Ed) Fluid movements- element transport and the composition of the deep crust, NATO Advanced Study Institute Series C vol 281, 111-113 pp

Bol LCGM, Bos A, Sauter PCC, Jansen JBH (1989) Barium-titanium rich phlogopites in marbles from Rogaland, southwest Norway (chapter II of this thesis). Am Mineral 74:439-447

Brimhall GH, Dietrich WE (1987) Constitutive mass balance relations between chemical composition, volume, density, porosity, and strain in metasomatic hydrochemical systems: Results on weathering and pedogenesis. Geochim Cosmochim Acta 51:567-587

Brimhall GH, Lewis CJ, Ague JJ, Dietrich WE, Hampel J, Teague T, Rix P (1988) Metal enrichment in bauxites by deposition of chemically mature eolian dust. Nature 333:819-824

Bruin M de (1983) Instrumental neutron activation analysis - a routine method. PhD Thesis, Delft University Press, Delft, 270 pp

Button A, Tyler N (1981) The character and Economic significance of Precambrian paleoweathering and erosion surfaces in southern Africa. Econ Geol 75th Anniv Vol (1905-1980) 686-709 pp

Condie KC (1976) Trace element geochemistry of Archean greenstone belts. Earth Sci Rev 12:393-417

Dekker AGC (1978) Amphiboles and their host-rocks in the high-grade Precambrian of Rogaland, SW Norway. PhD Thesis, Geol Ultraiectina 17, 277 pp

Duchesne JC Maquil R, Demaiffe D (1985) The Rogaland anorthosites: facts and speculations. In: Toby AC and Touret JLR (eds) The deep Proterozoic crust in the North Atlantic provinces, NATO ASI Series C Vol 158, Reidel, Dordrecht 449-476 pp

Duddy IR (1980) Redistribution of rare earth and other elements in a weathering profile. Chem Geol 30:363-381

Esson J (1983) Geochemistry of a nickeliferous laterite profile, Liberdade, Brazil. In: Wilson RCL (ed) Residual deposits: surface related weathering processes and materials. Geol Soc London Spec Publ 11:69-76

Feenstra A (1985) Metamorphism of Bauxites on Naxos, Greece. PhD thesis, Geol Ultraiectina 39, 206 pp

Floyd PA, Winchester JA (1978) Identification and discrimination of altered and metamorphosed volcanic rocks using immobile elements. Chem Geol 21:291-306

Gay AL, Grandstaff DE (1980) Chemistry and mineralogy of Precambrian paleosols at Elliot Lake, Ontario, Canada. Precambrian Res 12:349-373

Golani PR (1989) Sillimanite-Corundum deposits of Sonaphar, Meghalaya, India: a metamorphosed Precambrian paleosol. Precambrian Res 43:175-189

Golightly JP (1981) Nickeliferous Laterite Deposits. In: BJ Skinner (ed) Econ Geol 75th Anniv Vol (1905-1980): 710-734

Grandstaff DE, Edelman MJ, Foster RW, Zbinden E, Kimberly MM (1986) Chemistry and mineralogy of Precambrian paleosols at the base of the Dominion and Pongola Groups (Transvaal, South Africa). Precambrian Res 32:97-131

Gresens RL (1967) Composition-volume relationships of metasomatism. Chem Geol 2:47-65

Haskin LA (1979) On rare-earth element behavior in igneous rocks. In: Ahrens LH (ed) Physics and chemistry of the earth, vol 11. Pergamon Press, Oxford, 175-189 pp

Haskin MA, Haskin LA (1966) Rare Earths in European shales: a redetermination. Science 154:507

Haskin LA, Haskin MA, Frey FA, Wildeman TR (1968) Relative and absolute terrestrial abundances of the rare earths. In: Ahrens LH (ed) Origin and distribution of the elements. Pergamon, Oxford, 889-912 pp

Hermans GAEM, Tobi AC, Poorter RPE, Maijer C (1975) The high- grade metamorphic Precambrian of the Sirdal-Ørsdal area, Rogaland/Vest-Agder, South-west Norway. Nor Geol Unders 318:51-74

Holland HD (1984) The chemical evolution of the atmosphere and oceans. Princeton Univ Press, Princeton, NJ, 582 pp

Huijsmans JPP, Kabel ABET, Steenstra SE (1981) On the structure of a high-grade metamorphic Precambrian terrain in Rogaland, south Norway. Nor Geol Tidsskr 61:183-192

Huijsmans JPP (1985) Calc-alkaline lavas from the volcanic complex of Santorini, Aegean Sea, Greece. PhD Thesis, Geol Ultraiectina 41, 316 pp

Jacques de Dixmude S (1978) Geothermometrie comparée de roches du faciès granulite du Rogaland (Norvège méridionale). Bull Mineral 101:57-65

Jansen JBH, Schuiling RD (1976) Metamorphism on Naxos: Petrology and Geothermal gradients. Am J Sci 276:1225-1253

Jansen JBH, Blok RJP, Bos A, Scheelings M (1985) Geothermometry and Geobarometry in Rogaland and preliminary results from the Bamble Area, S Norway. In: Toby AC, Touret JLR (eds) The deep Proterozoic crust in the North Atlantic provinces, NATO ASI Series C Vol 158. Reidel, Dordrecht, 499-516 pp

Kars H, Jansen JBH, Tobi AC, Poorter RPE (1980) The metapelitic rocks of the polymetamorphic Precambrian of Rogaland, SW Norway - Part 2. Mineral relations between cordierite, hercynite and magnetite within the osumilite-in isograd. Contrib Mineral Petrol 74:235-244

Kimberley MM, Grandstaff DE (1986) Profiles of elemental concentrations in Precambrian paleosols on basaltic and granitic parent materials. Precambrian Res 32:133-154

Kronberg BI, Fyfe WS, Leonardos IR, OH, Santos AM (1979) The chemistry of some Brazilian soils: element mobility during intense weathering. Chem Geol 24:211-299

Maignien R (1966) Review of research on laterites. UNESCO natural resources research IV. Vaillant-Carmanne, Liège, 148 pp

Maijer C, Andriessen PAM, Hebeda EH, Jansen JBH, Verschure RH (1981) Osumilite, an approximately 970 Ma old high-temperature index mineral of the granulite-facies metamorphism in Rogaland, SW Norway. Geol Mijnb 60:267-272

Maijer C, Padget P (eds) (1987) The Geology of southernmost Norway. An excursion guide. Nor Geol Unders Spec Publ 1, 109 pp

McFarlane MJ (1983) A low level laterite profile from Uganda and its relevance to the question of parent material influence on the chemical composition of laterites. In: Wilson RCL (ed) Residual deposits: Surface related weathering processes and materials. Geol Soc London Spec Publ 11:69-76

Michot P (1960) La géologie de la catazone: Le problème des anorthosites, la palingénèse basique et la tectonique catazonale dans le Rogaland méridional (Norvège méridionale). In: Dons A (ed) Norway, Guidebook g. Witussen & Jensen AJS, Oslo, 52 pp

Millot G, Bonifas M (1955) Transformation isovolumétriques dans les phénomènes de latéritisation et de bauxitisation. Bull Serv Carte Geol Alsace Lorraine 8(1):3-19

Nance WB, Taylor SR (1977) Rare earth element patterns and crustal evolution -II Archean sedimentary rocks from Kalgoorlie, Australia. Geochim Cosmochim Acta 41:225-231

Nesbitt HW (1979) Mobility and fractionation of rare earth elements during weathering of a granodiorite. Nature 279:206-210

Nesbitt HW, Young GM (1989) Formation and diagenesis of weathering profiles. J Geol 97:129-147

Patterson SH (1971) Investigations of ferruginous bauxite and other mineral resources on Kauai and a reconnaissance of ferruginous bauxite deposits on Maui, Hawaii. US Geol Survey Prof Pap 656, 74 pp

Pearce JA (1982) Trace element characteristics of lavas from destructive plate boundaries. In: Thorpe RS (ed) Andesites: Orogenic andesites and related rocks. Wiley, Chichester, 526-548 pp

Persons BS (1970) Laterite. Genesis, location, use. Monographs in geoscience. In: RW Fairbridge (ed), Plenum Press, New York London, 103 pp

Reimer TO (1986) Alumina-rich rocks from the early Precambrian of the Kaapvaal craton as indicators of paleosols and as products of other decompositional reactions. Precambrian Res 32:155-179

Reinhardt J, Sigleo WR (eds) (1988) Paleosols and weathering through geologic time: Principles and applications. Geol Soc Am Spec Pap 216, 181 pp

Retallack G (1986) Reappraisal of a 2200 Ma-old paleosol near Waterval Onder, South Africa. Precambrian Res 32:195-232

Sauter PCC (1981) Mineral relations in siliceous dolomites and related rocks in the high-grade metamorphic Precambrian of Rogaland, SW Norway. Nor Geol Tidsskr 61:35-45

Sauter PCC (1983) Metamorphism of siliceous dolomites in the high-grade Precambrian of Rogaland, SW Norway. PhD Thesis, Geol Ultraiectina 32, 143 pp

Sauter PCC, Hermans GAEM, Jansen JBH, Maijer C, Spits P, Wegelin A (1983) Polyphase Caledonian metamorphism in the Precambrian basement of Rogaland/Vest-Agder, Southwest Norway. Norg Geol Unders 380:7-22

Schau M, Henderson JB (1983) Archean chemical weathering at three localities on the Canadian shield. Precambrian Res 20:189-224

Tobi AC, Hermans GAEM, Maijer C, Jansen JBH (1985) Metamorphic zoning in the high-grade Proterozoic of Rogaland-Vest Agder. In: Tobi AC, Touret JLR (eds) The deep Proterozoic crust in the North Atlantic provinces, NATO ASI Series Vol 158, Reidel, Dordrecht, 499-516 pp

Tracy RJ, McLellan EL (1985) A natural example of the kinetic controls of compositional and textural equilibration. In: Thompson AB, Rubie DC (eds) Metamorphic reactions: kinetics, textures and deformation. Advances in physical chemistry, vol 4. Springer, New York Berlin Heidelberg, 118-137 pp

Tracy RJ, Thompson AB (1979) Partial fusion and magma hybrydisation, Cortland complex, New York (abstract). EOS Trans Am Geophys Union 60:411.

Valeton I (1972) Bauxites. Elsevier, Amsterdam, 226 pp

Valeton I (1983) Paleoenvironment of lateritic bauxites with vertical and lateral differentiation. In: Wilson RCL (ed) Residual deposits: Surface related weathering processes and materials. Geol Soc London Spec Publ 11:77-90

Verschure RH, Andriessen PAM, Boelrijk NAIM, Hebeda EH, Maijer C, Priem HN, Verdurmen EA (1980) On the thermal stability of Rb-Sr and K-Ar biotite systems: Evidence from coexisting Sveconorwegian (ca 870 Ma) and Caledonian (ca 400 Ma) biotites in SW Norway. Contrib Mineral Petrol 74:245-252

Voncken JHL, Vriend SP, Kocken JWM, Jansen JBH (1986) Determination of beryllium and its distribution in rocks of the Sn-W granite of Regoufe, northern Portugal. Chem Geol 56:93-103

Wielens JBW, Andriessen PAM, Boelrijk NAIM, Hebeda EH, Priem HNA, Verdurmen EA, Verschure RH (1980) Isotope geochronology in the high-grade metamorphic Precambrian of southwestern Norway: new data and reinterpretations. Nor Geol Unders 359: 1-30

Wilson RCL (ed) (1983) Residual deposits: Surface related weathering processes and material. Blackwell, London, 259 pp

Winchester JA, Floyd PA (1977) Geochemical discrimination of different magma series and their differentiation products using immobile elements. Chem Geol 20:325-343

Winkler HGF (1979) Petrogenesis of metamorphic rocks. Springer, New York Berlin Heidelberg, 348 pp

CHAPTER IV: REGIONAL OXYGEN AND CARBON ISOTOPIC TRENDS IN GRANULITE-FACIES MARBLES FROM ROGALAND, SW NORWAY

4.0 ABSTRACT

Oxygen and carbon isotopic ratios of calcites in marbles from the very high-grade Precambrian terrane of Rogaland, SW Norway, show a regional trend from $\delta^{18}O = 21.5$ (SMOW) and $\delta^{13}C = -3.2$ (PDB) near the contact with the Rogaland anorthositic complex to $\delta^{18}O = 13.1$ and $\delta^{13}C = -8.2$ respectively ±30 km further north. This isotopic trend is geographically the opposite of the regular $\delta^{18}O$ and $\delta^{13}C$ depletion trends which are observed in carbonate rocks from other thermometamorphic aureoles. In the marbles, the calcite (O,C) isotopic trend is in accordance with oxygen isotope ratios of high-grade metamorphic silicate minerals (diopside, phlogopite). In contrast, no regional $\delta^{18}O$ has been observed either for quartz and diopside in quartz-diopside gneisses and quartzites of the metasedimentary succession which includes the marbles, nor in quartz, plagioclase and orthopyroxene in enderbites enveloping the metasediments. It is concluded that the intrusion of the magmatic complex, which is held responsible for the dry peak metamorphic granulite facies conditions, merely preserved bulk isotopic characteristics that already existed in the marbles. Evidence for preservation of premetamorphic $\delta^{18}O$ systematics in a metalateritic layer associated with the marbles is ambiguous from $\delta^{18}O$ values of individual metalaterite minerals (magnetite, sillimanite, plagioclase, orthopyroxene). The isotopic inhomogeneity of distinct metamorphic minerals (calcite, quartz, diopside) in various lithologies (marbles, quartz-diopside gneisses, quartzites, metalaterites and enderbites), both in outcrop- and in regional scale, preclude pervasive regional passage of isotopically homogeneous oxygen-bearing metamorphic fluids. The absence of such fluids is in accordance with petrographic observations throughout the area.

4.1 INTRODUCTION

Systematic relations between oxygen and carbon isotope ratios are observed in carbonate rocks and minerals of many contact-metamorphic aureoles. Invariably marbles become progressively depleted in $^{18}O/^{16}O$ and $^{13}C/^{12}C$ ratio as the degree of metamorphism increases with decreasing distance from the pluton (Valley 1986, and

references therein). The processes invoked to explain these trends include volatilization reactions, introduction of meteoric water, infiltration of magmatic/metamorphic fluids, isotopic exchange with graphite or combinations thereof, and may cause shifts of 15 permil or more for $\delta^{18}O$ and 5 permil or more for $\delta^{13}C$. Large regional stable isotopic shifts are less common and isotopic homogeneity of distinct metamorphic minerals in various lithologies over considerable distances have been proposed to be related to large scale pervasive fluid movements (Taylor et al. 1963).

The Proterozoic metamorphic envelope of the Rogaland anorthosite complex, SW Norway, represents one of the best studied high-temperature granulite-facies terranes (Michot 1960; Hermans et al. 1975; Tobi and Touret 1985; Maijer and Padget 1987). Excellent field control exists due to extensive mapping over more than two decades. The isograd pattern and the peak metamorphic temperatures involved are reminiscent of contact metamorphism (Tobi et al. 1985). However, the very high-grade metamorphic events related to the complex multistage intrusion of the anorthositic bodies affected both the country rocks and the magmatic complex (Duchesne et al. 1985) on a regional scale. Hence, the term "regional thermometamorphism" is more appropriate than "contact metamorphism" (Maijer et al. 1981).

In this study, systematic regional-scale, oxygen and carbon isotopic shifts are reported for calcites from impure dolomitic marbles that occur as intercalations in one particular granulite facies metasedimentary unit at various distances from the Rogaland anorthosite complex. In contrast to what is normally seen in metamorphic aureoles, the calcites closest to the intrusive complex are isotopically closer to sedimentary values than calcites from more distant marble exposures. The calcite isotopic data are related to the modal composition of the marbles and discussed in view of oxygen isotopic ratios in silicate minerals (*Di,Phl,Kfs*[1]) associated with the calcites, in silicate minerals (*Di,Qtz*) from diopside gneisses that sandwich the marbles and silicate (and oxide) minerals (*Qtz, Pl, Opx, Amp, Bt, Sil, Mag, Spl*) from country rocks that are part of or envelop the metasedimentary units. The (O,C) isotopic compositions of calcites and graphites from other units are used to bracket the scale and timing of isotopic exchange. The ultimate purpose of this study is to put

[1]see Appendix A for mineral abbreviations

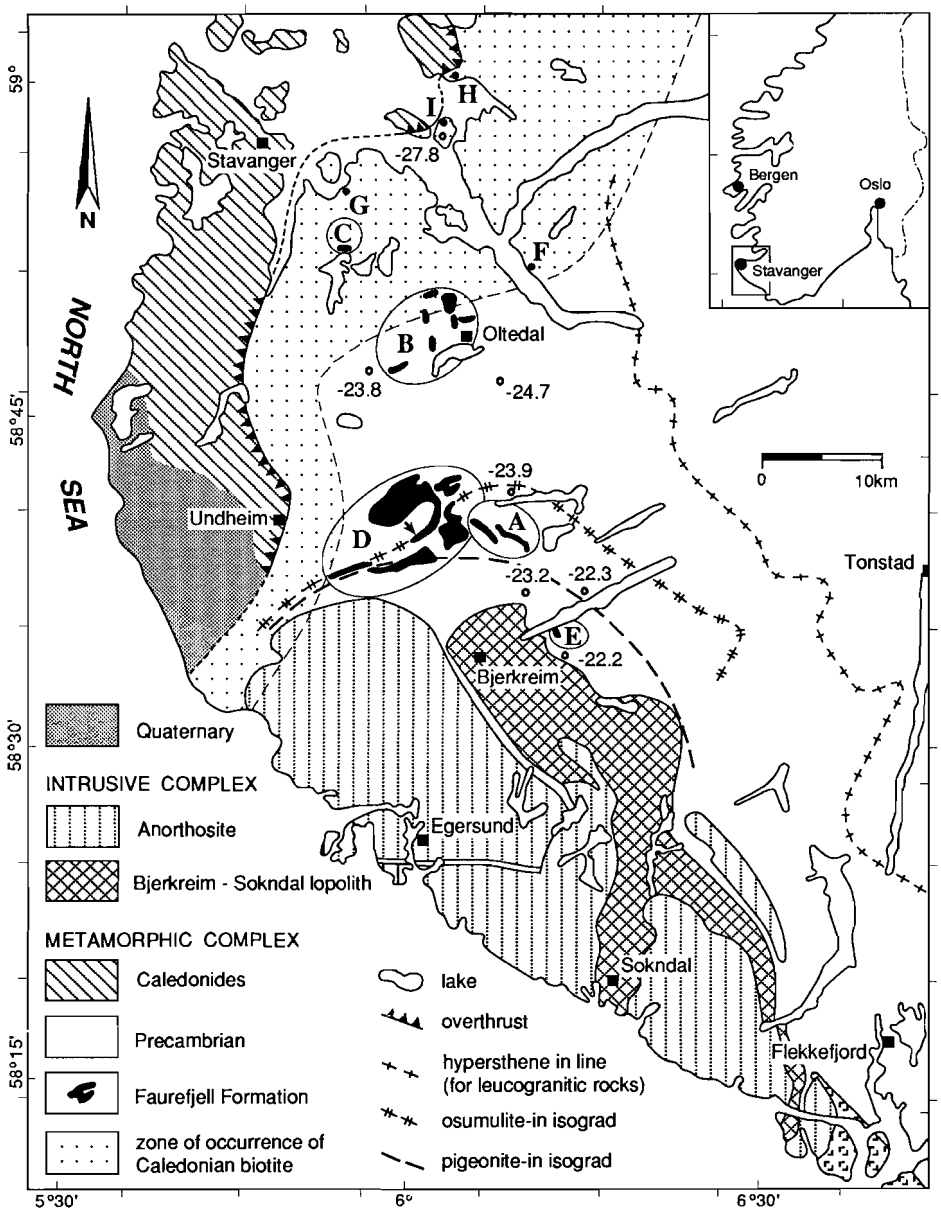

Fig. 4.1: Simplified geological map of SW Norway. A-E: Exposures of the **FF**. F-I: Locations of carbonate samples outside the **FF**. Numbers (-22.2 etc.): $\delta^{13}C$ values of graphite in garnetiferous migmatites and breccia. The arrow indicates the sole occurrence of marble in area D.

constraints on fluid budgets during granulite-facies conditions in the Rogaland area.

4.2 GEOLOGICAL SETTING

Massif-type anorthosites and the folded anorthositic to mangeritic Bjerkreim-Sokndal lopolith are exposed in the western part of the Precambrian basement in S.W. Norway (**Fig. 4.1**; Duchesne et al. 1985). These intrusive units are surrounded by a Precambrian polymetamorphic complex of Charnockitic and Granitic Migmatites with intercalations of augen gneisses and metasupracrustal rocks (Hermans et al. 1975). The latter are comprised of the Gyadal Garnetiferous Migmatites (Huijsmans et al. 1981) and the Faurefjell Metasediment Formation (**FF**) (Sauter 1981).

On the basis of mineral assemblages, four stages of metamorphism (**M1-M4**) have been recognized in the metasupracrustal units and in their enveloping migmatitic complex (**Fig. 4.2**).

The **M1** phase (about 1200 Ma) has been related to an old upper amphibolite to granulite facies metamorphism (Wielens et al. 1980; Maijer and Padget 1987).

The granulitic high temperature-intermediate pressure **M2** stage (1050 Ma) is essentially a thermal overprint induced by the intrusion of the leuconoritic phase of the Bjerkreim-Sokndal lopolith (Maijer et al. 1981). Metamorphic zoning related to the **M2** stage (Tobi et al. 1985) is manifest by **a**) a pigeonite-in isograd, **b**) an osumilite-in isograd, **c**) a garnet decomposition isograd, **d**) a (amphibole + quartz)-out isograd, and **e**) a hypersthene line (see **Fig. 4.1** for position of **a**, **b** and **e**; **c** approximately coincides with **b**, and **d** occurs a few km west of **e**). Geothermometric calculations yield temperatures of about 1050°C between the pigeonite-in isograd and the igneous complex, decreasing to about 750°C near the hypersthene line (Jacques de Dixmude 1978; Jansen et al. 1985).

The **M3**-stage of medium-grade metamorphism represents a period of retromorphism during slow, almost isobaric, post-**M2** regional cooling (Kars et al. 1980). **M3** features include exceptionally well developed exsolution phenomena and partial decomposition of typical **M2** minerals (e.g., osumilite, Al-rich orthopyroxene) into symplectites of lower grade minerals. In the vicinity of pegmatites and granites, **M3** micas and amphiboles may form rims around **M1** and **M2** minerals. Isotopic ages for osumilite (970 Ma (K-Ar; Rb-Sr), Maijer et al. 1981), hornblendes (950 Ma (K-Ar), Dekker 1978; Wielens et al. 1980), and brown biotite (870 Ma (K-

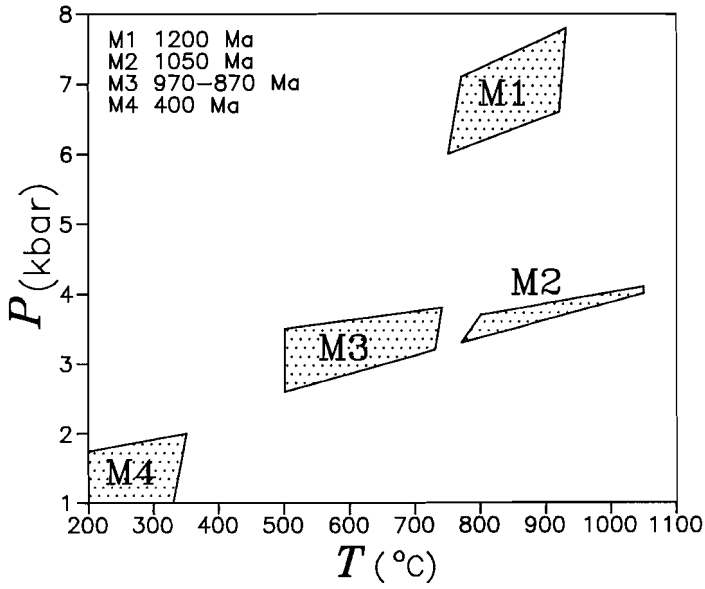

Fig. 4.2: Compilation of P-T-t estimates for **M1-M4** (see text) (after: Jansen et al. 1985; Maijer and Padget 1987).

Ar; Rb-Sr), Verschure et al. 1980) reflect passage through Rb-Sr and K-Ar closure temperatures during **M3** cooling.

Finally an **M4**-stage of retrograde prehnite-pumpellyite to greenschist facies metamorphism (400 Ma) is weak and omnipresent in the west and is attributed to the Caledonian orogeny (Verschure et al. 1980). An isograd of Caledonian green biotite follows the Caledonian front at a distance of 5-15 km in the Precambrian basement (**Fig. 4.1**) and is related to Caledonian overthrusting (Sauter et al. 1983).

Exposures of the **FF** are largely concentrated in five areas (A - E, **Fig. 4.1**) where it crops out as thin folded layers or boudinaged lenses with a total thickness varying from 10 to 50 meters. The contacts with the surrounding migmatites are usually concordant. Locally, in areas B and C, leucogranites intrude the metasediments discordantly. Diagnostic for the **FF** is the joint occurrence of thick quartzite layers and impure dolomitic marbles. Generally, the **FF** is composed of various intercalations of quartz-diopside gneisses, diopside marbles, forsterite marbles, quartzites, quartz-K-feldspar rocks, diopside-K-feldspar rocks, K-feldspar rocks, diopside rocks, leuco-charnockites, and heterogeneous basic layers consisting of basic granulites and Fe-Al rich granofelses (lacking in area C). The basic granulites and the Fe-Al granofelses have transitional bulk compositions that are interpreted as resulting from the combined effects of premetamorphic lateritization and syndiagenetic

metasomatism (Bol et al. 1989b).

The marbles cover only a very small part of the total mapped area (<0.01%). Most of them occur in areas A, B and C, usually as intercalations in quartz-diopside gneisses or, alternatively, in quartzo-feldspathic rocks. The marbles are generally separated from their host lithology by thick, almost monomineralic, diopside-layers. Marbles are subordinate in area E, and only one marble exposure is found in area D (see arrow in **Fig. 4.1**).

Seven distinct rock types from the metamorphic complex are considered in this study: 1) marbles and diopside rocks; 2) quartzites; 3) quartz-diopside gneisses; 4) metalaterites; 5) enderbites; 6) graphite-bearing rocks; and 7) miscellaneous calcite-bearing rocks. 1-4 Belong to the **FF**, 5 occurs within the Charnockitic Migmatites that envelop the **FF**, 6 comprises rocks from various other calcite-bearing units (locations **F-I, Fig 1**) that are not considered to be part of the **FF** and 7 are samples from the Gyadal Garnetiferous Migmatites. In **Appendix A**, the general petrography of types 1-7 is summarized and sample descriptions are given. Mineral associations in individual samples are given in **Table 4.A.**

4.3 METHODS OF INVESTIGATION

Carbon and oxygen isotope analyses on 47 carbonate mineral separates (mainly high-Mg calcites) and 7 graphites were performed at the Utrecht Stable Isotope Laboratory. Carbonates were reacted with 100% H_3PO_4 (McCrea 1950), graphite was combusted with CuO. The reproducibility of replicate analyses was better than ±0.1 permil for the carbonates and better than 0.2 permil for graphite (values of $\delta^{18}O$ and $\delta^{13}C$ are reported in standard permil notation relative to SMOW and PDB respectively).

Oxygen isotope analyses on silicate minerals, magnetites and spinel were performed in the Department of Geology and Geophysics, University of Wisconsin, Madison, following the methods of Clayton and Mayeda (1963) using BrF_5 as the oxidizing reagent. The minerals were separated from the rock and purified using heavy-liquid and magnetic methods. The purity of the separates was checked by XRD and optical methods and was above 95% except a) in mixed *Pl+Qtz* (>85%*Pl*) separates from country-rocks (enderbites) and b) in some of the *Phl* separates from marbles and *Di*-rocks where variable amounts (up to 20%) of *Srp* were observed. The

mixed *Pl* + *Qtz* separates were reacted with concentrated HF in order to retain pure quartz. Both the quartz and the mixture were analyzed for $\delta^{18}O$. The separates with partly serpentinized *Phl* were further purified by hand-picking, and in one instance both the purified and the serpentinized separate were analyzed for $\delta^{18}O$. Of the 125 silicate and oxide mineral separates analyzed in Madison, 69 were duplicated, with an average standard deviation of < 0.15 permil for *Pl*, *Qtz* and *Opx*, 0.25 permil for *Phl*, 0.3 permil for *Di*, 0.4 permil for *Sil* and 0.7 permil for *Mag*. The value of NBS-28 was 9.42 ± 0.17 permil (based on 14 analyses).

Modal compositions are determined for 22 marbles and are based on the count of 1000 points or more per sample. In order to assess for these samples the F(C) and F(O) values (the mole fractions of carbon and oxygen remaining in the rock after the decarbonation reactions), for each silicate mineral and for *Spl* the mole equivalent of CO_2 was calculated, starting with the components *Qtz*, *Dol* and *Kfs* and using the simple mass balance equations:

$$2Dol + 1Qtz = 1Fo + 2Cal + 2CO_2 \quad (1)$$

$$1Dol + 2Qtz = 1Di + 2CO_2 \quad (2)$$

$$3Dol + 1Kfs + 1H_2O = 1Phl + 3Cal + 3CO_2 \quad (3)$$

$$13Dol + 2Kfs = 6Fo + 13Cal + 1Spl + 13CO_2 + 1K_2O \quad (4)$$

$$3Dol + 4Qtz + 1H_2O = 1Tlc + 3Cal + 3CO_2 \quad (5)$$

$$5Dol + 8Qtz + 1H_2O = 1Tr + 3Cal + 7CO_2 \quad (6)$$

This yields an equivalence of 2 mole CO_2 for each mole of *Fo*, $2CO_2$ for each *Di*, $3CO_2$ for each *Phl*, $13CO_2$ for $1Spl + 6Fo$, $3CO_2$ for each *Tlc* and $7CO_2$ for each *Tr*. Combining the amount of outgassing as calculated from these CO_2-equivalents and the modes of silicate minerals and spinel, with the amount of CO_2 still present in the rock as calculated from the mode of the carbonate minerals, estimates of F(C) and F(O) are obtained.

The wt% CO_2 in marble samples is obtained volumetrically upon dissolution in acid.

4.4 RESULTS

The $\delta^{18}O$ and $\delta^{13}C$ values for *Cal* in 42 marbles from areas A-E are presented in **Table 4.1** together with the $\delta^{18}O$ values of silicate minerals from the marbles and the *Di*-rocks, and the wt% CO_2 of the marbles. The $\delta^{18}O$ and $\delta^{13}C$ values of silicate minerals, oxides, carbonates and graphites from associated rocks are presented in

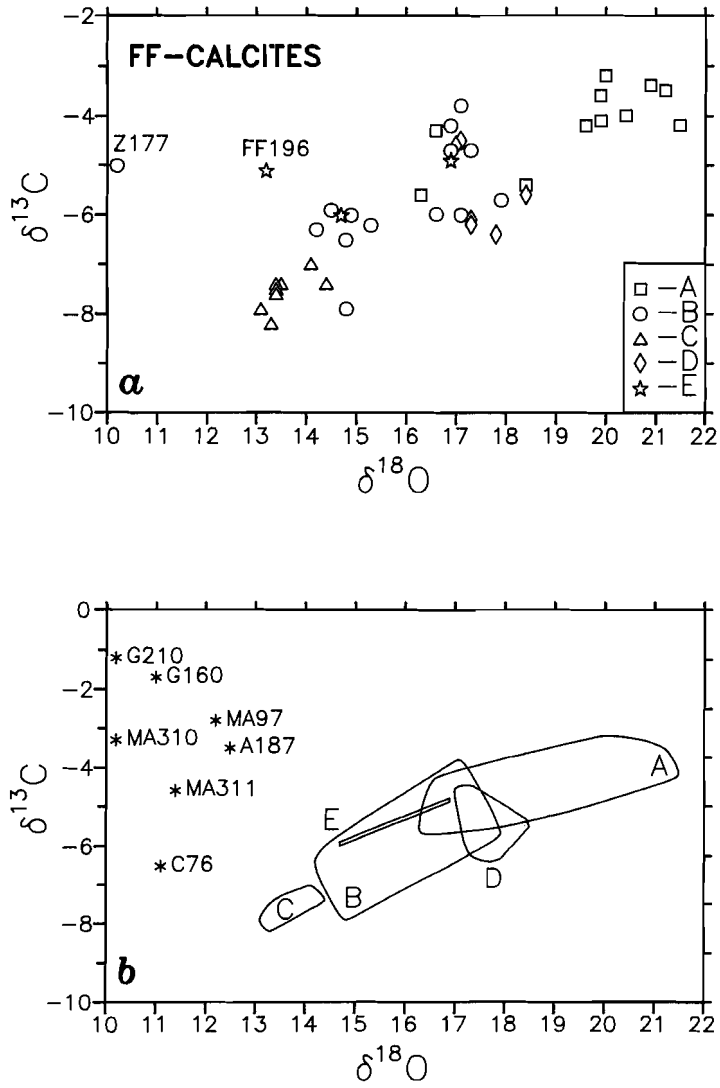

Fig. 4.3a-b:
a) $\delta^{18}O$ *vs.* $\delta^{13}C$ values of calcites from **FF marbles** in areas A-E.
b) $\delta^{18}O$ *vs.* $\delta^{13}C$ values of carbonate minerals from locations F-I (=*). Generalized fields are drawn for calcite data from area A-E, omitting the anomalous isotopic compositions of Z177 (B) and FF196 (E) (see text).

Tables 2-7. In **Table 4.8** the results of the modal analyses of 22 marbles from areas A-C are reported along with the F(O) and F(C) values. Additional information on the degree of retrogradation of the silicate minerals and the degree of recrystallization of the calcites is included in **Table 4.8.**

Table 4.1: Isotopic data (O,C) for marbles and diopside rocks

Sample#		Type	Loc	$\delta^{13}C$	$\delta^{18}O$				wt% CO_2
				Cal	*Cal*	*Di*	*Phl*	*other*	
A122	▪	*Fo*-marble	A	-4.0	20.4	-	16.1	-	24
A164	▪	*Fo*-marble	A	-3.2	20.0	21.1	17.5	-	16
A169		*Fo*-marble	A	-	-	-	16.2	-	24
C322	▪	*Di*-marble	A	-4.3	16.6	16.6	-	-	2
C324	▪	*Fo*-marble	A	-5.6	16.3	-	-	-	13
C335	▪	*Fo*-marble	A	-4.2	19.6	-	-	-	21
C346	▪	*Fo*-marble	A	-4.2	21.5	-	-	-	34
C480	▪	*Fo*-marble	A	-3.5	21.2	-	11.2	-	26
C481	▪	*Fo-Di*-marble	A	-3.6	19.9	20.4	19.1	-	21
FF167		*Di*-rock	A	-	-	15.0	-	-	-
FF171A		*Di*-rock	A	-	-	15.7	-	-	-
FF174		*Fo*-marble	A	-5.4	18.4	-	-	-	11
FF175		*Di*-rock	A	-	-	15.5	-	-	-
FF179		*Di*-rock	A	-	-	14.6	-	-	-
FF182		*Di*-rock	A	-	-	14.2	-	-	-
FF185		*Di*-rock	A	-	-	15.2	-	-	-
FF273		*Di*-nodule	A	-3.4	20.9	19.3	-	-	1
FF277		*Di*-nodule	A	-	-	18.1	-	17.3[a]	-
FF283		*Fo*-marble	A	-4.1	19.9	-	-	-	19
C372	▪	*Fo*-marble	B	-3.8	17.1	-	-	-	32
C397		*Di*-rock	B	-6.5	14.8	-	12.0	-	1
C499A		*Kfs*-vein	B	-	-	-	-	14.9[a]	-
C500A		*Di*-rock	B	-	-	14.0	10.7	-	-
C500B		*Di*-marble	B	-	-	14.3	11.4	-	26
C502A		*Di-Kfs*-rock	B	-7.9	14.8	14.0	-	14.6[a]	1
C502B		*Di*-rock	B	-	-	14.2	-	-	-
C509	▪	*Fo*-marble	B	-6.0	16.6	-	11.2	-	30
C510	▪	*Fo*-marble	B	-5.7	17.9	-	-	-	30
C511	▪	*Fo*-marble	B	-6.0	17.1	-	-	-	28
C512		*Fo*-marble	B	-7.9	15.3	-	-	-	29
C514		*Fo*-marble	B	-6.0	14.9	-	-	-	27
Q128	▪	*Tr*-marble	B	-4.7	16.9	16.3	12.8	-	28
Q138		*Fo*-marble	B	-4.7	17.3	-	-	-	28
Q201		*Fo*-marble	B	-4.2	16.9	-	-	-	30
Z52	▪	*Fo*-marble	B	-5.9	14.5	-	-	-	29
Z75	▪	*Fo*-marble	B	-6.3	14.2	-	-	-	24
Z177	▪	*Di*-marble	B	-5.0	10.2	18.7	-	-	7
C163		*Tr*-vein	C	-7.5	13.4	-	-	-	26
C165		*Di-Phl*-rock	C	-	-	12.3	9.1	8.6[b]	-
C235		*Di*-marble	C	-7.7	13.4	12.8	-	-	18

Table 4.1: - *continued*

Sample#	Type	Loc	$\delta^{13}C$	$\delta^{18}O$				wt% CO_2
			Cal	*Cal*	*Di*	*Phl*	*other*	
C236	▪ *Fo*-marble	C	-7.4	13.4	-	-	-	30
C264	▪ *Di*-marble	C	-7.5	14.4	-	8.9	-	33
C273	▪ *Fo*-marble	C	-7.4	13.5	-	9.5	-	24
C521	▪ *Di*-marble	C	-7.0	14.1	12.2	9.7	-	13
C522	▪ *Di-Fo*-marble	C	-8.2	13.3	9.8	8.6	-	15
C533	▪ *Fo*-marble	C	-7.9	13.1	-	12.0	-	23
FF4B	*Di*-marble	D	-6.2	17.3	-	-	-	13
FF4C	*Di*-marble	D	-6.1	17.3	-	-	-	16
FF47	*Di*-marble	D	-6.4	17.8	-	-	-	9
FF51	*Di-Kfs*-rock	D	-4.5	17.1	-	-	-	1
FF52	*Di*-rock	D	-4.6	17.0	-	-	-	1
FF53	*Di*-marble	D	-5.6	18.4	-	-	-	1
FF260	*Di-Kfs-Q*-vein	D	-	-	14.4	-	17.4[c)]	-
FF142	*Fo*-marble	E	-6.0	14.7	-	-	-	25
FF190	*SpDiPhl* vein rim		-	-	13.1	12.7	-	-
FF190	core	E	-	-	-	13.3	12.7[d)]	-
FF192	*Fo*-marble	E	-4.9	16.9	-	-	-	23
FF196	*Fo*-marble	E	-5.1	13.2	-	-	-	18

▪ = Modal compositions are determined for the marked samples, see **Table 4.8**.
a) = K-Feldspar; **b)** = Partly serpentinized (20% *Srp*) phlogopite; **c)** = Quartz; **d)** = Spinel; correlation coefficient for $\delta^{18}O$(cal) vs. $\delta^{13}C$(cal) = 0.72; for $\delta^{18}O$(Cal) vs. $\delta^{18}O$(Di) = 0.72; for $\delta^{18}O$(Cal)vs.$\delta^{18}O$(Phl) = 0.70; for $\delta^{18}O$(Di)vs.$\delta^{18}O$(Phl) = 0.97.

1 marbles and diopside rocks

The **calcites** from the major marble outcrops define a $\delta^{18}O$-$\delta^{13}C$ trend from about $\delta^{18}O = +21.5$ and $\delta^{13}C = -3.2$ for the southernmost areas A, D and E to about $\delta^{18}O = 13.1$ and $\delta^{13}C = -8.2$ for those of the northern area C (**Fig. 4.3a**). Calcites from area B have intermediate values of about $\delta^{18}O = +17$ and $\delta^{13}C = -5$. There are some notable deviations from the mean values within each area. In **area A** ($\delta^{18}O = 16.3$ to

Fig. 4.4a-b (opposite page): $\delta^{18}O$ values of *Cal*, *Di*, *Phl* and *Kfs* of **marbles** and **diopside rocks** in areas A-E. b) Relative oxygen isotopic compositions of *Cal*, *Di*, *Phl* and *Kfs* at various temperatures (°C) as inferred from isotopic fractionation factors reported by Bottinga and Javoy (1973,1975) and O'Neil et al. (1969). Fractionation factors for *Phl* are not defined for temperatures above 800°C.

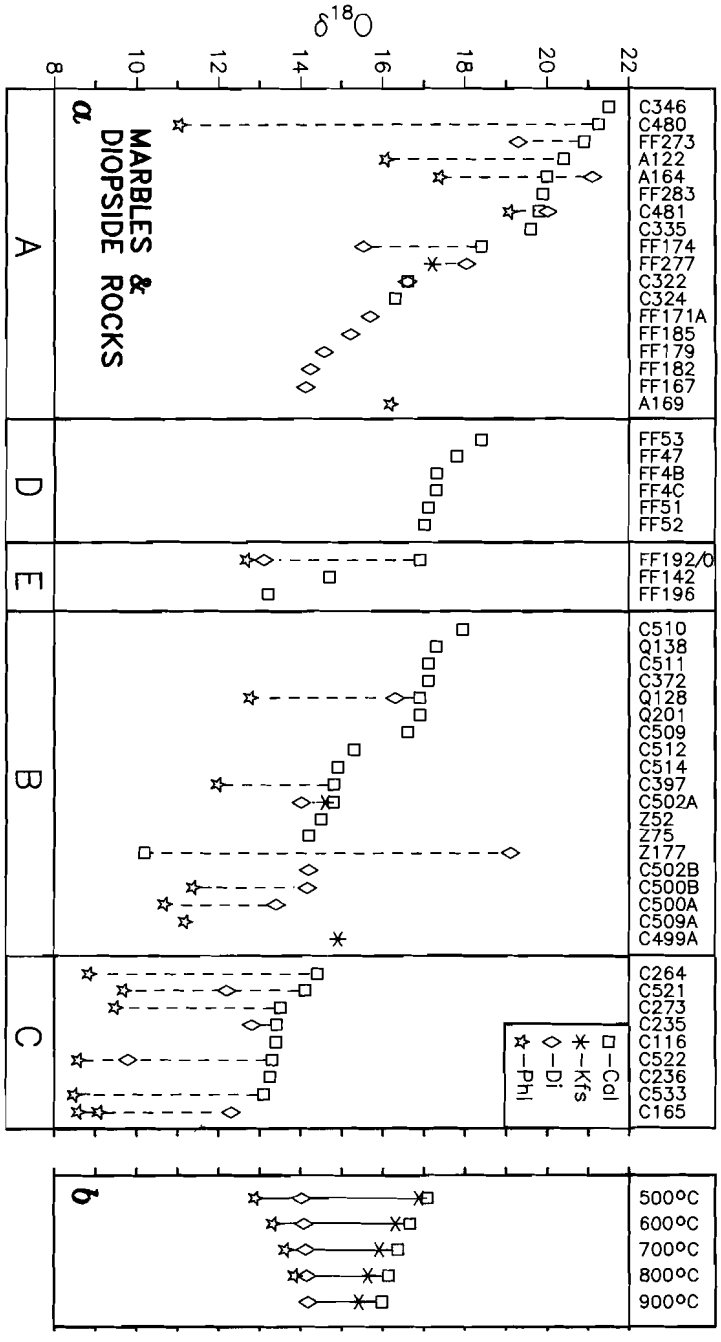
δ18O
8
10
12
14
16
18
20
22
a
MARBLES & DIOPSIDE ROCKS
A
C346
C480
FF273
A122
A164
FF283
C481
C335
FF174
FF277
C322
C324
FF171A
FF185
FF179
FF182
FF167
A169
D
FF53
FF47
FF4B
FF4C
FF51
FF52
E
FF192/0
FF142
FF196
B
C510
Q138
C511
C372
Q128
Q201
C509
C512
C514
C397
C502A
Z52
Z75
Z177
C502B
C500B
C500A
C509A
C499A
C
C264
C521
C273
C235
C116
C522
C236
C533
C165
□—Cal
✳—Kfs
◇—Di
☆—Phl
b
500°C
600°C
700°C
800°C
900°C

21.5; $\delta^{13}C = -5.6$ to -3.2), three samples contain calcites which are distinctly lower in $\delta^{18}O$ and slightly lower in $\delta^{13}C$, and which fall in the generalized data field of area B. In **area B** ($\delta^{18}O = 10.2$ to 17.9; $\delta^{13}C = -7.9$ to -4.2), the chloritized *Di*-marble, Z177, has the lowest $\delta^{18}O$ value of all **FF** calcites ($\delta^{18}O = 10.2$) and does not fall on the main $\delta^{13}C$-$\delta^{18}O$ trend for calcites (**Fig. 4.3a**). The (O,C) isotopic ratios in calcites from **area C** define a narrow range ($\delta^{18}O = 13.1$ to 14.4; $\delta^{13}C = -8.2$ to -7.0). The isotopic composition of *Cal* from the *Cal-Tr* vein C163 does not deviate notably from those of the marble calcites (**Table 4.1**). Calcites in six silica-rich *Di*-marble samples from the small marble exposure in **area D** ($\delta^{18}O = 17.0$ to 18.4; $\delta^{13}C = -6.4$ to -4.5), coincide isotopically more or less with the low $\delta^{18}O$ calcites in samples from the nearby area A. Calcites in three samples from the marble layer in **area E** have a limited $\delta^{13}C$ (-6.0 to -5.1), and a wide $\delta^{18}O$ variability (13.2 to 16.9). The marble FF196 is most heavily retrograded and does not fall on the main trend (**Fig. 4.3a**).

Phlogopites in *Di*-marbles, *Fo*-marbles and intimately associated *Phl*-bearing *Di*-rocks from the principal marble occurrences (A, B and C) roughly follow the regional $\delta^{18}O$ trend of the calcites (**Fig. 4.4a**). In sample C165 (area C), partially serpentinized *Phl* (20% *Srp*) is slightly lower in $\delta^{18}O$ than its fresh counterpart ($\delta^{18}O = 8.6$ and 9.1, respectively, see **Table 4.1** and **Fig. 4.4a**).

Diopsides in *Di*-marbles, and, less prominently, in *Di*-rocks also show a regional $\delta^{18}O$ shift. *Di* in six samples from a profile across a >5m thick *Di*-rock layer in **area A** ($\delta^{18}O = 14.2$-15.7; **Fig 15**) is notably lower in $\delta^{18}O$ than *Di* in marbles from the same area ($\delta^{18}O = 16.6$-21.1). *Di* in two *Di*-nodules from **area A** have oxygen isotopic compositions ($\delta^{18}O = 18.1$-19.3) similar to *Di* in the *Di*-marbles. In **area B**, *Di* in *Di*-rocks ($\delta^{18}O = 14.0$-14.2) also has lower oxygen isotopic ratios than *Di* in marbles ($\delta^{18}O = 14.3$-18.7), whereas in **area C**, *Di* from a *Di*-rock ($\delta^{18}O = 12.3$) falls within the range of values for *Di* in marbles ($\delta^{18}O = 9.8$-12.8). *Di* ($\delta^{18}O = 14.4$) in *Di-Kfs-Qtz* vein FF260 from **area D** and *Di* from the rim ($\delta^{18}O = 13.1$) and the core ($\delta^{18}O = 12.7$) of *Spl-Di-Phl* vein FF190 in **area E** are isotopically similar to *Di* in *Di*-rocks from areas A-C (see **Table 4.1**). For comparison, $\delta^{18}O$ of *Di* and *Phl* from the rim of vein FF190 is plotted in **Figure 4.4a** below $\delta^{18}O$ of *Cal* from FF192, which represents the *Fo*-marble directly adjacent to this vein.

Within most samples the order of minerals (if present) with increasing $\delta^{18}O$ is: *Phl* < *Di* < *Cal*, as would be expected (**Fig. 4.4a**). *Cal-Di* reversals are observed in area A for A164 and C481, and in area B for Z177, the latter also having an

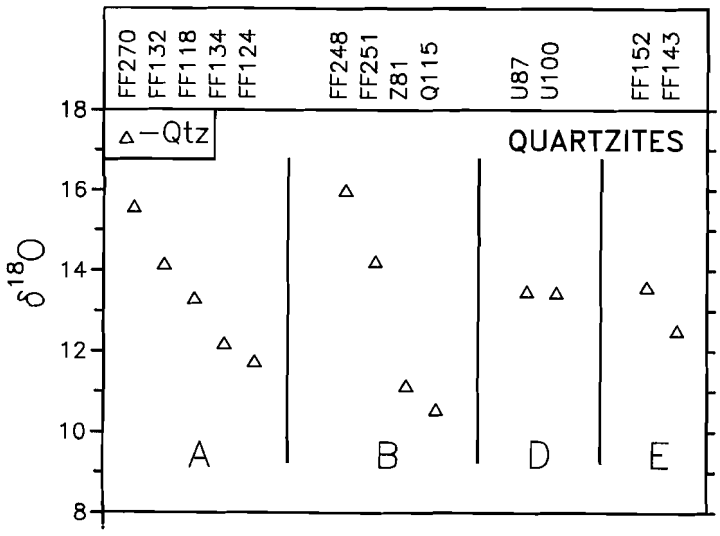

Fig. 4.5: $\delta^{18}O$ values of quartz in **quartzites** from areas A,B,D and E.

Table 4.2: Isotopic data (O) of quartzites

Sample#	Type	Loc	$\delta^{18}O$
			Qtz
FF118	quartzite	A	13.3
FF124	quartzite	A	11.7
FF132	quartzite	A	14.2
FF134	quartzite	A	12.2
FF270	quartzite	A	15.6
FF248	quartzite	B	16.0
FF251	quartzite	B	14.2
Q115	quartzite	B	10.6
Z81	quartzite	B	10.9
U87	quartzite	D	13.5
U100	quartzite	D	13.5
FF143	quartzite	E	12.5
FF152	quartzite	E	13.6

anomalously low calcite $\delta^{18}O$. A *Di-Kfs* reversal is observed in FF277 (A).

2 quartzites

Qtz in thirteen samples from the basal quartzite layer of the **FF** in areas A, B, D and E has a considerable variation in oxygen isotopic composition (**Table 4.2; Fig. 4.5**). The range of $\delta^{18}O$ values within area A (11.7-15.6) and B (10.6-16) covers the variation encountered in area D (13.5) and E (12.5-13.6). No systematic regional $\delta^{18}O$-shift is indicated by the quartzite data.

3 quartz-diopside gneisses

Oxygen isotopic compositions of *Qtz* and *Di* in eight *Qtz-Di* gneisses from areas A, B and D similarly do not seem to reflect the regional $\delta^{18}O$ trend observed for the marble minerals (**Table 4.3; Fig. 4.6a**). *Di* ($\delta^{18}O = 8.6$ to 13.6) is generally lower in $\delta^{18}O$ than *Di* from marbles and *Di*-rocks in area A and B and about equal to *Di* from area C. *Qtz* in *Qtz-Di* gneisses yields a limited $\delta^{18}O$ spread (12.0-15.2), well within the

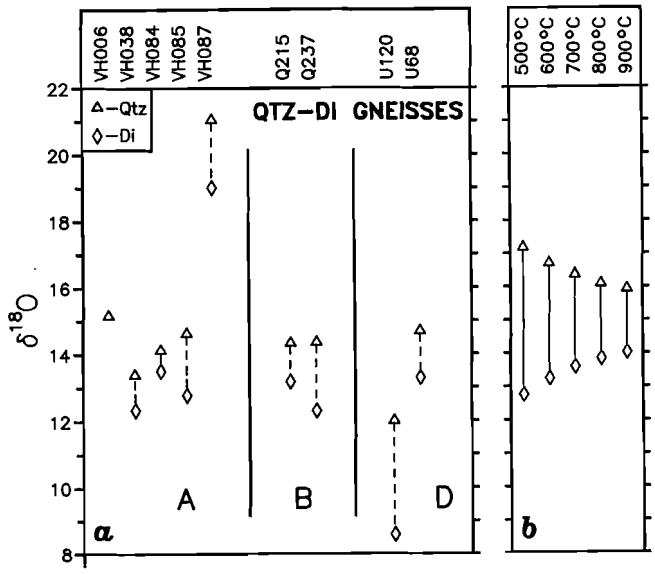

Fig. 4.6a-b: a) $\delta^{18}O$ values of *Qtz* and *Di* in *Qtz-Di* gneisses from areas A, B and D. b) Relative oxygen isotopic compositions of *Qtz* an *Di* at various temperatures (°C) as inferred from isotopic fractionation factors reported by Bottinga and Javoy (1975).

Table 4.3: Isotopic data (O) of quartz-diopside gneisses

Sample#	Type	Loc	$\delta^{18}O$	
			Qtz	*Di*
VH6	*Qtz-Di*-gneiss	A	15.2	-
VH38	*Qtz-Di*-gneiss	A	13.4	12.3
VH84	*Qtz-Di*-gneiss	A	14.2	13.6
VH85	*Qtz-Di*-gneiss	A	14.7	12.8
VH87	*Kfs-Di*-gneiss	A	21.1	19.0
Q215	*Qtz-Di*-gneiss	B	14.4	13.0
Q237	*Qtz-Di*-gneiss	B	14.4	12.2
U68	*Qtz-Di*-gneiss	D	14.7	13.3
U120	*Qtz-Di*-gneiss	D	12.0	8.6

oxygen isotopic variation in *Qtz* from the quartzites (c.f., **Fig. 4.5**). Anomalously high values are observed for *Di* ($\delta^{18}O = 19.0$) and *Qtz* ($\delta^{18}O = 21.1$) in VH087, which represents a *Di-Kfs* rock with small amounts of *Qtz*, intercalated within *Qtz-Di* gneisses.

4 metalaterites

Oxygen isotopic compositions of *Mag* (7.6-11.0), *Sil* (12.2-13.8), *Opx* (11.2-12.0) and *Pl* (10.2-13.0; **Table 4.4**) in ten samples from one specific metalateritic layer in area A are plotted against their bulk silica content in **Figure 4.7a**. *Mag* and *Sil* have, on average, higher $\delta^{18}O$ values in silica poor metalaterites (Fe-Al-rich granofelses) than in silica-rich metalaterites (basic granulites). In contrast, *Pl* has lowest $\delta^{18}O$ values in silica poor metalaterites. These vague trends are not related to whole-rock alkaline (earth) content or degree of saussuritization of feldspars (see Bol et al. (1989b) and

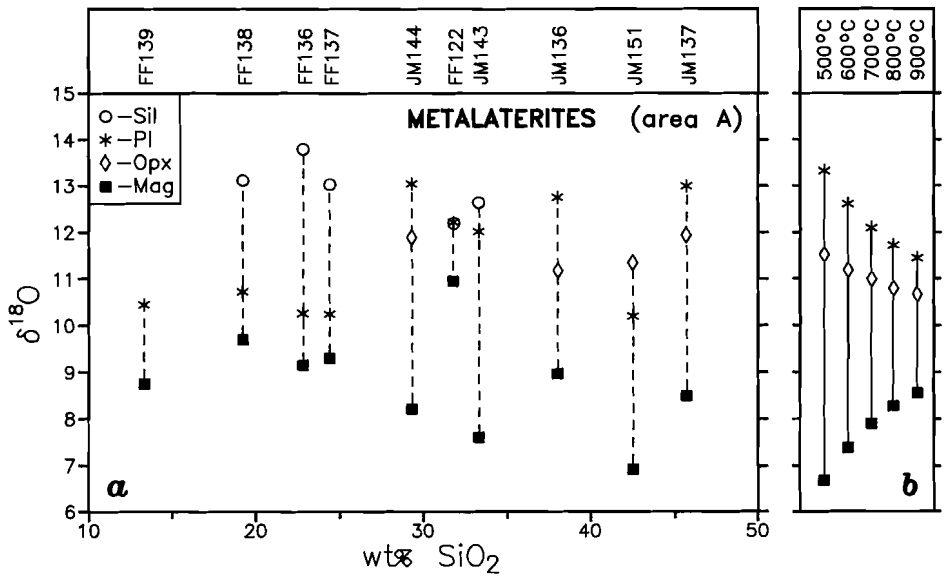

Fig. 4.7a-b: a) $\delta^{18}O$ in *Pl*, *Opx*, *Mag*, and *Sil vs.* bulk wt% SiO_2 in **basic granulites** and **Fe-Al rich granofelses** from one particular metalateritic layer of the **FF** in area A (see text). b) Relative oxygen isotopic compositions of *Pl* (An = 40%), *Opx*, *Mag* at various temperatures (°C) as inferred from isotopic fractionation factors reported by Bottinga and Javoy (1975).

Table 4.4: Isotopic data (O) of metalaterites

Sample#	Type	Loc	$\delta^{18}O$			
			Pl	*Opx*	*Mag*	*Sil*
JM137	basic granul	A	13.0	12.0	8.5	-
JM151	basic granul	A	10.2	11.4	6.9	-
JM136	Fe-Al granof	A	12.8	11.2	9.0	-
JM143	Fe-Al granof	A	12.0	-	7.6	12.6
FF122	Fe-Al granof	A	12.2	-	11.0	12.2
JM144	Fe-Al granof	A	13.0	11.9	8.2	-
FF137	Fe-Al granof	A	10.2	-	9.3	13.0
FF136	Fe-Al granof	A	10.3	-	9.2	13.8
FF138	Fe-Al granof	A	10.7	-	9.7	13.1
FF139	Fe-Al granof	A	10.5	-	8.8	-

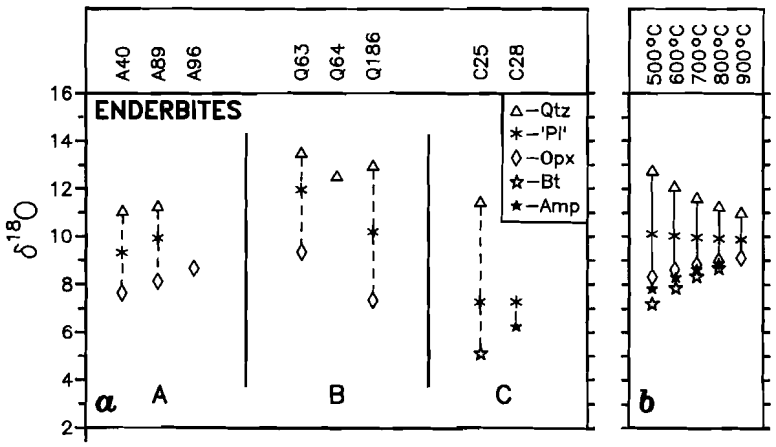

Fig. 4.8a-b: a) $\delta^{18}O$ values of *Qtz*, *Pl*, *Opx*, *Bt* and *Amp* in **enderbites** from migmatitic units directly underlying or overlying the FF. b) Relative oxygen isotopic compositions of *Qtz*, *Pl* (An = 35%), *Opx*, *Bt* and *Amp* at various temperatures (°C) as inferred from isotopic fractionation factors of Bottinga and Javoy (1975). Fractionation factors for *Bt* and *Amp* are not defined for temperatures above 800°C.

Table 4.5: Isotopic data (O) of enderbites

Sample#	Type	Loc	$\delta^{18}O$ (°C)				
			Qtz	*Pl*[a)]	*Opx*	*Bt*	*Amp*
A40	enderbite	A	11.8	9.3	7.6	-	-
A89	enderbite	A	11.4	9.9	8.1	-	-
A96	enderbite	A	-	-	8.7	-	-
Q63	enderbite	B	13.5	12.0	9.4	-	-
Q64	*Grt-Bt*-enderb	B	12.5	-	-	-	-
Q186	enderbite	B	13.0	10.2	7.6	-	-
C25	*Bt*-enderbite	C	11.5	7.3	-	5.1	-
C28	norite	C	-	7.3	-	-	6.2

a) = Plagioclase separates from enderbites are mixtures of *Pl* and *Qtz* (up to 15 wt% *Qtz*).

Bol and Jansen (1989) for a detailed discussion on the chemistry of the metalaterites). *Mag* in FF122 is unaltered in thin section and proved to be pure by XRD. Yet, it has an anomalously high $\delta^{18}O$ (11.0 permil). In general, within the metalaterites the sequence of minerals with increasing $\delta^{18}O$ is: *Mag* < *Opx* < *Pl* or *Mag* < *Pl* < *Sil.* In sample JM151 a $\delta^{18}O$ reversal occurs for the *Opx-Pl* pair and in FF122 for the *Sil-Pl* pair.

5 enderbites

A regional isotopic shift could not be substantiated from $\delta^{18}O$ values of *Qtz* (6.2-13.0), *Opx* (7.6-9.4) and *Pl* with up to 15% *Qtz* admixture (7.3-12.0) in eight enderbites from the Charnockitic Migmatites that envelop the **FF** in areas A, B and C (**Table 4.5; Fig. 4.8a**). *Bt* in C25 and *Amp* in C28 yield $\delta^{18}O = 5.1$ and 6.2 respectively.

Table 4.6: Isotopic data (O,C) of other calcite-bearing rocks

Sample#	Type	Loc	$\delta^{13}C$ *Cal*	$\delta^{18}O$ *Cal*
A187	*Ap*-marble	F	-3.5	12.5
MA97	*Ap*-marble	F	-2.8	12.2
C76	*Cal*-vein	G	-6.5	11.1
MA310	Breccia	H	-3.3	10.2
MA311	Breccia	H	-4.6	11.4
G160	*Qtz*-marble	I	-1.7	11.0
G210	*Qtz*-marble	I	-1.2	10.2

Table 4.7: Carbon isotope data of graphite-bearing rocks

Sample#	Type	$\delta^{13}C$ *Graphite*
A75	*Grt*-granofels	-22.3
BE51	*Grt*-granofels	-23.2
LI56	*Grt*-granofels	-22.2
Q96	*Grt*-granofels	-23.8
Y33	*Grt*-granofels	-24.7
Y121	*Grt*-granofels	-23.9
G80	Breccia matrix	-27.8

Sample positions are indicated on **Fig. 4.1**

6 miscellaneous carbonate-bearing rocks

Isotopic compositions of calcites from **locations F-I** (see **Fig. 4.1**) do not have any systematic relation with the regional trend observed for **FF** calcites (**Table 4.6; Fig. 4.3b**). The $\delta^{18}O$ values of these calcites are all relatively low, from +10.2 to +12.5, while $\delta^{13}C$ has a wide spread, from -1.2 to -6.5.

7 graphite-bearing rocks

Carbon isotope ratios in graphite from six granofelses of the Gyadal Garnetiferous Migmatites (see **Fig. 4.1** for location) show a small spread from -22.2 to -24.7 (**Table 4.7**). Carbonaceous material from the matrix of a

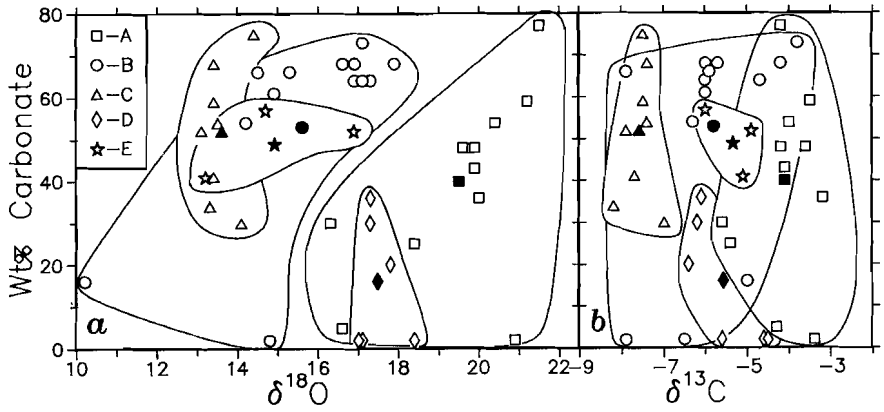

Fig. 4.9a-b: a) $\delta^{18}O$ and b) $\delta^{13}C$ *vs.* weight percent carbonate minerals in marbles from areas A-E.

breccia (G80) yields $\delta^{13}C = -27.8$.

4.5 DISCUSSION

At elevated temperatures (T > 200°C), both decarbonation reactions (Bottinga 1968, Shieh and Taylor 1969) and interaction with magmatic fluids (Sheppard 1986) are expected to lower initially high carbonate $\delta^{18}O$ and $\delta^{13}C$ values inherited from sedimentary precursor minerals. Oxygen and carbon isotopic shifts, similar in magnitude to the shift observed for the **FF** calcites, are reported for silicate-bearing carbonaceous rocks from many contact metamorphic aureoles (e.g., Deines and Gold 1969; Lattanzi et al. 1980; Nabelek et al. 1984; Bowman et al. 1985; Valley 1986). Within the aureoles, $\delta^{18}O$ and $\delta^{13}C$ values of carbonate minerals often decrease systematically with decreasing distance from the pluton and, hence, with increasing metamorphic grade (Valley 1986). However, most analyses of **FF** calcites from marble exposures in the vicinity of the anorthosite complex, i.e., from areas A, D and E, where **M2** peak metamorphic temperatures were extremely high (≥900°C), yield higher $\delta^{18}O$ and $\delta^{13}C$ values than those of calcites from the more remote marble outcrops within area B (±800°C), and still higher values than those from the northernmost outcrop in area C (±750°C). Therefore, in addition to the fluid-rock

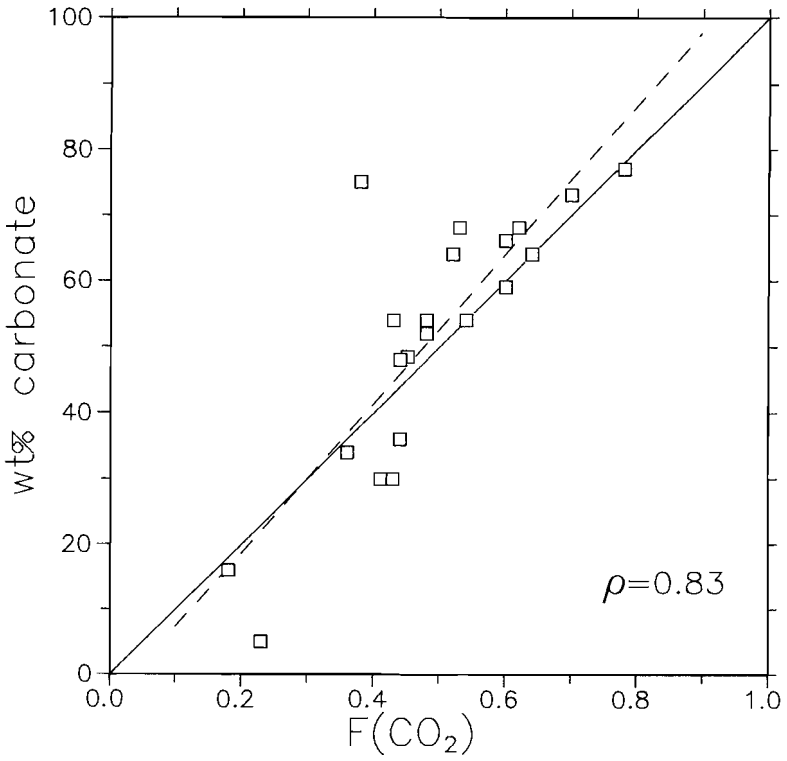

Fig. 4.10: Weight percent carbonate *vs.* $F(CO_2)$ for 22 point counted marble samples from the principal marble exposures A, B and C (see **Table 4.8**). The dashed line is a linear best fit through the data points (y = 113x-4; correlation coefficient = 0.83).

interaction processes commonly associated with the intrusion of igneous masses, other isotope exchange mechanisms may have been dominant. In the ensuing discussion we will evaluate the importance of several processes which were potentially key factors in reaching the final isotopic compositions observed within the **FF**. These are: decarbonation reactions; interaction with fluids derived from the anorthositic complex; interaction with fluids derived from the Caledonian nappe system; isotopic re-equilibration and exchange with low $\delta^{18}O$ fluids during post-**M2** cooling; reservoir effects between neighboring and isotopically contrasting lithologies; isotopic variations inherited from a premetamorphic stage.

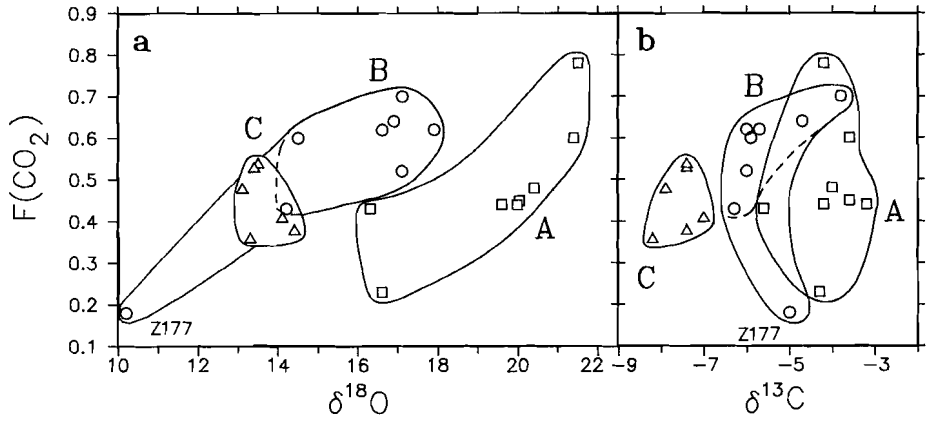

Fig. 4.11a-b: a) $\delta^{18}O$ and b) $\delta^{13}C$ of calcite *vs.* $F(CO_2)$ for the 22 point-counted marble samples from exposures A-C. Symbols are as in **Figure 4.9a.**

4.5.1 decarbonation reactions versus interaction with externally derived fluids

During the formation of metamorphic silicate minerals (*Fo,Di,Phl*) by reaction of carbonates (*Cal,Dol*) and siliceous material, either mixed in during sedimentation or introduced during metasomatic processes, devolatilization reactions *must* have occurred within the **FF** marbles (and within the *Qtz-Di* gneisses). If the isotopic trend observed for the **FF** calcites was caused entirely by such reactions, some systematic relationship between the wt% carbonate in the marbles and the degree of isotopic depletion may be expected. This is not apparent from diagrams of $\delta^{18}O$ and $\delta^{13}C$ in calcite *vs.* wt% carbonate in the marbles (**Figs. 9a,b**; the wt% carbonate is obtained from the wt% CO_2 (**Table 4.1**), assuming that the carbonate mineral composition in the marbles is purely calcitic). The correlation is slightly improved when calculated F(C) values (**Table 4.8**; see analytical techniques for explanation) are used instead of wt% carbonate. Since neither graphite nor scapolite were observed in the **FF** marbles, the F(C)'s equal the $F(CO_2)$ values (mole fraction of CO2 remaining in the rock after decarbonation). The $F(CO_2)$'s in turn, would ideally be inversely related to the amount of CO_2 outgassing from the marbles. As expected, $F(CO_2)$ correlates fairly well with the wt% carbonate (**Fig. 4.10**; cor. coef. = 0.83). In **Figure 4.11a**, the $F(CO_2)$ values are plotted *vs.* the calcite $\delta^{18}O$ and $\delta^{13}C$ values of the 22 marbles in **Table 4.8**

Table 4.8: Modal compositions of 22 *Fo*-marbles and *Di*-marbles from locations A, B and C

Sample#	Loc	Mode% *Cal*	*Dol*[a]	*Fo*	*Di*	*Phl*	*Spl*	F(C)[b]	F(O)[b]	Retro%[c]	Recryst[d] *Cal*	Exsol[d] *Dol*
A122	A	57		31	2	10		0.48	0.72	1	o	
A164	A	49		25	7	18		0.44	0.71	5	o	a
C322	A	27		(13)	60			0.23	0.64	15		a
C324	A	53		(39)		8		0.43	0.69	85	x	a
C335	A	53		(33)	3	12		0.44	0.70	70	a	a
C346	A	85		13		3	<1	0.78	0.87	<1		
C480	A	71		24	1	<1	4	0.60	0.77	<1		a
C481	A	51		19	20	10		0.45	0.72	2	x	
C372	B	47	31[e]	19	<1	<1	3	0.70	0.82	20		x
C509	B	67	5	(23)	4	2		0.62	0.78	20		x
C510	B	65	6	(21)	5	3		0.62	0.78	25		x
C511	B	50	7	(21)[f]	7	15[h]		0.52	0.75	30		x
Q128	B	60		20[f]	17[g]	3[h]		0.64	0.81	"100"		a
Z52	B	66	4	(25)	(2)	4		0.60	0.77	25	x	x
Z75	B	52	3	(34)		6		0.43	0.67	80	o	o
Z177	B	18			64	18		0.18	0.72	20		a
C236	C	50	4	(27)	(59)	6		0.53	0.83	40	o	x
C264	C	40		(4)	39	17		0.38	0.71	10		o
C273	C	61	2	(29)	(1)	6		0.54	0.74	55		x
C521	C	41		(4)	36	18		0.41	0.73	10		o
C522	C	37		(12)	24	28		0.36	0.71	25		o
C533	C	53	3	(25)	8	11		0.48	0.72	45	o	o

a)=mainly "primary" dolomite (see text); b)=mole fractions of carbon (F(C)) and oxygen (F(O)) remaining in the system after decarbonation reactions (see text). c)=proportion of silicates which has been retrograded; d)=recrystallization calcite/exsolution dolomite: x=abundant, o=moderate, a=minor; e)=25% "primary" dolomite; f)=talc; g)=tremolite; h)=chlorite; Numbers within brackets refer to minerals that are partly or wholly retrograded to low-grade minerals.

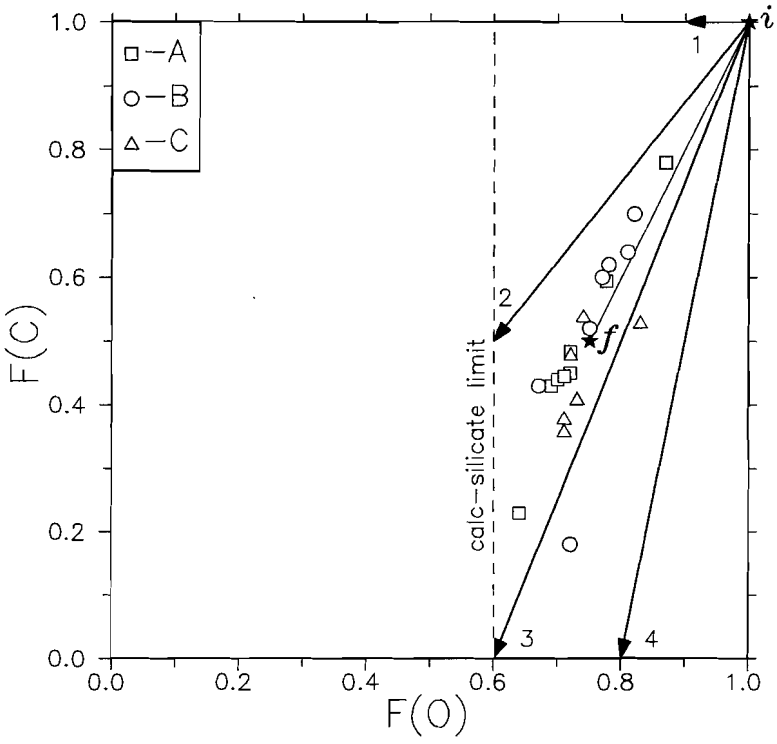

Fig. 4.12: F(O) *vs.* F(C) relationships for various devolatilization reactions. 1) Dehydration; 2) 50% "inert" carbon, e.g. $C + SiO_2 + CaCO_3 = C + CaSiO_3 + CO_2$; 3) normal calc-silicate decarbonation, e.g. $CaMg(CO_3)_2 + 2SiO_2 = CaMgSi_2O_6 + 2CO_2$; 4) 50% excess oxygen in silicates, e.g. $CaCO_3 + 2SiO_2 = CaSiO_3 + SiO_2 + CO_2$; F(O) and F(C) values of **Table 4.8** are plotted; i = initial F-values (F(O) = 1; F(C) = 1); f = average F-values of the marbles in **Table 4.8**.

which cover the isotopic range observed for the principal marble occurrences in areas A, B and C. Most samples have a $F(CO_2)$ (= F(C)) between 0.35 and 0.65, without systematic variation between marbles of different areas. However, within the single areas A and B, significant correlations between $\delta^{18}O$ in *Cal* and $F(CO_2)$ of the marble are seen (cor. coefs. are 0.77 (A) and 0.89 (B)). In area A, the silicate-rich sample C322 has a relatively low $\delta^{18}O$, whereas the *Cal*-rich sample C346 has a high value. Similarly, in area B, the silicate rich samples Z177 and Z75 have low $\delta^{18}O$ values, while other, silicate-poorer marbles from this area are higher in $\delta^{18}O$. The $\delta^{18}O$-$F(CO_2)$ trend in area B is less marked when sample Z177 (with anomalous $\delta^{18}O$

values for *Di* and *Cal*) is omitted. The $\delta^{18}O$-$F(CO_2)$ correlations in areas A and B may be taken to indicate that decarbonation reactions produced isotopic shifts in the order of magnitude of the isotopic variability observed within these areas. Although significant $\delta^{13}C$ depletions may be expected in low $F(CO_2)$ rocks (where decarbonation is nearly complete), analogous positive covariations between $\delta^{13}C$ and $F(CO_2)$ are not observed within areas A and B (**Fig. 4.9b**). Therefore, other factors besides decarbonation may have contributed to the significant $\delta^{18}O$-$F(CO_2)$ correlations within areas A and B (see later).

The calculated F(O) and F(C) values allow evaluation of the possible magnitude of O,C isotopic shifts effected by decarbonation reactions. In **Figure 4.12**, F(O)-F(C) relationships for various decarbonation paths are depicted together with the F-values of the marbles in **Table 4.8**. For example, the final F-values of a stoichiometric carbonate-silica mixture which reacts to a calc-silicate end product without excess C or O (normal calc-silicate decarbonation) are $F(O) = 0.6$ and $F(C) = 0.0$. If the **FF** marbles, apart from volatile loss, represent closed systems, they can be regarded as excess carbonate systems where all decarbonation reactions went to completion. In that case the calculated F-values are final F-values.

Shifts in calcite $\delta^{18}O$ and $\delta^{13}C$ due to devolatilization reactions are usually modelled as one of two endmember processes: 1) **batch volatilization** ($\delta f = \delta i$-(1-F)1000lnα; one step fluid escape) or 2) **Rayleigh volatilization** ($\delta f = \delta i + 1000(F(\alpha\text{-}1)\text{-}1)$; gradual fluid escape; Valley 1986). In fact, most metamorphic degassing reactions will exhibit intermediate behaviour (c.f., Nabelek et al. 1984). At high F-values (> 0.6), the difference between the two models is small compared to analytical errors. Rayleigh processes, however, produce larger shifts in $\delta^{13}C$ if nearly all of the carbon is volatilized ($F(C) < 0.2$).

Calcite O,C isotopic trends resulting from Rayleigh devolatilization reactions are calculated (**Figs. 13a,b**) for various values of α (the fluid-rock isotopic fractionation factor), in order to assess the maximum isotopic shifts which can be attributed to decarbonation. Average values for α throughout the devolatilization process between evolved fluid (CO_2 + H_2O) and rock (carbonate + silicate minerals) are used (see Valley (1986) for explanation). Bearing in mind that a) most devolatilization reactions in the impure dolomites of the **FF** occurred between 400°C and 700°C (Sauter 1983); b) the dominant component of the evolved fluid is CO_2; c) up to 65% of the oxygen may have been present in (precursor) silicate minerals; we

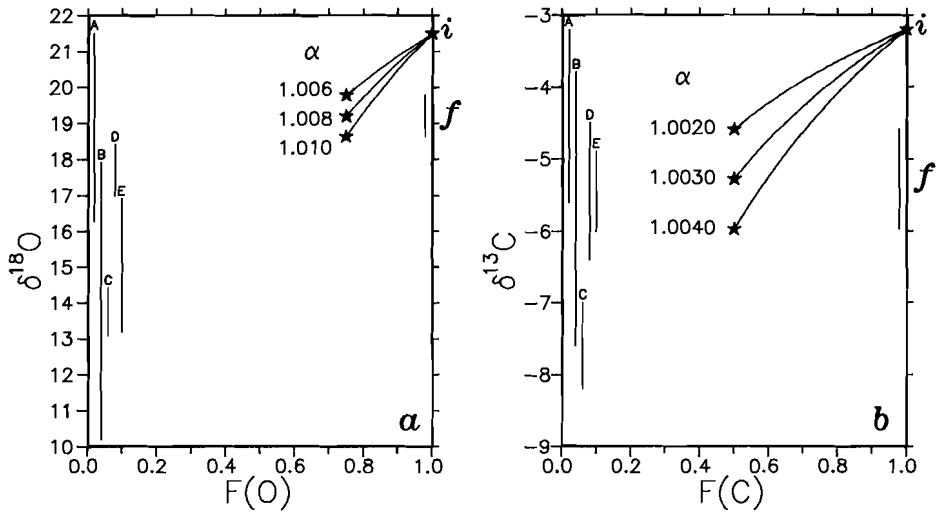

Fig. 4.13a-b: a) Calculated Rayleigh fractionation paths of a) F(O) *vs.* carbonate $\delta^{18}O$ and b) F(C) *vs.* carbonate $\delta^{13}C$ for various values of $\alpha^{18}O$(fluid-rock) and $\alpha^{13}C$(fluid-rock), respectively (see text). Calcite isotopic ranges observed in areas A-E are indicated along the Y-axes.

assumed a range of average $\alpha^{18}O$(fluid-rock) = 1.006-1.010 and a range of average $\alpha^{13}C$(fluid-rock) = 1.0020-1.0040 (cf, Friedman and O'Neil 1977; cf, Chacko et al. 1989). In **Figures 13a,b**, the highest $\delta^{18}O$ (=21.5 permil) and $\delta^{13}C$ (=-3.2 permil) values observed for *Cal* are arbitrarily selected as the initial isotopic composition (δi). Picking other initial isotopic compositions will simply shift the onset of the decarbonation curves without changing their shape. The final isotopic ratios (δf) are obtained by substituting the average F-values of the marbles (**Table 4.9**) for F in the Rayleigh equation. Along the y-axes the calcite $\delta^{18}O$ and $\delta^{13}C$ ranges observed within each area are indicated.

Unless unrealistically high values for α are used (average $\alpha^{18}O$(fluid-rock) > 1.040; average $\alpha^{13}C$(fluid-rock) > 1.0070), the Rayleigh decarbonation model cannot produce calcite $\delta^{18}O$ and $\delta^{13}C$ shifts equal in magnitude to the entire O,C isotopic ranges observed for calcites within the **FF** (**Figs. 13a,b**). Even *within* the individual areas A-E, the observed ranges in $\delta^{18}O$ and, to a lesser degree, in $\delta^{13}C$ may only partly be explained by isotopic shifts due to decarbonation reactions. The

Table 4.9: Average δ-, wt% CO_2- and F-values for various areas

Area	$\delta^{18}O$	$\delta^{13}C$	wt% CO_2	F(O)	F(C)
A	19.5(1.7)	-4.1(0.8)	17.7 (9.7)	0.73 (0.07)	0.48 (0.16)
B	15.6(1.7)	-5.8(1.2)	23.3 (10.8)	0.76 (0.05)	0.54 (0.17)
C	13.6(0.4)	-7.6(0.4)	22.8 (7.0)	0.74 (0.05)	0.45 (0.08)
D	17.5(0.5)	-5.6(0.8)	6.8 (6.7)	- -	
E	14.9(1.9)	-5.3(0.6)	22.0 (3.6)	- -	
A-C	16.4(2.8)	-5.6(1.6)	21.3 (9.6)	0.74 (0.06)	0.49 (0.14)
A-E	16.5(2.6)	-5.6(1.5)	19.3 (10.3)	- -	

Numbers within brackets are standard deviations (1σ)

isotopic differences *among* the areas A-E can not (at all) be explained by simple decarbonation models, since for marbles from different areas no systematic relationship between the average amount of CO_2 outgassing and the average isotopic composition is inferred (**Table 4.9, Figs. 4.9,4.11**).

In order to compare the calcites of areas A-C with unmetamorphosed Precambrian carbonates, the original calcite isotopic compositions (δi's, i.e before decarbonation), are estimated by substituting the observed $\delta^{18}O$-, $\delta^{13}C$-values (δf's) along with the appropriate F-values (**Table 4.8**) in the Rayleigh equation. The average α-values used are: $\alpha^{18}O$(fluid-rock) = 1.008 and $\alpha^{13}C$(fluid-rock) = 1.0030. The "corrected" calcite data points (δi's) for areas A-C are plotted in **Figure 4.14**, together with generalized calcite O,C isotopic data fields for areas A-C (δf's, without Z177). Also indicated is the field for *Cal* and *Dol* in Proterozoic unmetamorphosed chalks and limestones (after: Schidlowski et al. 1975; Veizer and Hoefs 1976). Positive $\delta^{13}C$ excursions (up to $\delta^{13}C$ = 10 permil) from the Proterozoic carbonate record, as indicated by (inferred) premetamorphic carbonate compositions in 2 Ga old marbles from Lofoten-Vesteralen (Norway; Baker and Fallick 1989) and the Lomagundi Province (Zimbabwe; Schidlowski et al. 1976) are not included in the unmetamorphosed carbonate field. The average magnitude of the combined $\delta^{18}O$-$\delta^{13}C$ depletion in the **FF** marbles due to carbonation is calculated using the average F-values of areas A-C (**Table 4.9**) at the same α's, and is shown in the inset of **Figure 4.14**.

All **FF** calcite $\delta^{18}O$ compositions fall within the range reported for unmetamorphosed Precambrian carbonates, whereas most **FF** calcites are lower in

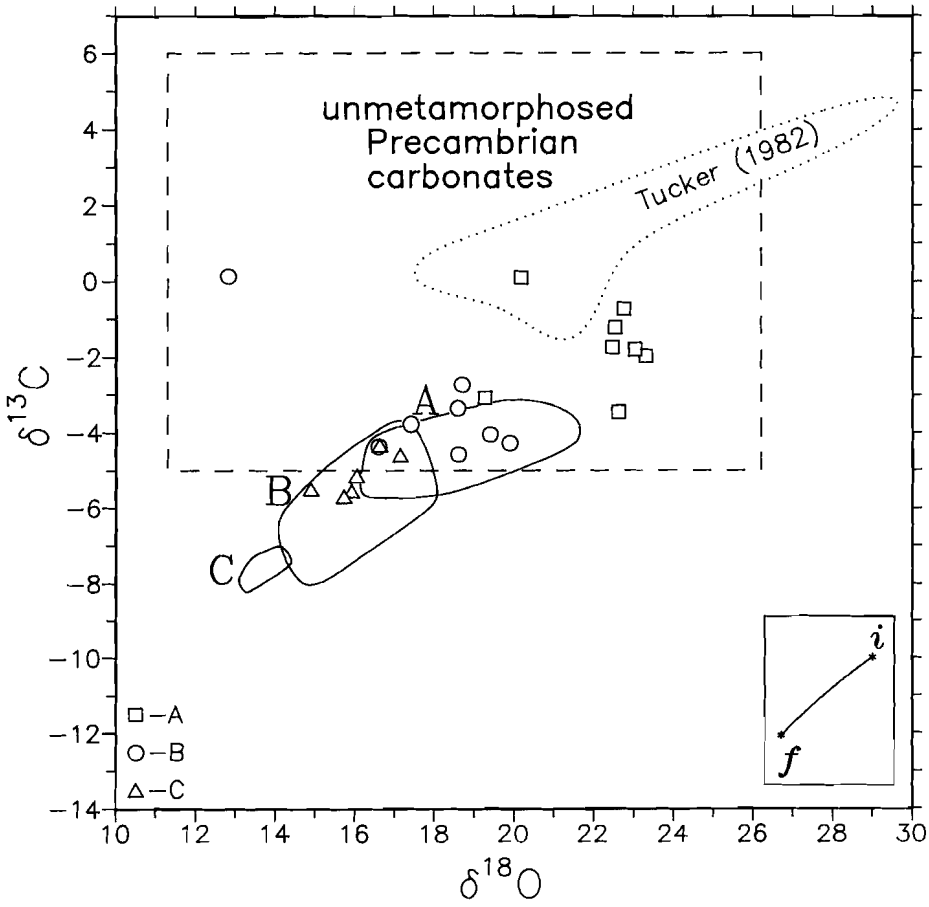

Fig. 4.14: Initial $\delta^{18}O$ vs. initial $\delta^{13}C$ inferred for 22 marbles in areas A-C. The F(O) and F(C) values (F's) in **Table 4.8** were combined with the corresponding O,C isotopic compositions (δf's) in the Rayleigh equation in order to obtain initial isotopic ratios. The α's used are: $\alpha^{18}O$(fluid-rock) = 1.008 and $\alpha^{13}C$(fluid-rock) = 1.0030, respectively. The inset shows the magnitude of the average isotopic shift due to decarbonation in the marbles, substituting the above α's, and the average F's the Rayleigh equation. The generalized O,C isotopic data fields (δf's) of areas A-C are included for comparison. The rectangle represents the approximate compositional field for unmetamorphosed Proterozoic sedimentary carbonates (after: Schidlowski et al. 1975; Veizer and Hoefs 1976). Also indicated is the field of isotopic compositions of various depositional and diagenetic dolomite species separated from the Precambrian Beck Spring Dolomite, California (after: Tucker 1982).

$\delta^{13}C$. When corrected for decarbonation effects, most calcites plot inside the Precambrian carbonate field, but the generally low $\delta^{13}C$-values remain a striking feature. It is important to note that the calcite isotopic data, even when "corrected" for the amount of decarbonation indicated by the $F(CO_2)$ value of their host, still show a considerable (and coupled) O,C isotopic trend (**Fig. 4.14**).

It is unlikely that the regional (O,C) isotopic trend in the **FF** calcites simply reflects the isotopic variability of the sedimentary precursor carbonate minerals. Detrital silicate minerals with low $\delta^{18}O$ values that were mixed in during sedimentation potentially have shifted the $\delta^{18}O$-values of the presently metamorphic calcites away from the field of sedimentary carbonates, as inferred in other areas (Valley and O'Neil 1984). Indeed, the positive covariation between $\delta^{18}O$ and $F(CO_2)$ within area A and B (**Fig. 4.11a**) may be partly related to original variations in carbonate/silicate ratio, especially since similar covariations between $\delta^{13}C$ and $F(CO_2)$ are absent (A) or less clear (B; **Fig. 4.11b**). However, variable amounts of sedimentary silicate admixture probably did not cause the entire regional $\delta^{18}O$ shift observed in the marbles, since the average silica content of the marbles in distinct areas, as reflected by the average wt% CO_2 within each area, does not vary systematically with $\delta^{18}O$ (**Table 4.9; Fig. 4.9a**). Moreover, whether corrected for decarbonation or not, the calcite $\delta^{18}O$ and $\delta^{13}C$ values *are* significantly correlated, a feature not easily explained by sedimentary admixture of (O-bearing, C-free) silicate minerals.

Although most calcite isotopic compositions plot outside the field for unmetamorphosed Precambrian carbonates, it is impossible to rule out the possibility that the unmetamorphosed precursor of the marbles had sedimentary carbonate grains with a range in isotopic compositions comparable to those presently observed for the calcites. Also, there is a possibility that the original sediments contained organic matter. Even if there is no graphite now, organic matter may have been present once, exchanged ^{13}C at low grade, and than have been oxidized to CO_2. However it is more likely that the **FF** calcite compositions point towards interaction with external fluids.

Summarizing, we conclude that decarbonation processes alone cannot account for the large regional $\delta^{18}O$ variability observed in *Cal* (**Figs. 11a,13a**). Also, pure decarbonation cannot produce the observed $\delta^{13}C$ values, that clearly set apart the different areas, but seem unrelated to F(C) (**Fig. 4.11b**). Similarly, variation in the

carbonate/silicate ratio inherited from the sedimentary marble protolith may have caused part of the O isotopic variation presently seen in the calcites, but again, it cannot account for the entire regional $\delta^{18}O$ and $\delta^{13}C$ range. Therefore, besides decarbonation reactions and sedimentary variations, interaction with externally derived, oxygen- and carbon-bearing fluids is likely to have occurred in the **FF** marbles, in order to produce the observed isotopic shifts between and, partly, within the areas. These interactions may be hypothesized to have occurred before, during or after the main metamorphic events.

4.5.2 fluids associated with the anorthositic complex

Oxygen isotopic ratios of the Rogaland anorthosites and related magmatic units range from 5.2 to 7.1 permil (whole-rock; Taylor 1969; Demaiffe and Javoy 1980) and any fluid that equilibrated at high temperatures with these igneous masses must be accordingly low in $\delta^{18}O$. Within the anorthosite complex, some subsolidus isotopic exchange is indicated by relatively low isotopic temperatures (500-700°C) calculated from oxygen isotopic fractionations between mineral pairs (Demaiffe and Javoy 1980). This may be related to slow post-orogenic ascent of the igneous bodies under wet conditions, or to deuteric readjustment by a fluid phase. Catazonal gneisses directly surrounding the isotopically fairly homogeneous anorthosite bodies have a wide $\delta^{18}O$ range (whole rock 4.3-9.8 permil; Demaiffe and Javoy 1980). This puts serious constraints on the possibility of large scale fluid fluxes from the magmatic complex into the granulitic envelope. Furthermore, the calcite $\delta^{18}O$ values of the **FF** marbles are highest in the vicinity of the anorthositic complex, and interaction with high-temperature (low $\delta^{18}O$) fluids derived therefrom, if any, can thus be excluded as a possible cause of the regional isotopic trends seen in the marble minerals.

*4.5.3 Caledonian alteration effects (**M4**)*

Retrogression resulting from the Caledonian orogenesis (**M4**) is widespread in both the **FF** and its country rocks from area C, less prominent in area B, and only weakly present in area A (see the zone of Caledonian green biotite in **Fig. 4.1**). It is interesting to note that the south to north decrease in calcite $\delta^{18}O$ and $\delta^{13}C$ within the **FF** marbles coincides with the increase of retrograde metamorphism towards the

Caledonian nappe system. Hence, the hypothesis that the regional calcite isotopic trend is a systematic isotopic shift due to differential interaction with fluids derived from the Caledonian nappe system may be further tested.

In **Table 4.8**, the proportion of silicate minerals which has been altered to typical **M4** minerals (*Srp*, *Chl*, *Tr*, *Tlc* and *Chu)* is indicated, providing a rough measure of the amount of retrogradation in the marbles. In fact, some retrograde marbles (C324, Z52, Z75, Z177, FF196) have lower calcite $\delta^{13}C$ and especially $\delta^{18}O$ values, than most other marbles from the corresponding areas. However, within the distinct areas A-E no unambiguous relation could be established between the presence of retrograde minerals and the degree of calcite $\delta^{18}O$ and $\delta^{13}C$ depletion (c.f. **Table 4.1** with **Table 4.8**). For instance, *Cal* in *Tr*-bearing samples Q128 (B) and C163 (C) is isotopically similar to *Cal* in the bulk of the samples in areas B and C respectively (**Table 4.1**). Nevertheless it is conceivable that low $\delta^{18}O$, low $\delta^{13}C$ fluids derived from Caledonian nappes, that once covered a large part of the Rogaland area (Sauter et al. 1983), interacted with marbles from the various areas in different degrees. If so, these fluid/rock interactions took place without destroying the beautifully preserved *Dol* exsolution textures that are observed in calcites of all areas, but mostly in areas B and C, and which record the complex cooling history during **M3** (Sauter 1983).

Indeed, calcites in other carbonate bearing rocks from locations F through I, which lie close to or just below the Caledonian thrust front (**Fig. 4.1**), are low in $\delta^{18}O$ (10.2-12.5 permil; **Table 4.6**; **Fig. 4.3b**). If the quartz marbles G160 and G210 (I) originally had isotopic compositions somewhere in the field of unmetamorphosed Precambrian carbonates (cf. **Fig. 4.14**), their present calcite $\delta^{18}O$ compositions would indicate extreme $\delta^{18}O$ depletions. The calcite $\delta^{18}O$ values of other samples from this group also suggest that fluids associated with the Caledonian events were low in $\delta^{18}O$. The calcite $\delta^{13}C$ values from locations F-I range from -2.8 to -6.5, the lowest value is observed in the calcite vein C76 (G). At the temperatures inferred for **M4** (**Fig. 4.2**) still lower $\delta^{13}C$ values are expected for calcite in equilibrium with any Caledonian fluid that may be related to the regional calcite $\delta^{13}C$ shift observed for the **FF** marbles.

Moreover, conclusive evidence against a dominant role of Caledonian fluids in the formation of the regional calcite isotopic trend is found within the marbles themselves. Oxygen isotopic compositions of typical high-grade (**M1**, **M2**)

Table 4.10: Coefficients for the oxygen isotope fractionation equation used to calculate "isotopic temperatures"

Equation[a]: $1000\ln\alpha(Qtz, \text{mineral}) = A + B*10^6/T^2$

Mineral	A	B	Temperature range (°C)
Calcite[b]	0.00	0.38	>600
Feldspar[b]	0.00	0.95 + An*1.02	>600
Pyroxene[c]	0.00	2.20	400-845
Amphibole[d]	-0.30	3.15	500-800
Biotite[d]	-0.60	3.69	500-800
Magnetite[e]	0.00	6.29	600-1300

a) Bottinga and Javoy 1973; b) Clayton et al. 1989; c) Matthews et al. 1983 (their wollastonite fractionation data are assumed to be applicable to all pyroxenes in this study); d) Bottinga and Javoy 1975; e) Chiba et al. 1989;
An = mole fraction anorthite in feldspar.

metamorphic minerals (*Di,Phl*) that occur within the **FF** marbles reflect the regional $\delta^{18}O$ trend observed for the calcites (see **Table 4.1**, for $\delta^{18}O$ correlation coefficients for various mineral pairs). *Di* and *Phl* within the marbles are highest in $\delta^{18}O$ in area A, intermediate in B, and are lowest in area C (**Fig. 4.4a**). It is extremely unlikely that low $\delta^{18}O$ Caledonian fluids exchanged significantly oxygen isotopes with silicate minerals in the marbles without concomitant recrystallization of the calcites.

Although some retrograde effects can be recognized throughout the Rogaland terrane in high-grade minerals of most rock types investigated (see below), no systematic regional trends were found in quartzites (**Fig. 4.5**), *Qtz-Di* gneisses (**Fig. 4.6a**) and enderbites (**Fig. 4.8a**) surrounding the marbles. The uniformly low $\delta^{13}C$ values for the graphites (-27.8 to -22.2 permil; **Table 4.7**; **Fig.1**) suggest an organic origin, without later large scale exchange with fluids. It is difficult to envisage, that Caledonian fluids selectively exchanged with calcites *and* high-grade silicate minerals within the **FF** marbles on a regional scale, without producing similar regional shifts, at least to some degree, in minerals from other units.

Therefore, we conclude that the regional isotopic shifts observed within the marble minerals can not be attributed to differential interaction with Caledonian metamorphic fluids.

4.5.4 partial oxygen isotopic re-equilibration and exchange with low $\delta^{18}O$ fluids during post-M2 cooling

Valley and O'Neil (1984) proposed that "isotopic temperatures" are not as accurate as "petrologic temperatures". This is due to a) the generally poor calibration and low temperature sensitivity of isotopic geothermometers; b) unknown effects of solid solution; c) analytical error; and d) the possible presence of isotopic zoning and/or resetting. We calculated ^{18}O-temperatures merely to test temperature concordance among mineral pairs and to compare them with petrologic temperatures. As such, isotope thermometry may provide insight in the degree of retention of metamorphic isotope compositions and isotope equilibrium between minerals.

Isotopic temperatures obtained from ^{18}O fractionations between *Di-Phl* pairs within marbles from areas A-C are low ($<640°C$, most fall between 420-320°C) compared to peak metamorphic temperatures inferred from the **M2** isograd pattern (**Table 4.11**). This cannot simply be attributed to poor analytical precision. For example, if the $\Delta^{18}O$(*Di-Phl*) of C500A in reality is 0.5 permil less than the difference between the measured $\delta^{18}O$ compositions of *Di* and *Phl*, the isotopic temperature should be 389°C, instead of 345°C. Coefficients which are substituted in the fractionation equation used for ^{18}O-thermometry are listed in **Table 4.10**. Other combinations of appropriate published coefficients generally yield similar or lower (by up to 100°C) *Di-Phl* isotopic temperatures. Whichever coefficients used, the ^{18}O-temperatures calculated for *Di-Phl* pairs display no regional variation. This is in contrast with the Fe/Mg distribution between these minerals in areas A-C, which still reflect the different peak metamorphic temperatures experienced by marbles from distinct areas (Sauter 1983). The isotopic temperature calculated for a *Di-Phl* pair from the rim of a *Spl-Di-Phl* vein in marbles from area E (948°C) compares favorably with the petrologic temperature (950°C), which may be fortuitous.

The generally low, fairly constant ^{18}O-temperatures inferred for *Di-Phl* pairs may be taken to indicate partial subsolidus oxygen isotopic exchange between these minerals, as result of the extremely slow cooling rates that prevailed during **M3**. However, partial serpentinization of *Fo* and *Phl* observed in the marbles is related to introduction of aqueous fluids during **M4** (Sauter 1983). The slightly lower $\delta^{18}O$ in partly serpentinized *Phl* (20% *Srp*) in C165 (**Table 4.1**) indicates that, besides subsolidus re-equilibration, isotopic exchange with external fluids may have affected

Table 4.11: Isotopic Temperatures

-marbles and diopside rocks

	T(isotopic)°C				T(petrologic)°C
Sample#	*Cal/Di*	*Cal/Phl*	*Di/Phl*	*Qtz/Di*	
A122	-	638	-	-	900
A164	rev	873	323	-	900
C322	rev	-	-	-	900
C480	-	347	-	-	900
C481	rev	>1000	613	-	900
FF273	997	-	-	-	900
C397	-	821	-	-	800
C500A	-	-	345	-	800
C500B	-	-	379	-	800
C502A	>1000	-	-	-	800
C509	-	551	-	-	800
Q128	>1000	658	330	-	800
Z177	rev	-	-	-	800
C165	-	-	353 (316)[a]	-	750
C235	>1000	-	-	-	750
C264	-	544	-	-	750
C273	-	668	-	-	750
C521	892	629	420	-	750
C522	586	603	637	-	750
C533	-	>1000	-	-	750
FF260	-	-	-	583	900
FF190	-	-	948	-	950

-quartz diopside gneisses

	T(isotopic)°C	T(petrologic)°C
Sample#	*Qtz/Di*	
VH38	>1000	900
VH84	>1000	900
VH85	803	900
VH87	751	900
Q215	981	800
Q237	727	800
U68	981	900
U12	531	900

Table 4.11 - *continued*

-metalaterites

	T(isotopic)°C			T(petrologic)°C
Sample#	*Pl/Opx*	*Pl/Mag*	*Opx/Mag*	
JM137	645	774	808	900
JM151	rev	950	680	900
JM136	452	866	> 1000	900
JM143	-	786	-	900
FF122	-	> 1000	-	900
JM144	602	741	778	900
FF137	-	> 1000	-	900
FF136	-	> 1000	-	900
FF138	-	> 1000	-	900
FF139	-	> 1000	-	900

-enderbites

	T(isotopic)°C			T(petrologic)°C
Sample#	*Qtz/Opx*	*Qtz/Bt*	*Qtz/Pl* [b]	
A40	451	-	450-413	900
A89	543	-	660-612	900
Q63	460	-	660-613	800
Q186	365	-	410-374	800
C25	-	453	285-256	750

"Isotopic temperatures" are obtained using the mineral-pair fractionation equations specified in **Table 10.** The averaged anorthite content for *Pl* in metalaterites (An = 40%) and in enderbites (An = 35%) is used. **a)** *Di/Phl* temperature within brackets corresponding to partly serpentinized (20% *Srp*) phlogopite in C165; **b)** Two isotopic temperatures are calculated for each *Qtz/Pl* pair in the enderbites: The first is calculated by substituting $\delta^{18}O$ of the *Pl-Qtz* mixture for $\delta^{18}O$ of *Pl* in the formula, the second is corrected for an average 10% *qtz* admixture; rev = no temperature calculated due to isotopic reversal, indicating disequilibrium. "Petrologic temperatures" are peak metamorphic temperatures estimated from the **M2** isograd pattern.

the value of $\Delta^{18}O(Di\text{-}Phl)$.

The ^{18}O-temperatures calculated for *Cal-Phl* pairs are generally higher, again with no regional variation. *Cal-Di* fractionations are commonly small or even reversed, and, of the ^{18}O-temperatures of *Cal-Di* pairs, all but one exceed those

reached during **M2**. It is important to realize however, that at high temperatures the oxygen isotope fractionation factor for mineral pairs becomes small, and analytical and calibration errors as well as small deviations from isotopic equilibrium drastically influence the calculated temperatures. For instance, using the fractionation coefficients in **Table 4.10** and assuming that the minerals once equilibrated isotopically at the peak metamorphic temperatures listed in **Table 4.11**, we find that, on average, $\Delta^{18}O(Cal\text{-}Di)$ values are 0.9 permil too low; $\Delta^{18}O(Cal\text{-}Phl)$ values are 0.85 permil too high; $\Delta^{18}O(Di\text{-}Phl)$ values are 1.9 permil too high. Hence, in terms of isotopic temperatures, the degree of isotopic disequilibrium may sound worse than when expressed in permil.

Carbonates are commonly more subject to retrograde exchange than silicate minerals (Eslinger and Savin 1973; Magaritz and Taylor 1976). An exception may be K-feldspar which is reported to be more readily altered than calcite (Valley and O'Neil 1984) though the reverse may be true at low P (Clayton et al. 1968). Wada (1988) demonstrated that $\delta^{18}O$ values in calcite grains from a high-grade marble from the Hida belt, Japan, decrease from core to rim within 200-300 μm by up to 7 permil, due to exchange with metamorphic fluids. Assuming an average calcite grain size of 5 mm he estimated that the bulk calcite $\delta^{18}O$ composition was lowered by up to 0.6 permil. In fact, *Cal* grains in many **FF** marbles are recrystallized (**Table 4.8**), as indicated by grain size reduction (down to 0.25 mm) and by growth of new clear *Cal* at the expense of old dusty grains. Hence, the higher temperatures calculated from *Cal-Di* and *Cal-Phl* pairs are possibly caused by differential interaction of retrograde metamorphic fluids with the various metamorphic minerals. This implies that $^{18}O/^{16}O$ ratios in many calcites were presumably higher before retrograde recrystallization, and part of the calcite $\delta^{18}O$ range within each area may be caused by interaction with low $\delta^{18}O$ fluids after **M2**. However, on average, post-**M2** lowering of calcite $\delta^{18}O$ values due to the combined effects of subsolidus re-equilibration and interaction with external low $\delta^{18}O$ fluids is likely less than 1 permil, since the observed $\Delta^{18}O(Cal\text{-}Di)$ values are, on average, within 1 permil from peak-metamorphic equilibrium (see above).

Within the enderbites, isotopic temperatures of *Qtz-Opx* (365-543°C), *Qtz-Bt* (453°C) and *Qtz-Pl* (285-660°C) are lower than peak metamorphic temperatures. After correcting $\delta^{18}O$ of *Pl* for *Qtz* admixture, the calculated *Qtz-Pl* temperatures in enderbites are lower (256-613°C). Again, these temperatures may tentatively be

attributed to partial subsolidus re-equilibration. Alternatively, the low temperatures may reflect interaction with low $\delta^{18}O$ post-**M2** fluids, since, analogous to *Cal* in the marbles, *Pl* in the silicate rocks has a high susceptibility to isotopic exchange at low-grade conditions (O'Neil and Taylor 1967). However, caution is necessary in interpreting ^{18}O-fractionations between *Qtz-Pl* pairs: the inferred temperatures are almost meaningless due to the small fractionation coefficient (**Table 4.10**). On average, 1.5 permil must be added to the observed plagioclase $\delta^{18}O$ values, in order to yield ^{18}O-temperatures equal to the peak metamorphic temperatures.

Similarly, preferential lowering of $\delta^{18}O$ in *Pl* by low $\delta^{18}O$ retrograde metamorphic fluids may explain the unrealistically high ^{18}O-temperatures ($> 1000°C$) calculated for five *Pl-Mag* pairs in the metalaterites from area A, whereas *Opx-Mag* and *Sil-Mag* pairs may have partly retained higher grade oxygen isotopic compositions. On average, the $\Delta^{18}O$(*Pl-Mag*) values observed in the metalaterites are 0.9 permil lower than may be expected at peak metamorphic equilibrium.

Qtz-Di fractionations in *Qtz-Di* gneisses yield temperatures ranging from well above 900°C in area A to about 500°C in area D. On average, $\Delta^{18}O$(*Qtz-Di*) values are 0.1 permil above peak metamorphic equilibrium.

Summarizing, it may be stated that, in the marbles, the *Qtz-Di* gneisses, the metalaterites and the enderbites, average deviations from isotopic equilibrium up to 2 permil are indicated by oxygen isotopic fractionations between mineral pairs (**Figs. 4,6-8**). From our data set, and from data given by Demaiffe and Javoy (1980), it can be concluded that both the Rogaland anorthosite complex and its high-grade metamorphic envelope were affected to some degree by subsolidus isotopic exchange, with no clear geographic trends. Similar limited amounts of isotopic exchange are commonly found in other granulite terranes (Matthews et al. 1983; Chiba et al. 1989).

4.5.5 reservoir effects

From the above discussion it is clear that, during or after **M2**, pervasive fluids did not cause significant oxygen isotope exchange at high-grade metamorphic temperatures with the various rock types. Isotopic heterogeneity, occasionally within a meter (**Fig. 4.15**), is observed for *Cal* and *Phl* in marbles, for *Qtz* in quartzites, in *Qtz-Di* gneisses and in enderbites, for *Pl* in enderbites and in metalaterites, for *Di* in marbles and in *Qtz-Di* gneisses, and for *Mag* in metalaterites (**Figs. 4-8**). Similarly, isotopic

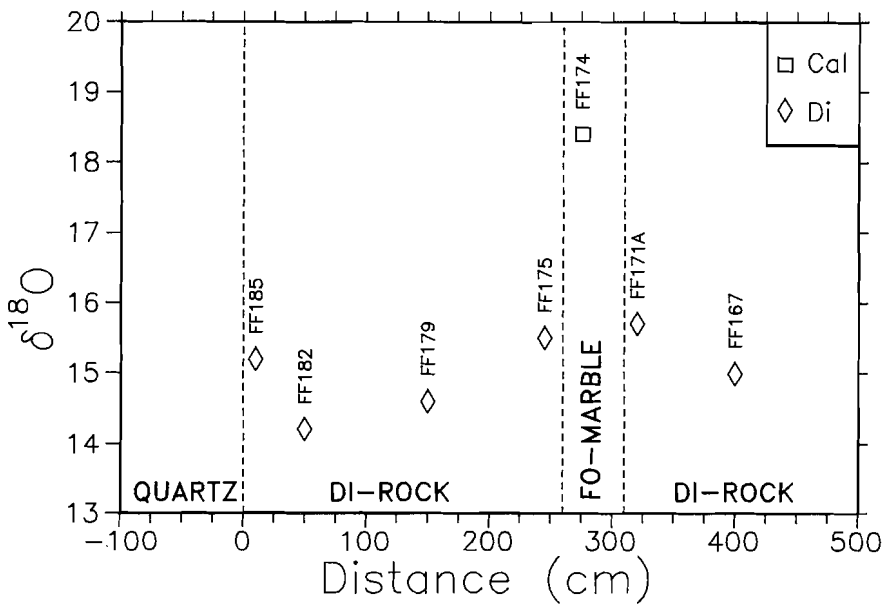

Fig. 4.15: Diopside (and calcite) $\delta^{18}O$ values in *Di*-rock *vs.* distance from a quartzite layer in area A.

heterogeneity is reported for noritic and felsic gneisses directly surrounding the anorthosite complex (Demaiffe and Javoy 1980). "Carbonic metamorphism" as proposed for granulite formation in other areas (Janardhan et al. 1979; Newton et al. 1980; Janardhan et al. 1982) is not supported for the Rogaland terrane by the present isotopic data. Permeating rocks with large quantities of CO_2 from some deep-seated reservoir, at temperatures recorded by **M2** granulite facies mineral assemblages, would likely have a pronounced and homogenizing effect on the isotopic composition of distinct minerals, regardless the mineralogical or original isotopic composition of their host-rock (Rumble 1982). This is simply not observed. Besides, the effects of **M2** are least prominent within area C, where the isotopic composition of *Cal* seems most altered. Any regional isotopic trend in marbles produced by variable CO_2 introduction hypothetically related to the degree of granulite facies metamorphism would topologically be opposite to the one documented in this study.

Sigmoidal $\delta^{18}O$ profiles across marble-schist contacts are reported, for example, from Naxos (Rye et al. 1976; Baker et al. 1989), from Sifnos (Ganor et al. 1989), both

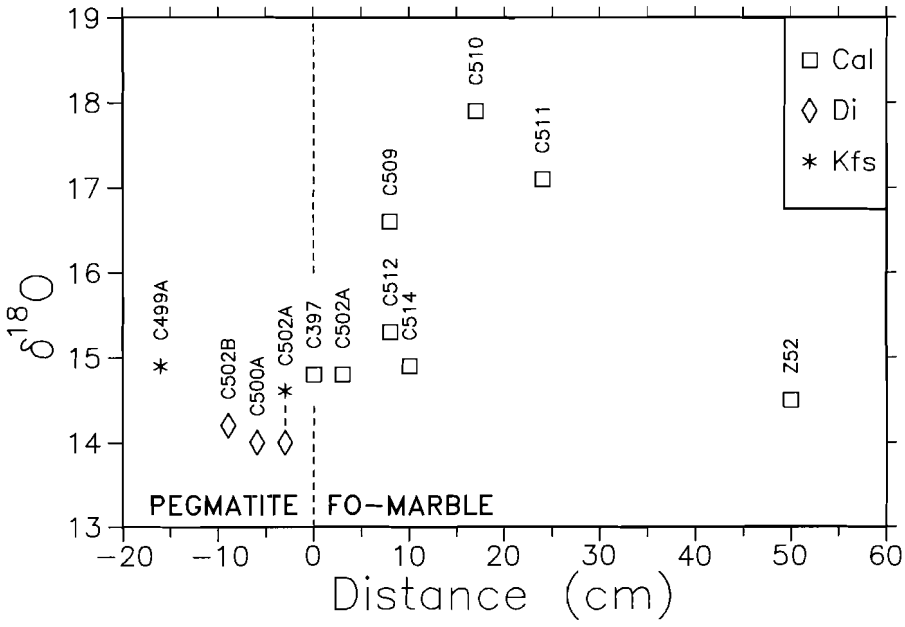

Fig. 4.16: Calcite, diopside and K-feldspar $\delta^{18}O$ values in *Fo*-marbles and *Di*-rocks *vs.* distance from the diopside front enveloping a pegmatite in area B.

Greece, and from several locations in the Adirondack Mountains, New York (e.g., at Cascade Slide, Valley and O'Neil 1984; see also Cartwright in Bohlen et al. 1989, pp 37-38). Such profiles evidence (limited) isotopic communication *via* a fluid phase between lithological units in a boundary zone. Similar subtle isotopic "reservoir effects" between **FF** marbles and contacting country-rocks are not substantiated, since for the marble minerals no clear relation between isotopic composition and position within the marble layer (see **Appendix A, Figs. 4A.1-4A.3** for sample positions) or distance from a pegmatite **(Fig. 4.16)** is noticed. Presumably, any preexisting $\delta^{18}O$ gradients in the marbles resulting from earlier isotopic interactions with adjacent silicate layers are wiped out by later deformation events.

On a larger scale, oxygen isotopic interactions between the bulk of the **FF** marbles and the bulk of the enveloping silicate-rich rocks may have occurred. The magnitude of the bulk $\delta^{18}O$ effect in the marbles depends, besides upon the availability and accessibility of fluids, on the volumes of the isotopic reservoirs involved. The $\delta^{18}O$ values of *Pl* separates from enderbites more or less equal the bulk

isotopic compositions of their host and may be taken to represent the isotopic composition of the country-rock of the **FF** as a whole. It can easily be demonstrated that isotopic compositions of *Cal* (and *Di* and *Phl*) in marbles from all areas are grossly out of equilibrium with those of the enderbite *Pl* separates, for all temperatures of interest. However, the marble occurrences in areas C, D and E represent approximately equal carbonate volumes, as estimated from their outcrop area, that are small compared to those from A and B. Yet, marbles from C, D and E have widely different isotopic compositions. Therefore, we do not suppose that lithologic reservoir effects were an important factor in reaching the present isotopic compositions of *Cal*.

4.5.6 timing of the marble trend

Complex intergrowths (symplectites, coronas) composed of mixed **M1-M2**, **M2-M3** and even **M1-M2-M3** anhydrous mineral assemblages are found in many rock types throughout the Rogaland terrane (Tobi et al. 1985). Together with the regional observation that compositional equilibrium is often restricted to small domains (< 1cm), the intergrowths provide evidence that metamorphic reactions were controlled by solid state volume diffusion (cf., Tracy and McLellan 1985). In general, the textures and the minerals observed in the granulite facies rocks surrounding the anorthositic bodies are indicative for vapor deficient **M2** granulite-facies metamorphism, induced in rocks that were already "dried out" during **M1**, and followed by an equally "dry" cooling period during **M3** (Maijer and Padget 1987). Important deviations from this generalized scheme are manifest in the vicinity of some granites and pegmatites where hydrous **M3** minerals developed, but such rocks are not considered in this study. Therefore, it may well be that the **M2** and **M3** stages merely preserved pre-existing bulk isotopic characteristics of many rocks, without inducing significant isotopic alterations.

Apparently, the regional (O,C) isotopic trend is exclusively a property of the impure dolomitic marbles, since similar systematic regional shifts are not observed in minerals from other lithologies. The marbles may have acted as an aquifer sometime before **M2**. A pre-**M2** "plumbing system", although looked for, is not identified in the marbles, but vestiges of former veinlets, e.g. arrays of recrystallized *Cal* grains, may easily be obliterated by subsequent high-temperature **M2** events. Isoclinically folded

pegmatitic veins with thick *Di* rims and, locally, with desilicified cores are still visible. These (macroscopic) pegmatites represent major conduits of aqueous fluids wherefrom silica metasomatically invaded the marbles and many of them intruded the **FF** prior to **M2** (Bol and Jansen, in preparation). *Di* from *Di*-rims of pegmatites and from other *Di*-rocks is generally lower in $\delta^{18}O$ than *Di* in the marbles (**Table 4.1, Figs. 4a,15**). It is conceivable that ^{18}O and ^{13}C depletions in the marbles are related to a pre-**M2** metasomatic influx of silica-bearing, low-$\delta^{18}O$ fluids with subsequent decarbonation reactions. However, in area B the isotopic composition of *Cal* seems unrelated to distance from a pegmatite with particularly well developed metasomatic rims (**Fig. 4.15**). Moreover, no difference in the abundance of veins is noted between areas A, B, C and E. In area D marbles are subordinate and intercalated in an intersecting *Di*±*Kfs* vein network. Yet, *Cal* in marbles from area D is less depleted in ^{18}O and ^{13}C than in those from B and C. The overall conclusion is that isotopic alterations associated with the pegmatitic veins are restricted to the *Di*-rims.

The bulk compositions of the marbles and the enveloping *Qtz-Di* gneisses differ mainly in silica/carbonate content (Sauter 1983), possibly reflecting differences in carbonate/silica ratios of the sedimentary precursors. If so, the fluid/rock interactions that caused the regional isotopic shift in the marbles presumably would have occurred sometime after the event in which the carbonates in the precursors of the *Qtz-Di* gneisses were exhausted by calc-silicate producing reactions, since the isotopic trends in the marbles are not reflected by $\delta^{18}O$ compositions of *Qtz* and *Di* in the associated *Qtz-Di* gneisses. Similarly, *Di*-marbles are on average higher in silica than *Fo*-marbles (Sauter 1983). This difference may also be due to sedimentary carbonate/silica variations. On the other hand it may reflect variable metasomatic input of silica that cannot be related to a vein system anymore. In this context it is interesting and important to note that, regionally, no systematic differences are observed between the isotopic compositions of *Cal* in *Fo*-marbles and *Cal* in *Di*-marbles. For example, in area C, calcites have higher $\delta^{18}O$ values in *Di*-marbles than in *Fo*-marbles, and in area B calcites have generally lower $\delta^{18}O$ values in *Di*-marbles. Calcites in *Di*-marbles from area A fall isotopically within the range of calcites in *Fo*-marbles (**Table 4.1**). Whatever process caused the variation in silica content within the marbles, apparently it is not simply related to the regional isotopic trends seen in marble minerals.

Alternatively, the present day regional isotopic variation in the impure dolomitic marbles may reflect bulk isotopic characteristics acquired during or shortly after

deposition, diagenesis, and lithification of their sedimentary precursors.

Dolomitization may have occurred in the **FF** if the marble precursor was a limestone. In that case, the replacement of primary $CaCO_3$ by $CaMg(CO_3)_2$ was complete, since the molar Ca/Mg ratio is about one in marbles from all areas. Large isotopic difference between marbles from various areas resulting from dolomitization alone must therefore be related to differences in dolomitization temperature, or to differences in isotopic composition or quantity of dolomitizing fluids.

Changes in the proportion of sedimentary and diagenetic components, may have a tremendous effect on the bulk isotopic composition. Tucker (1982) reports widely varying $\delta^{13}C$ and $\delta^{18}O$ values for distinct *Dol* components (sedimentary grains, internal sediments, cements) of the Beck Spring Dolomite, California (**Fig. 4.14**). In this unmetamorphosed marine Proterozoic dolostone, successive generations of diagenetic *Dol* cement become progressively lower in $\delta^{13}C$ (by 4 permil) and, especially, in $\delta^{18}O$ (by 12 permil), presumably in response to lowering of $\delta^{18}O$ in pore fluids as a result of influx of meteoric water.

The possibility of preservation of premetamorphic oxygen isotopic compositions is also explored for the isotopic composition of the adjacent metalaterites (see below).

4.5.7 oxygen isotopic composition of metamorphic minerals in the metalaterites

Desilification during premetamorphic weathering of a presumably basaltic protolith caused residual enrichment in Al, Fe, Ti, P, Zr, REE and other transition elements in the metalaterites, with superimposed supergene enrichment in Fe, Ni and Co in the silica poorest rocks. The expected loss of K and other alkaline (earth) elements during weathering is less systematic in the metalaterites, and may be partly compensated for during syn-diagenetic metasomatism (Bol et al. 1989b). Apart from H and O loss during and before **M1**, no notable modification of the bulk chemistry is supposed for the metalaterites.

Little is known about oxygen isotopic systematics in modern laterite profiles. Incipient subaerial or submarine weathering of volcanic and plutonic materials (perlitisation, hydration of fine grained mesostasis and feldspars) almost invariably leads to an increase in $^{18}O/^{16}O$ (Muehlenbachs 1987). Clay minerals and hydroxides formed during continued or severe continental weathering have oxygen and hydrogen

isotopic ratios approximately in equilibrium with downward percolating rainwater (Lawrence and Taylor 1972). Accordingly, many weathering minerals, when formed at constant temperatures, define trends on $\delta^{18}O$-δD diagrams parallel to the meteoric water line and have higher $\delta^{18}O$ and lower δD values than the related meteoric water (Savin 1981). At surficial temperatures (±25°C), the approximate $\alpha^{18}O$(mineral-H_2O) values of the bauxite/laterite minerals kaolinite ($Al_2Si_2O_5(OH)_4$), boehmite (AlO(OH)), gibbsite ($Al(OH)_3$) and goethite (αFeOOH) are: $\alpha(Kln\text{-}H_2O) = 1.026$ (Lawrence and Taylor 1972), $\alpha(Bhm\text{-}H_2O) = 1.018$ (Bird et al. 1989), $\alpha(Gbs\text{-}H_2O) = 1.014$ (Bird et al. 1989; c.f. Lawrence and Taylor 1972)), $\alpha(Gth\text{-}H_2O) = 1.006$ (Yapp 1987).

Upon weathering, the original rock mass, consisting of fresh unaltered protolith minerals, is progressively replaced and/or diluted by a combination of clay minerals, Al-Fe (hydr)oxides, and water (H_2O^+,H_2O^-). The $\delta^{18}O$ value of this blend is, besides being dependent on weathering temperature and on isotopic composition of the associated meteoric water, primarily a function of its mineralogical composition. Chemically and mineralogically unaltered parent minerals may retain essentially their primary isotopic composition (Taylor and Epstein 1964; Lawrence and Taylor 1972). Therefore, to a first approximation, the bulk $^{18}O/^{16}O$ systematics during lateritization processes may be represented by binary mixtures of oxygen isotopic ratios in the protolith and in the composite weathering product, analogous to a two component submarine weathering model for MORBs (Muehlenbachs and Clayton 1972). Progressive bauxitization is expected to increase the bulk $\delta^{18}O$ values of most substrates, whereas the formation and accumulation of large amounts of low $\delta^{18}O$ hydrous and anhydrous iron (III) oxides during lateritization may compensate for, or reverse this trend (Borshchevskiy 1976). Oxygen exchange and oxygen loss during subsequent diagenesis and metamorphism may partly erase the bulk $\delta^{18}O$ systematics in the weathering profile (Cf, Yapp 1990).

Possible premetamorphic trends in bulk $\delta^{18}O$ with progressive lateritization (i.e., with decreasing silica content) are ambiguous at best from the $\delta^{18}O$ variation of individual metalaterite minerals (**Fig. 4.7a**).

Mag and *Sil* tend to have high $\delta^{18}O$ values in silica poor metalaterites, and low values in silica-rich metalaterites. In contrast, *Pl* has lowest $\delta^{18}O$ values in silica poor rocks. These vague trends are not related to whole-rock alkaline (earth) content or to the degree of saussuritization of feldspars. *Mag* from JM137, JM136 and FF122 is

unaltered in thin section and proved to be pure by XRD. Yet, *Mag* from these samples is relatively high in $\delta^{18}O$. The relatively low $\delta^{18}O$ in *Mag* from FF139 may reflect the significant supergene iron (hydr)oxide enrichment, as anticipated for this sample (Bol et al. 1989b).

Mag-Opx, *Mag-Pl* and *Opx-Pl* fractionations in orthopyroxene-bearing metalaterites are not concordant, indicating a lack of oxygen isotopic equilibrium between these minerals. Although accurate isotopic fractionation factors for *Sil* are not known, the same probably holds true for *Sil*-bearing rocks. At equilibrium, it can be expected that ^{18}O is fractionated into *Pl* for all temperatures of interest (**Fig. 4.7B**). A $\delta^{18}O$ reversal for the *Opx-Pl* pair, such as in sample JM151, together with the lower $\delta^{18}O$ in *Pl* from the low silica rocks may be taken as evidence that *Pl* was altered by reaction with low-grade metamorphic (**M4**) or meteoric fluids whereas *Opx*, *Mag* and *Sil* crystals partly re-equilibrated to lower metamorphic temperatures during **M3**.

Hence, in the metalaterites, premetamorphic bulk oxygen isotopic systematics are not reflected by *Pl*, and their relation with the present $\delta^{18}O$ values of *Mag*, *Sil* and *Opx* is ambiguous. These results neither support nor exclude the possibility of preservation of premetamorphic bulk (O,C) isotopic characteristics in the marbles.

4.6 CONCLUSIONS

1) The isotopic composition of *Cal* in marbles from the granulite-facies metasedimentary Faurefjell Formation regionally varies from about $\delta^{18}O = 21.5$ and $\delta^{13}C = -3.2$ in the south (near the Rogaland anorthosite complex) to about $\delta^{18}O = 13.1$ and $\delta^{13}C = -8.2$ in the north (near the Caledonian thrust front). This isotopic trend is reflected by the $\delta^{18}O$ values of other marble minerals (*Di, Phl).* Silicate minerals from adjacent metasedimentary layers (quartzites, *Qtz-Di* gneisses) or from rocks enveloping the **FF** (enderbites) do not show similar regional $\delta^{18}O$ trends.

2) Several fluid/rock interaction processes may have operated successively or in concert in reaching the (O,C) isotopic compositions observed for the marble minerals. The main shift in $\delta^{18}O$ and $\delta^{13}C$ predates the peak metamorphic events, since the (O,C) isotopic trend in *Cal* is reflected in $\delta^{18}O$ values of high-grade silicate minerals (*Phl, Di*) in the marbles.

3) Decarbonation reactions must have occurred in the **FF** marbles, but, unaccompanied by other processes, they cannot account for the large local and regional range in $\delta^{18}O$ and $\delta^{13}C$ values observed for *Cal*. Even if significant variability is assumed in the mineralogical or isotopic composition of the sedimentary precursor of the marbles, interactions with externally derived fluids must have occurred, in addition to devolatilization reactions.

4) From the data presented in this paper, no notable (O,C) isotopic interactions between the Rogaland anorthosite complex and the enveloping granulite facies terrane can be substantiated. In general, isotopic communication between adjacent lithologies is not observed. Even within single metasedimentary layers, the isotopic compositions of distinct minerals varies widely. This is at variance with petrogenetic models invoked for other granulite facies terranes which involve large quantities of all-pervading fluids during metamorphism.

5) Both the Rogaland anorthosite complex and its high-grade metamorphic envelope were affected by subsolidus isotopic exchange. Isotopic alteration by low $\delta^{18}O$ fluids during **M3/M4** regionally affected several minerals (most notably *Pl* and *Cal*). However, the regional isotopic shifts observed for the marble minerals can not be attributed to differential interaction with Caledonian metamorphic fluids.

6) Premetamorphic processes may have caused regional and local bulk (O,C) isotopic variations in the marble precursors, which are currently expressed by the isotopic trends seen for individual marble minerals. Bulk oxygen isotopic systematics inherited from premetamorphic weathering are not unambiguously identified from $\delta^{18}O$ values of minerals in a metalaterite layer directly adjacent to the marbles in area A.

4.7 ACKNOWLEDGMENTS

A. Hakstege, A. Hilversum, C. Maijer, J. Meertens, G. Venhuis and H. Teske collected some of the samples, K. Koop provided some of her unpublished data. J. Meesterburrie is thanked for analytical assistance with stable isotope measurements in Utrecht. Special thanks are due to K. Baker, who performed part of the $\delta^{18}O$ measurements on silicates and patiently supervised all other stable isotope work in

Madison. C. Maijer guided fieldwork in Rogaland. The manuscript benefitted from constructive remarks of R.D. Schuiling and B.H.W.S. de Jong. This research has been supported by grants from the Netherlands Organisation for Scientific Research (751-353-016, LCGMB; 18-21-06, PCCS), by the Gas Research Institute (5086-260-1425, JWV) and the US National Science Foundation (EAR 88-05470, JWV).

4.8 REFERENCES

Baker AJ, Fallick AE (1989) Heavy carbon in two-billion-year old marbles from Lofoten-Vesteralen, Norway: Implications for the Precambrian carbon cycle. Geochim Cosmochim Acta 53:1111-1115

Baker J, Bickle MJ, Buick IS, Holland TJB, Matthews A (1989) Isotopic and petrological evidence for the infiltration of water-rich fluids during the Miocene M2 metamorphism on Naxos, Greece. Geochim Cosmochim Acta 53:2037-2050

Bird MI, Chivas AR, Andrew AS (1989) A stable-isotope study of lateritic bauxites. Geochim Cosmochim Acta 53:1411-1420

Birkeland T (1981) The geology of Jaeren and adjacent districts. A contribution to the Caledonian nappe tectonics of Rogaland, southwest Norway. Nor Geol Tidsskr 61:213-292

Bohlen SR, Valley JW, Whitney PR (1989) The Adirondack Mountains, a section of deep Proterozoic crust. 28th IGC, Field Trip Guidebook T164

Bol LCGM, Bos A, Sauter PCC, Jansen JBH (1989a) Barium-titanium- rich phlogopites in marbles from Rogaland, southwest Norway (Chapter II of this thesis). Am Mineral 74:439-447

Bol LCGM, Jansen JBH (1989) Proterozoic metasediments from the deep crust of Rogaland, SW Norway: Chemistry of metabasites and granofelses (*ext abstr*). In D Bridgwater (ed) Fluid movements-element transport and the composition of the deep crust, NATO Advanced Study Institute Series C vol 281 pp 111-113

Bol LCGM, Jansen JBH (in preparation) REE distribution among minerals in marbles and pegmatites from the high-grade Precambrian, Rogaland, SW Norway

Bol LCGM, Maijer C, Jansen JBH (1989b) Premetamorphic lateritization in proterozoic metabasites of Rogaland, SW Norway (Chapter III of this thesis). Contrib Mineral Petrol 103:299-309

Borshchevskiy YuA, Ananenko NA, Ustinov VI, Amosova KhB (1976) Oxygen isotopes of bauxites as geochemical indicators of the conditions of its formation. Dokl Akad Nauk SSSR 222:223-224

Bottinga Y (1968) Calculation of fractionation factors for carbon and oxygen exchange in the system calcite-carbon-dioxide-water. J Phys Chem 72:800-808

Bottinga Y, Javoy M (1973) Comments on oxygen isotope geothermometry. Earth Planet Sci Lett 20:250-265

Bottinga Y, Javoy M (1975) Oxygen isotope partitioning among the minerals in igneous and metamorphic rocks. Rev Geophys Space Phys 13,2:401-418

Bowman JR, O'Neil JR, Essene EJ (1985) Contact skarn formation at Elkhorn, Montana. II: Origin and evolution of C-O-H skarn fluids. Am J Sci 285:621-660

Chacko T, Mayeda TK, Clayton RN, Goldsmith JR (1989) An experimental determination of $^{18}O/^{16}O$ and $^{13}C/^{12}C$ fractionations between CO_2 and calcite at 10 kbar. GSA Abstr Vol 21, pp A11

Chiba H, Chacko T, Clayton RN, Goldsmith JR (1989) Oxygen isotope fractionations involving diopside, forsterite, magnetite and calcite: Application to geothermometry. Geochim Cosmochim Acta 53:2985-2995

Clayton RN, Goldsmith JR, Mayeda TK (1989) Oxygen isotope fractionation in quartz, albite, anorthite and calcite. Geochim Cosmochim Acta 53:725-733

Clayton RN, Mayeda TK (1963) The use of pentafluoride in the extraction of oxygen from oxydes and silicates for isotopic analyses. Geochim Cosmochim Acta 27:43-52

Clayton RN, Muffler LJP, White DE (1968) Oxygen isotope study of calcite and silicates of the River Ranch No. 1 Well, Salton Sea Geothermal Field, Calif. Am J Sci 266:968-979

Deines P, Gold DP (1969) The change in carbon and oxygen isotopic composition during contact metamorphism of Trenton limestone by the Mount Royal pluton. Geochim Cosmochim Acta 33:421-424

Dekker AGC (1978) Amphiboles and their host-rocks in the high-grade Precambrian of Rogaland, SW Norway. PhD Thesis, Geol Ultraiectina 17, pp 277

Demaiffe D, Javoy M (1980) $^{18}O/^{16}O$ Ratios of anorthosites and related rocks from the Rogaland complex (SW Norway). Contrib Mineral Petrol 72:311-317

Duchesne JC Maquil R, Demaiffe D (1985) The Rogaland anorthosites: facts and speculations. In: Toby AC, Touret JLR (eds) The deep Proterozoic crust in the North Atlantic provinces, NATO ASI Series C Vol 158 Reidel, Dordrecht Boston Lancaster, pp 449-476

Eslinger EV, Savin SM (1973) Oxygen isotope geothermometry of the burial metamorphic rocks of the Precambrian Belt Supergroup, Glacier National Park, Montana. Bull Geol Soc Am 84:2549-2560

Friedman IR, O'Neil JR (1977) Compilation of stable isotope fractionation factors of geochemical interest. In: Fleischer M (Ed) Data of geochemistry, USGS Professional Paper 440-KK

Ganor J, Matthews A, Paldor N (1989) Constraints on effective diffusivity during oxygen isotope exchange at a marble-schist contact, Sifnos (Cyclades), Greece. Earth Planet Sci Lett 94:208-216

Hermans GAEM, Tobi AC, Poorter RPE, Maijer C (1975) The high- grade metamorphic Precambrian of the Sirdal-Ørsdal area, Rogaland/Vest-Agder, South-west Norway. Nor Geol Unders 318:51-74

Huijsmans JPP, Kabel ABET, Steenstra SE (1981) On the structure of a high-grade metamorphic Precambrian terrain in Rogaland, south Norway. Nor Geol Tidsskr 61:183-192

Jacques de Dixmude S (1978) Géothermometrie comparée de roches du faciès granulite du Rogaland (Norvège méridionale). Bull Minèralogique 101:57-65

Janardhan AS, Newton RC, Hansen EC (1982) The transformation of amphibolite facies gneiss to charnockite in southern Karnataka and northern Tamil Nadu, India. Contrib Mineral Petrol 79:130-149

Janardhan AS, Newton RC, Smith JV (1979) Ancient crustal metamorphism at low p_{H_2O}: charnockite formation at Kabbaldurga, south India. Nature 278:511-514

Jansen JBH, Blok RJP, Bos A, Scheelings M (1985) Geothermometry and Geobarometry in Rogaland and preliminary results from the Bamble Area, S Norway. In: Toby AC, Touret JLR (eds) The deep Proterozoic crust in the North Atlantic provinces, NATO ASI Series C Vol 158. Reidel, Dordrecht, pp 499-516

Kars H, Jansen JBH, Tobi AC, Poorter RPE (1980) The metapelitic rocks of the polymetamorphic Precambrian of Rogaland, SW Norway - Part 2. Mineral relations between cordierite, hercynite and magnetite within the osumilite-in isograd. Contrib Mineral Petrol 74:235-244

Kretz R (1983) Symbols for rock-forming minerals. Am Mineral 68:277-279

Lattanzi P, Rye DM, Rice JM (1980) Behavior of ^{13}C and ^{18}O in carbonates during contact metamorphism at Marysville, Montana: Implications for isotope systematics in impure dolomitic limestones. Am J Sci 280:890-906

Lawrence JR, Taylor HP (1972) Hydrogen and oxygen isotope systematics in weathering profiles. Geochim Cosmochim Acta 36:1377-1393

Magaritz M, Taylor HP (1976) Oxygen, hydrogen and carbon isotope studies of the Franciscan formation, Coast Ranges, California. Geochim Cosmochim Acta 40:215-234

Matthews A, Goldsmith JR, Clayton RN (1983) Oxygen isotope fractionations involving pyroxenes: The calibration of mineral-pair geothermometers. Geochim Cosmochim Acta 47:631-644

Maijer C, Andriessen PAM, Hebeda EH, Jansen JBH, Verschure RH (1981) Osumilite, an approximately 970 Ma old high-temperature index mineral of the

granulite-facies metamorphism in Rogaland, SW Norway. Geol Mijnb 60:267-272

Maijer C, Padget P (eds) (1987) The Geology of southernmost Norway. An excursion guide. Nor Geol Unders Spec Publ 1, pp 109

Michot P (1960) La géologie de la catazone: Le problème des anorthosites, la palingenese basique et la tectonique catazonale dans le Rogaland méridional (Norvège méridionale). In: Dons A (ed) Norway, Guidebook g. Witussen & Jensen AJS, Oslo, pp 52

McCrea JM (1950) On the isotopic chemistry of carbonates and a paleotemperature scale. J Chem Phys 18:849-857

Muehlenbachs K (1987) Oxygen isotope exchange during weathering and low temperature alteration. In: Kyser TK (ed) Stable isotope geochemistry of low temperature fluids. Mineralogical Association of Canada Short Course vol 13, pp 162-186

Muehlenbachs K, Clayton RN (1972) Oxygen isotope studies of fresh and weathered submarine basalts. Can Jour Earth Sci 9:172-184

Nabelek PI, Labotka TC, O'Neil JR, Papike JJ (1984) Contrasting fluid/rock interaction between the Notch Peak granitic intrusion and argilites and limestones in western Utah: evidence from stable isotopes and phase assemblages. Contrib Mineral Petrol 86:25-34

Newton RC, Smith JV, Windley BF (1980) Carbonic metamorphism, granulites and crustal growth. Nature 288:45-50

O'Neil JR, Taylor HP (1967) The oxygen isotope and cation exchange chemistry of feldspars. Am Mineral 52:1414-1437

Rumble D (1982) Stable isotope fractionation during metamorphic devolatilization reactions. In: JM Ferry (ed) MSA Reviews in Mineralogy Vol 10, pp 327-353

Rye RO, Schuiling RD, Rye DM, Jansen JBH (1976) Carbon, hydrogen and oxygen isotope studies of the regional metamorphic complex at Naxos. Geochim Cosmochim Acta 40:1031-1049

Sauter PCC (1981) Mineral relations in siliceous dolomites and related rocks in the high-grade metamorphic Precambrian of Rogaland, SW Norway. Nor Geol Tidsskr 61:35-45

Sauter PCC (1983) Metamorphism of siliceous dolomites in the high-grade Precambrian of Rogaland, SW Norway. PhD Thesis, Geol Ultraiectina 32, pp 143

Sauter PCC, Hermans GAEM, Jansen JBH, Maijer C, Spits P, Wegelin A (1983) Polyphase Caledonian metamorphism in the Precambrian basement of Rogaland/Vest-Agder, Southwest Norway. Nor Geol Unders 380:7-22

Savin SM (1981) Oxygen and hydrogen isotope effects in low-temperature mineral-

water interactions. In: Fritz P, Fontes JCh (eds) Handbook of environmental isotope geochemistry, Vol 1, The terrestrial environment. Elsevier, Amsterdam, pp 283-327

Schidlowski M, Eichmann R, Junge CE (1975) Precambrian sedimentary carbonates: carbon and oxygen isotope geochemistry and implications for the terrestrial oxygen budget. Precambrian Res 2:1-69

Schidlowski M, Eichmann R and Junge CE (1976) Carbon isotope geochemistry of the Precambrian Lomagundi carbonate province. Geochim Cosmochim Acta 40:449-455

Sheppard SMF (1986) Characterization and isotopic variations in natural waters. In: PH Ribbe (ed) MSA Reviews in Mineralogy Vol 16, pp 165-183

Shieh YN, Taylor HP (1969) Oxygen and carbon isotope studies of contact metamorphism of carbonate rocks. J Petrol 10,2:307-331

Taylor HP (1969) Oxygen isotope studies of anorthosites with particular reference to the origin of the bodies in the Adirondacks Mountains, New York. In: YW Isachsen (ed) NY State Mus Sci Serv, Mem 18, 111-134

Taylor HP, Albee AL, Epstein S (1963) $^{18}O/^{16}O$ of coexisting minerals in three assemblages of kyanite zone pelitic schist. J Geol 71:513-522

Taylor HP, Epstein S (1964) Comparison of oxygen isotope analyses of tektites, soils, and impactite glasses. In: Craig H, Miller SL, Wasserburg GJ (eds) Isotopic and cosmic chemistry (dedicated to HC Urey on his seventieth birthday). North Holland, Amsterdam, pp 181-199

Tobi AC, Hermans GAEM, Maijer C, Jansen JBH, (1985) Metamorphic zoning in the high-grade Proterozoic of Rogaland-Vest Agder. In: Tobi AC, Touret JLR (eds) The deep Proterozoic crust in the North Atlantic provinces, NATO ASI Series C Vol 158 Reidel, Dordrecht, pp 499-516

Tobi AC, Touret JLR (eds) (1985) The deep Proterozoic crust in the North Atlantic provinces, NATO ASI Series C Vol 158 Reidel Publishing Company, Dordrecht, pp 614

Tracy RJ, McLellan EL (1985) A natural example of the kinetic controls of compositional and textural equilibration. In: Thompson AB, Rubie DC (eds) Metamorphic reactions: kinetics, textures and deformation. Advances in physical chemistry, vol 4. Springer, New York Heidelberg Berlin, pp 118-137

Tucker ME (1982) Precambrian dolomites: Petrographic and isotopic evidence that they differ from Phanerozoic dolomites. Geology 10:7-12

Valley JW (1986) Stable isotope geochemistry of metamorphic rocks. In: PH Ribbe (ed) MSA Reviews in Mineralogy Vol 16, pp 445-489

Valley JW, O'Neil JR (1984) Fluid heterogeneity during granulite facies metamorphism in the Adirondacks: Stable isotope evidence. Contrib Mineral Petrol 85:158-173

Veizer J, Hoefs J (1976) The nature of $^{18}O/^{16}O$ and $^{13}C/^{12}C$ secular trends in sedimentary carbonate rocks. Geochim Cosmochim Acta 40:1387-1395

Verschure RH, Andriessen PAM, Boelrijk NAIM, Hebeda EH, Maijer C, Priem HN, Verdurmen EA (1980) On the thermal stability of Rb-Sr and K-Ar biotite systems: Evidence from coexisting Sveconorwegian (ca 870 Ma) and Caledonian (ca 400 Ma) biotites in SW Norway. Contrib Mineral Petrol 74:245-252

Wada H (1988) Microscale isotopic zoning in calcite and graphite crystals in marble. Nature 331:61-63

Wielens JBW, Andriessen PAM, Boelrijk NAIM, Hebeda EH, Priem HNA, Verdurmen EA, Verschure RH (1980) Isotope geochronology in the high-grade metamorphic Precambrian of southwestern Norway: new data and reinterpretations. Nor Geol Unders 359: 1-30

Wilmart E, Duchesne J-C (1987) Geothermobarometry of igneous and metamorphic rocks around the Åna-Sira anorthosite massif: Implications for the depth of emplacement of the south Norwegian anorthosites. Nor Geol Tidsskr 67:185-196

Yapp CJ (1987) Oxygen and hydrogen isotope variations among goethites (α-FeOOH) and the determination of paleotemperatures. Geochim Cosmochim Acta 51:355-364

Yapp CJ (1990) Oxygen isotope effects associated with the solid-state α-FeOOH to α-Fe_2O_3 phase transformation. Geochim Cosmochim Acta 54:229-236

4.A APPENDIX A: SAMPLE INFORMATION

Additional sample information for rock types 1-7 is given below, with emphasis on carbonate-bearing rocks. The position of some of the marble samples is indicated on three sketches of exposures in areas A, B and C (**Figs. 4A1-4A3**). In Chapter I of this thesis, detailed petrographic information on marbles and metalaterites (types 1 and 4) can be found. The mineral associations in samples investigated for O,C isotopes are given in **Table 4A.1**.

4.A.1 marbles and diopside rocks

The grain size of **carbonate minerals** in the marbles greatly varies. It may amount to 6 mm in several samples, but in those samples where recrystallisation has played a role (see **Table 4.3**) it does not exceed 1 mm. In general, the grain size of the **silicate minerals** in the *Fo*-marbles varies between 1 and 2 mm. In some samples it amounts 4mm. In the *Di*-marbles the overall grain size does generally not exceed 1mm.

In **area A** all marble samples except A122, C346, and FF174 were collected in the same, 5 to 10m thick, marble bed, within a distance of about 100 m (**Fig. 4A.1**). A164, C322 and C324 were collected from the basal parts of the marble, C481 from the middle, and C335 C480 and FF283 from the top. Samples A122 and C346 were taken from a marble layer in the same area, 600m southwest from the other samples. The samples A122, A164, A169, C480 and C481 are fresh samples with varying amounts of *Cal, Fo, Di, Phl* and *Spl. Cal* may form large or recrystallized small grains. Sample C346, also fresh, contains only a small amount of silicate and oxide minerals, mainly *Di. Fo* is completely altered to *Srp*. This sample represents the transition zone between a *Di*-rock and a *Fo*-marble. In the samples C324 and C335 *Fo* is completely serpentinized, in samples A169, FF174 and FF283 partly. *Cal* in C324 is fine-grained and recrystallized, in C335 it is coarse-grained. In samples from this area, *Dol* is only present as minute exsolved particles. The diopside-nodules FF273 and FF277 were collected in the vicinity of C335. Besides *Di*, they contain varying amounts of *Kfs, Phl, Cal* and *Spn*. The *Di*-rocks FF167, FF171A, FF175, FF179, FF182 and FF185 are nearly monomineralic *Di* parts of a sample profile across a >5m thick *Di* ± *Kfs* layer that is sandwiched by quartzites and that has a core of *Fo*-marble (FF174).

In **area B** samples C509, C510, C511, C512, C514 and Z52 were collected from the same marble lens, approximately 50 m long and 5 m thick. They were taken at 8, 17, 24, 8, 10 and 50 cm distance from a pegmatite cross-cutting the marble lens (**Fig. 4A.2**). The *Di*-rocks C397, C500A, C502B represent the outer portions of this pegmatite and the *Kfs*-rich samples C499A and C502A were taken from the pegmatite core. Q128 and Z177 were collected from two strongly retrogressive exposures. Q138, Q201, C372 and Z75 were taken from three small, isolated marble lenses. The samples C372, C509, C510, C511, C512, C514, Q128 and Q201 contain varying amounts of *Cal, Dol, Fo, Di, Phl* and *Spl. Dol*-exsolution is volumetrically important especially in C372, where large *Dol* lamellae occur. In C509, C510 and C511, *Dol* tablets and coarse-grained symplectitic *Dol* are the predominant exsolution types. The samples Z52 and Z75 are more retrogressively altered, *Fo* and *Di* are largely serpentinized, Z75 contains a large amount of *Chu,* overgrowing *Srp*. In Q128 newly formed *Tr* and *Tlc* have completely replaced *Fo* and/or *Di. Cal* has old, dusty cores, with new, clear rims. Some *Chl* has replaced *Phl*. Z177 is a *Di*-marble in which *Phl* is almost completely retromorphosed to Mg-*Chl*.

All samples from **area C** were taken within a distance of 20 m within this small exposure (**Fig. 4A.3**). The forsterite marbles C236, C273 and C533 have varying

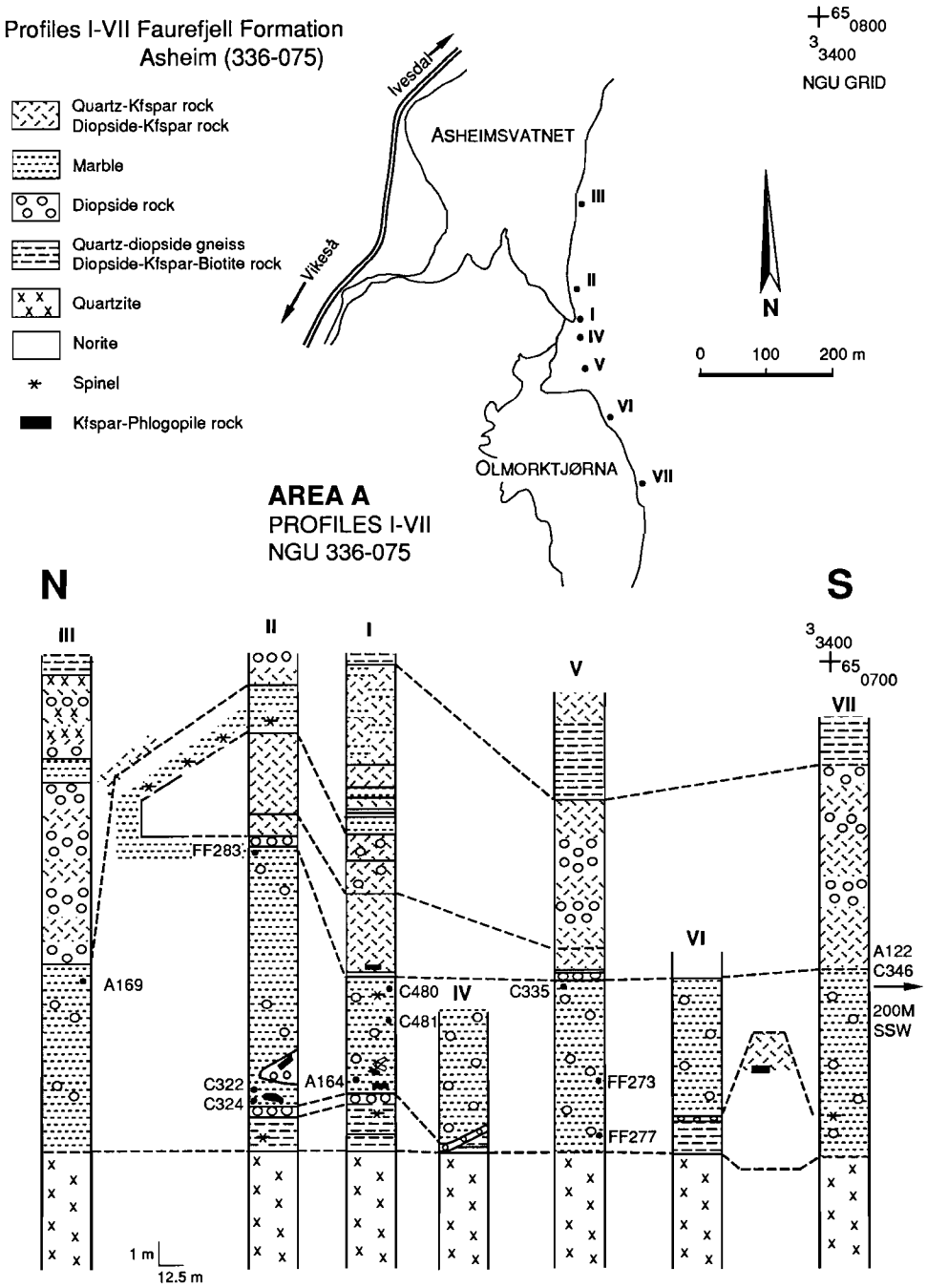

Fig. 4A.1: Sample locations in area A.

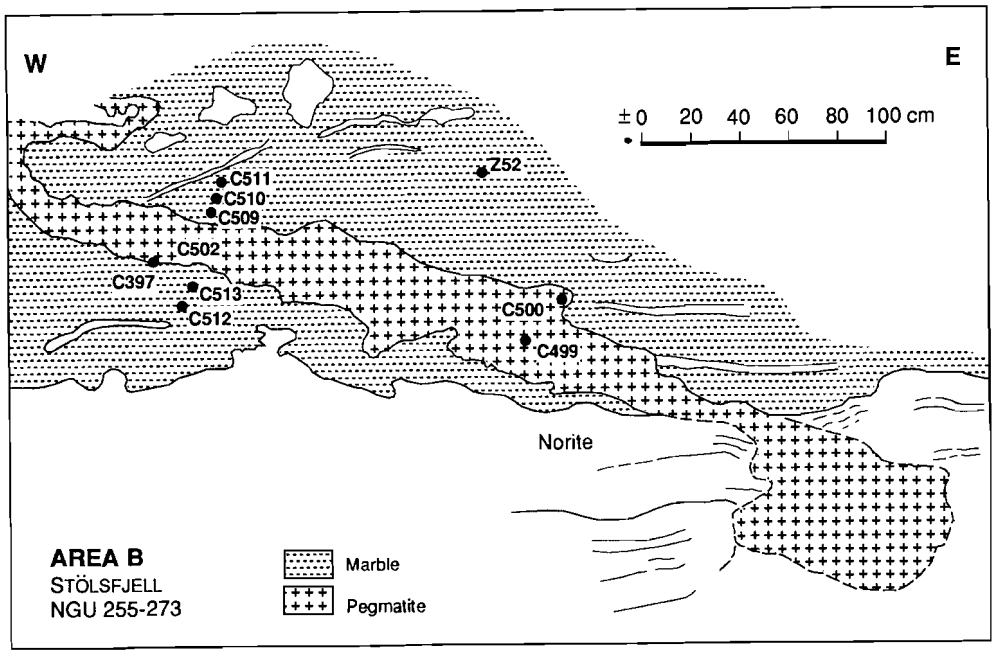

Fig. 4A.2: Sample locations in area B.

amounts of *Cal*, *Dol*, *Fo*, *Di* and *Phl*. In C533 *Cal* has undergone extensive recrystallisation. C235, C264 and C521 are *Di* marbles with a relatively high silica content. C522 is intermediate between *Fo*-marble and *Di*-marble, the result of a fine layering. *Fo* and *Di* in the analyzed *Fo*-marble samples from area C are partly serpentinized. *Dol* exsolution is extensive in the form of tablets and of rhombohedral *Dol*. C163 represents a small, coarse-grained, *Tr-Cal* vein, which intersects a *Di*-rock. Along this vein *Di*, is replaced by *Tr*. Sample C165 represents the central portion of a thick (3m) *Di±Phl±Kfs*layer

All samples from **area D** except FF260 are silica rich *Di*-marbles that were collected within 5m from a roadcut near Bue, the sole occurrence of marble in D (see arrow in **Fig. 4.1**). The marbles are intercalated within a banded vein network of *Di±Phl, Kfs±Qtz,* and *Di-Kfs±Phl* rocks. FF260 is a finely banded specimen from a similar *Di-Kfs-Qtz* veining system 5km further west.

Samples FF142, FF192 and FF196 are *Fo*-marbles from **area E** collected along strike from an intensely folded 5m thick marble bed. *Fo* grains are wholly serpentinized in FF196 and partly in FF142 and FF192. FF190 represents a thin (7cm) *Di-Spl-Phl* vein crosscutting FF192. The vein has a *Di + Spl* core, symmetrically jacketed by *Phl* and, further towards the marble, by *Di*.

4.A.2 quartzites

Quartzites occur at several stratigraphic levels within the **FF**, the most prominent being a thick layer at the base of the formation also known as "Quartzite de base de la série de Gjestal" (Michot 1960). They consist almost entirely of quartz. Feldspars,

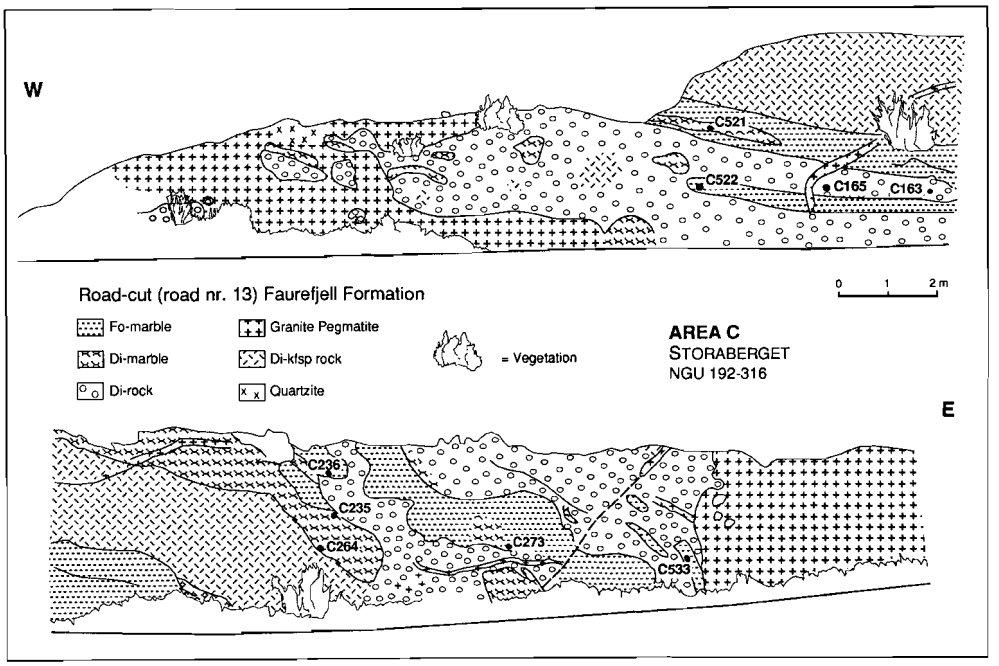

Fig. 4A.3: Sample locations in area C.

Bt, *Di*, *Ep* and *Mag* are minor or accessory minerals. Quartzites from area A were sampled along strike from the thick basal quartzite layer. The same layer was probably sampled in areas B, D and E, although the exact stratigraphic position of the quartzites is not as clear in these areas. Quartz grains often display undulatory extinction and have interlobate grain boundaries.

4.A.3 quartz-diopside gneisses

Qtz-Di gneisses occur at three stratigraphic levels within the **FF**, together with marbles and the diopside rocks. Their bulk composition differs from the marbles mainly in silica content. In general, they contain $Qtz + Di \pm Kfs \pm Pl$ with accessory amounts of *Bt*, *Spn*, *Zrn* and ore minerals. The *Qtz-Di* gneisses are generally thinly banded (0.3-1cm) due to alternation of *Qtz*-rich and *Di*-rich layers. Occasionally diopside nodules (up to 5cm) occur. In area B the gneisses may have a mosaic fabric due to intense recrystallization. The isotopically investigated *Qtz-Di* gneisses are from various layers with distinct stratigraphic positions within the **FF** at areas A, B and D. In samples from area A, *Ep* is observed and two of them contain *Pmp*. Some retrogression is also evident in Q237 were newly formed albitic *Pl* is observed. VH87 is a *Di-Kfs* rock intercalated within the *Qtz-Di* gneisses. It differs from similar *Di-Kfs* rocks within the marbles in that it contains some *Qtz*.

4.A.4 metalaterites

All metalaterites are sampled from the same heterogeneous basic layer of the **FF** in area A (**Fig. 3.3**; see Bol et al. (1989b) for exact position of the samples within the "Upper Basic Layer"). The basic granulites (massive hypersthene-plagioclase

granolites) are medium-grained inequigranular granoblastic rocks with coarser grained lenticular aggregates of ferromagnesian minerals that define a weak foliation. The Fe-Al granofelses (spinel-cordierite-sillimanite granoblastites) have textures similar to those of the basic granulites and are generally coarse-grained. Sillimanite defines a weak foliation. Retrograde metamorphic minerals and/or alteration of *Pl*, *Opx* and *Crd* is virtually absent in these rocks.

4.A.5 enderbites

The enderbites are a prominent rock-type within the Charnockitic Migmatites and they are selected in this study to represent the country rock surrounding the **FF** in areas A-C. They consist predominantly of *Pl* (An = 25-40), *Qtz*, and *Opx* with minor amounts of *Bt*, *Kfs* (microcline), *Cpx* and *Amp*. Accessory minerals are *Ap*, *Zrn*. *Opx* may be partly serpentinized in enderbites from area B (slightly) and C (severely).

Samples A40, A89, A96, Q64, C25 and C28 are from the "mainly banded" units of the Charnockitic Migmatites, as defined by Hermans et al. (1975), Q63 and Q186 are from the "mainly massive" parts. Generally, the degree of serpentinization and/or chloritization of *Opx* in the Rogaland enderbites decreases with distance from the Caledonian front. *Opx* in area A is fresh, in B slightly altered, and in C wholly replaced by lower grade minerals.

4.A.6 miscellaneous carbonate-bearing rocks

Apart from the **FF**-marbles in areas A-E, some other calcite-bearing rocks from locations F-I (see **Fig. 4.1**) were investigated.

A187 and MA97 (location F) are apatite marbles from a 50 to 100cm thick lens intercalated in garnetiferous migmatites. Having a very dissimilar chemistry and occurring in a very different geological setting, these Precambrian marbles are not assumed to belong to the **FF**. The samples contain coarse-grained, subhedral *Ap* crystals, in some cases exceeding 5mm. They constitute 30% to 40% of the rock volume. The grain size of *Cal* occasionally is 5 mm, but most grains seem to have recrystallized to a grain size of 0.5mm. Other minerals are *Chl*, *Ep*, *Qtz* and *Spn*.

C76 (location G) is a small calcite vein in retrograde augen gneisses. Its location is close to the Caledonian overthrust. The vein contains coarse grained *Cal* (up to several centimeters large) and some *Qtz* and feldspars. These latter minerals are fragments from the country rocks. Locally *Fl* is associated with this kind of calcite veins.

MA310 and MA311 (location H) are breccias, presumably the result of explosive volcanism (C. Maijer, pers.comm.). These breccias occur in the Precambrian basement, mainly close to the Caledonian front. The fragments are angular and represent material from adjacent silicate country rocks. The matrix is fine-grained and often consists of small fragments of *Qtz*, feldspars and green *Bt*. Occasionally (in samples MA310 and MA311) *Cal* forms the matrix. The *Cal* presumably precipitated at or after the time of brecciation. The grain size of *Cal* varies from 20 μm to 3mm. Textures indicate that the grain size reduction is the result of deformation and recrystallization. Some small *Qtz*, feldspar and *Bt* grains are observed in the *Cal* matrix.

Samples G160 and G210 (location I) were collected from a mylonitized zone just above the Precambrian basement. They are supposed to be parautochtonous units of Cambro-Ordovician age (AC Tobi, pers.comm), although Birkeland (1981) suggests a more allochtonous origin, of possible Precambrian age. These rocks mainly consist of *Cal* and *Qtz*. G160 is a fine grained rock (50-100 μm), consisting of a polygonal texture of *Cal* and *Qtz*. locally streaks of green *Bt* are present. G210 contains semi-

rounded, deformed and partly recrystallized *Qtz* grains, with a size of 1 to 2 mm and some large, deformed *Kfs* grains, lying in a matrix of fine-grained *Cal* and *Qtz* with a polygonal texture. Some *Kfs* and green *Bt* occur in the matrix.

4.A.7 graphite-bearing rocks
All but one (G80) graphite-bearing samples are optically fresh, coarse-grained *Grt*-granofelses from the Gyadal Garnetiferous Migmatites. This marker unit crops out throughout the Rogaland terrane and has a supracrustal origin (Huijsmans et al. 1981). The *Grt*-granofelses all contain *Qtz*, *Kfs*, *Pl* (An = 25-40) and *Grt*, and some of the minerals *Crd*, *Sil*, *Spl* and *Bt*. Graphite is present as large, elongated flakes. The matrix of the explosion breccia G80, nearby location I (**Fig. 4.1**), consists of very fine-grained *Qtz*, feldspars, green *Bt* and carbonaceous material.

Table 4.A: Mineral associations in the samples analyzed for oxygen and carbon isotope ratios

Sample#	Type	Loc	NGU-coord.	Mineral Association													
1) marbles and diopside rocks				*Cal*	*Dol*	*Fo*	*Di*	*Phl*	*Spl*	*Ep*	*Spn*	*Tr*	*Tlc*	*Ap*	*Brt*	*Srp*	*Kfs*	
A122	▪ *Fo*-marble	A	337-070	x	-	x	a	o	-	-	-	-	-	a	a	a	-	
A164	▪ *Fo*-marble	A	336-076	x	-	x	o	o	-	-	r	-	-	-	a	a	-	
A169	*Fo*-marble	A	337-076	x	-	x	-	o	a	-	-	-	-	a	a	a	-	
C322	▪ *Di*-marble	A	336-076	o	-	(o)	x	-	-	-	-	-	-	-	-	-	-	
C324	▪ *Fo*-marble	A	336-076	x	-	(x)	-	o	-	-	-	-	-	-	-	-	-	
C335	▪ *Fo*-marble	A	336-075	x	-	(x)	a	o	-	-	-	-	-	-	-	-	-	
C346	▪ *Fo*-marble	A	337-069	x	-	(x)	a	o	a	-	-	-	-	-	-	-	-	
C480	▪ *Fo*-marble	A	336-076	x	-	x	a	a	x	-	o	-	-	-	a	-	-	
C481	▪ *Fo-Di*-marble	A	336-076	x	e	x	o	o	-	-	-	-	-	-	-	-	-	
FF167	*Di*-rock	A	295-095	-	-	-	x	a	-	-	a	-	-	-	-	-	o	
FF171A	*Di*-rock	A	295-095	-	-	-	x	-	-	-	-	-	-	-	-	-	-	
FF174	*Fo*-marble	A	295-095	x	e	(x)	o	x	-	-	-	-	-	-	-	r	-	
FF175	*Di*-rock	A	295-095	-	-	-	x	-	-	-	a	-	-	-	-	-	a	
FF179	*Di*-rock	A	295-095	-	-	-	x	a	-	-	a	-	-	-	-	-	-	
FF182	*Di*-rock	A	295-095	-	-	-	x	-	-	-	-	-	-	-	-	-	-	
FF185	*Di*-rock	A	295-095	-	-	-	x	-	-	-	a	-	-	-	-	-	-	
FF273	*Di*-nodule	A	337-074	-	-	a	x	x	-	-	-	-	-	-	-	-	-	
FF277	*Di*-nodule	A	337-074	-	-	-	x	a	-	-	a	-	-	-	-	-	a	
FF283	*Fo*-marble	A	336-076	x	-	(x)	(x)	x	-	-	-	-	-	a	-	r	-	
C372	▪ *Fo*-marble	B	268-260	x	x,e	x	a	a	o	r	-	r	-	-	-	-	-	
C372	*Di*-rock	B	255-273	-	-	-	x	x	o	-	-	-	-	r	-	-	-	
C499A	*Kfs*-vein	B	255-273	-	-	-	-	-	-	-	-	-	-	-	-	-	x	
C500A	*Di*-rock	B	255-273	-	-	-	x	x	-	-	a	-	-	-	-	-	-	
C500B	*Di*-marble	B	255-273	x	a	a	x	x	-	-	-	-	-	-	-	-	-	
C502A	*Di-Kfs*-rock	B	255-273	-	-	-	x	a	-	-	-	-	-	a	-	-	x	
C502B	*Di*-rock	B	255-273	-	-	-	x	a	-	-	a	-	-	-	-	-	-	
C509	▪ *Fo*-marble	B	255-273	x	o	(x)	o	o	-	-	-	-	-	-	a	r	-	
C510	▪ *Fo*-marble	B	255-273	x	o	(x)	o	o	-	-	-	-	-	-	-	r	-	
C511	▪ *Fo*-marble	B	255-273	x	x	(x)	o	o	-	-	-	-	-	-	-	r	-	
C512	*Fo*-marble	B	255-273	x	o	x	(o)	o	-	-	-	-	-	a	-	r	-	
C514	*Fo*-marble	B	255-273	x	o	(x)	(o)	o	-	-	-	-	-	a	-	r	-	
Q128	▪ *Tr*-marble	B	257-274	x	o	-	o	o	-	-	-	x	o	-	-	-	-	*Chl*
Q138	*Fo*-marble	B	269-261	x	a	x	-	x	-	x	-	-	-	a	-	-	-	*Chl*
Q201	*Fo*-marble	B	269-261	x	a	(x)	-	x	o	-	-	-	-	-	-	r	-	Opaque
Z52	▪ *Fo*-marble	B	255-273	x	o	(x)	a	x	-	-	-	-	-	-	-	r	-	
Z75	▪ *Fo*-marble	B	274-261	x	a	(x)	-	(o)	-	-	-	-	-	-	-	r	-	*Chu, Chl*
Z177	▪ *Di*-marble	B	261-270	x	-	-	x	(x)	-	-	-	-	-	-	-	-	-	*Chl*

Table 4.A -*continued*

				Cal	*Dol*	*Fo*	*Di*	*Phl*	*Spl*	*Ep*	*Spn*	*Tr*	*Tlc*	*Ap*	*Brt*	*Srp*	*Kfs*	
C163	*Tr*-vein	C	192-316	x	-	-	-	-	-	-	-	o	-	-	-	-	-	
C165	*DiPhl*-rock	C	192-316	-	-	-	x	x	-	-	a	-	-	-	-	-	-	
C235	*Di*-marble	C	192-316	x	e	-	x	x	-	-	a	-	-	-	-	a	-	
C236	▪ *Fo*-marble	C	192-316	x	o	x	o	x	-	-	-	-	-	a	-	-	-	*Hu, Zrn*
C264	▪ *Di*-marble	C	192-316	x	-	(o)	x	x	-	-	-	-	-	-	-	r	-	
C273	▪ *Fo*-marble	C	192-316	x	o	(x)	a	x	-	-	a	-	-	a	-	r	-	
C521	▪ *Di*-marble	C	192-316	x	-	(o)	x	x	-	-	-	-	-	-	-	r	-	
C522	▪ *DiFo*-marble	C	192-316	x	-	(x)	x	x	-	-	-	-	-	-	-	r	-	
C533	▪ *Fo*-marble	C	192-316	x	a	(x)	o	x	-	-	-	-	-	-	-	r	-	
FF4B	*Di*-marble	D	245-062	x	e	-	x	o	-	-	-	-	-	-	-	-	-	
FF4C	*Di*-marble	D	245-062	x	a	-	x	o	-	-	-	-	-	-	-	-	-	
FF47	*Di*-marble	D	245-062	x	e	-	x	x	-	-	-	-	-	-	-	-	-	
FF51	*DiKfs*-rock	D	245-062	a	-	-	x	a	-	-	-	-	-	-	-	-	x	
FF52	*Di*-rock	D	245-062	a	-	-	x	o	-	-	-	-	-	-	-	-	-	
FF53	*Di*-marble	D	245-062	o	e	-	x	x	-	-	-	-	-	-	-	-	-	
FF260	*DiKfsQ*-vein	D	195-056	-	-	-	x	-	-	-	-	-	-	-	-	-	x	*Qtz*
FF142	*Fo*-marble	E	385-004	x	-	(x)	-	o	-	-	-	-	-	-	-	r	-	*Mag*
FF190	*SpDiPhl*-vein	E	385-004	-	-	-	x	x	x	-	-	-	-	-	-	-	-	
FF192	*Fo*-marble	E	385-004	x	-	(x)	-	o	-	-	-	-	-	-	-	r	-	
FF196	*Fo*-marble	E	385-004	x	-	(x)	-	-	-	-	-	-	-	-	-	r	-	*Mag*

2) quartzites

				Qtz	*Kfs*	*Pl*	*Bt*	*Di*	*Ep*	*Op*
FF118	quartzite	A	312-089	x	-	-	-	-	-	a
FF124	quartzite	A	297-092	x	-	-	-	-	-	a
FF132	quartzite	A	334-078	x	-	-	-	-	-	-
FF134	quartzite	A	332-086	x	-	-	a	-	-	-
FF270	quartzite	A	337-074	x	-	-	a	-	-	-
FF248	quartzite	B	255-273	x	-	-	-	-	-	-
FF251	quartzite	B	271-261	x	(o)	-	-	-	a	-
Q115	quartzite	B	257-274	x	-	-	-	-	-	-
Z81	quartzite	B	265-265	x	a	a	-	-	a	-
U87	quartzite	D	220-100	x	-	a	-	a	-	-
U100	quartzite	D	337-221	x	-	o	-	-	-	-
FF143	quartzite	E	385-004	x	-	-	-	-	-	-
FF152	quartzite	E	385-004	x	-	-	-	-	-	a

Table 4.A *-continued*

3) quartz-diopside gneisses				*Qtz*	*Di*	*Kfs*	*Pl*	*Bt*	*Ms*	*Opx*	*Ep*	*Spn*	*Zrn*	*Op*	*Pmp*	
VH6	*Qtz-Di*-gneiss	A	325-082	x	o	-	x	-	-	-	r	-	a	a	r	
VH38	*Qtz-Di*-gneiss	A	304-088	x	x	-	x	-	o	-	o	a	-	-	-	
VH84	*Qtz-Di*-gneiss	A	327-083	x	o	-	x	a	-	a	a	-	a	a	-	
VH85	*Qtz-Di*-gneiss	A	324-082	x	o	-	x	-	-	a	o	-	a	a	-	
VH87	*Kfs-Di*-gneiss	A	328-080	o	a	x	-	-	-	-	-	a	-	-	r	
Q215	*Qtz-Di*-gneiss	B	256-266	x	x	o	-	o	-	-	-	a	a	a	-	
Q237	*Qtz-Di*-gneiss	B	260-248	x	x	o	r	o	-	-	-	a	a	a	-	
U68	*Qtz-Di*-gneiss	D	195-054	x	x	x	x	a	-	-	-	-	a	a	-	*Ap*
U120	*Qtz-Di*-gneiss	D	245-084	x	x	-	x	a	-	-	-	a	a	-	-	

4) metalaterites				*Pl*	*Opx*	*Mag*	*Hc*	*Crd*	*Bt*	*Kfs*	*Sil*	*Zrn*	*Ap*	*Mnz*	*Spn*	*Crn*
JM137	basic granul	A	267-093	x	x	x	a	-	o	-	-	a	a	-	-	-
JM151	basic granul	A	326-081	x	x	x	a	-	o	o	-	a	a	-	-	-
JM136	Fe-Al granof	A	297-093	x	x	x	x	x	-	o	-	a	-	-	-	-
JM143	Fe-Al granof	A	302-085	x	-	x	x	x	o	-	x	a	-	-	a	-
FF122	Fe-Al granof	A	326-081	x	-	x	x	x	-	-	a	a	a	-	-	-
JM144	Fe-Al granof	A	302-085	x	x	x	x	x	o	o	-	a	a	-	-	-
FF137	Fe-Al granof	A	326-081	o	-	x	x	x	-	-	x	a	a	-	-	-
FF136	Fe-Al granof	A	326-081	o	-	x	x	x	-	-	x	a	a	a	-	a
FF138	Fe-Al granof	A	326-081	o	-	x	x	x	-	-	x	a	a	a	-	a
FF139	Fe-Al granof	A	326-081	o	-	x	x	x	-	-	-	a	a	a	-	-

5) enderbites				*Qtz*	*Cpx*	*Kfs*	*Pl*	*Bt*	*Amf*	*Opx*	*Ep*	*Ap*	*Zrn*	*Op*	*Grt*	*Spn*	
A40	enderbite	A	398-044	x	-	-	x	-	-	x	-	a	-	-	-	-	
A89	enderbite	A	323-095	x	-	-	x	-	-	x	-	a	-	-	-	-	
A96	enderbite	A	350-087	x	-	-	x	-	-	x	-	a	-	-	-	-	
Q63	enderbite	B	268-263	x	-	-	x	o	-	x	r	a	a	a	-	-	
Q64	*GrtBt*-enderb	B	278-252	x	-	-	x	x	-	x	-	a	a	a	x	-	
Q186	enderbite	B	272-283	x	-	-	x	o	-	x	r	a	a	a	-	-	
C25	*Bt*-enderbite	C	195-315	x	-	o	x	x	-	(o)	o	a	a	-	-	x	*Chl,Srp*
C28	norite	C	194-306	o	o	-	x	x	x	(o)	-	a	a	a	-	-	

Table 4.A *-continued*

6) other calcite-bearing rocks				*Cal*	*Qtz*	*Pl*	*Kfs*	*Bt*	*Ep*	*Spn*	*Zrn*	*Ap*	*Chl*	
A187	*Ap*-marble	F	343-305	x	x	-	-	-	o	a	-	a	-	
MA97	*Ap*-marble	F	343-305	x	x	-	x	-	o	a	-	-	a	
C76	*Cal*-vein	G	185-361	x	(x)	(x)	(x)	-	-	-	-	-	-	
MA310	Breccia	H	276-461	x	x	x	x	x	-	-	-	-	-	(*Cal* in matrix)
MA311	Breccia	H	276-461	x	x	x	x	x	-	-	-	-	-	(*Cal* in matrix)
G160	*Qtz*-marble	I	266-433	x	x	x	x	x	-	-	-	-	-	
G210	*Qtz*-marble	I	266-433	x	x	x	x	x	-	-	-	-	-	(*Cal* and *Bt* in matrix)

7) graphite-bearing rocks			*Grt*	*Qtz*	*Kfs*	*Pl*	*Gr*	*Spl*	*Crd*	*Sil*	*Bt*	
A75	*Grt*-granofels	384-033	x	x	x	x	o	-	-	-	-	
BE51	*Grt*-granofels	335-029	x	x	x	x	o	-	-	-	-	
LI56	*Grt*-granofels	370-984	x	x	x	x	o	o	x	x	-	
Q96	*Grt*-granofels	201-206	x	x	x	x	o	-	x	x	-	
Y33	*Grt*-granofels	311-212	x	x	x	x	o	-	-	-	-	
Y121	*Grt*-granofels	327-114	x	x	x	x	o	o	x	x	-	
G80	Breccia matrix	263-418	-	x	x	x	-	-	-	-	x	Carbonaceous material

x=abundant, o=moderate, a=accessory, e=exsolved phase, r=retromorphic.
Brackets indicate partly or wholly retrograded minerals.
▪ = Modal compositions are determined for marked samples, see **Table 3.**
Mineral abbreviations (after Kretz 1983): *Amf*=Amphibole; *Ap*=Apatite; *Bhm*=Boehmite; *Brt*=Barite; *Bt*=Biotite; *Cal*=Calcite; *Chl*=Chlorite; *Chu*=Clinohumite; *Cpx*=Clinopyroxene; *Crd*=Cordierite; *Crn*=Corundum; *Di*=Diopside; *Dol*=Dolomite; *Ep*=Epidote; *Fl*=Fluorite; *Fo*=Forsterite; *Gbs*=Gibbsite; *Ght*=Goethite; *Gr*=Graphite; *Grt*=Garnet; *Hc*=Hercynite; *Hu*=Humite; *Kfs*=K-Feldspar; *Kln*=Kaolinite; *Mag*=Magnetite; *Mn*=Monazite; *Ms*=Muscovite; *Op*="Opaque"; *Opx*=Orthopyroxene; *Phl*=Phlogopite; *Pl*=Plagioclase; *Pmp*=Pumpellyite; *Qtz*=Quartz; *Sil*=Sillimanite; *Spl*=Spinel; *Spn*=Sphene; *Srp*=Serpentine; *Tlc*=Talc; *Tr*=Tremolite; *Zrn*=Zircon.

CHAPTER V: GENERAL CONCLUSIONS

With reference to the scope of this thesis, as defined in Chapter I, the following inferences can be made:

1) Chemical compositions of high-grade metamorphic minerals in marbles of the Faurefjell Metasediment Formation show evidence for local (< mm scale) buffering of element activities (Sauter 1983). For example, high activities of barium and titanium in some phlogopites are probably buffered by phase relations involving neighboring barite and ilmenite grains. The concentrations of Ba and Ti in nearby phlogopites are much lower in the absence of directly adjacent high-Ba or high-Ti phases (Chapter II), indicating low mobilities for these elements. This low mobility on its turn, may be combined with the proposed low hydrogen content of the hydroxyl-site (Chapter II) to infer low water activities in the marbles after the peak metamorphic conditions (**M2**). Rock volumes in late veins (ie, veins consisting of low-grade hydrous minerals) represent an exception.

2) Open system behaviour is demonstrated for various chemical elements in heterogeneous basic layers (basic granulites and Fe-Al-rich granofelses) which occur together with the marbles. These layers acquired their present bulk compositions by premetamorphic interaction with rain water (weathering) and groundwater (syn-diagenetic metasomatism; Chapter III). During the subsequent high-grade metamorphic events, the basic rocks were not notably altered. The conservation of premetamorphic bulk compositions, and the absence of reaction with chemically contrasting neighboring lithologies (quartzites, marbles) provide evidence for very limited metamorphic mass transfer in these rocks. The low mobilities of elements during metamorphism imply low amounts of transporting fluids.

3) The Faurefjell Metasediments were open to fluid-fluxes which caused significant oxygen and carbon isotopic shifts in the marbles or in their sedimentary precursors sometime before the peak metamorphic events (**M2**; Chapter IV). Locally, and in some minerals, rehydration during post-**M2** low-grade events may have caused alteration of oxygen isotopic compositions. However, bulk isotopic compositions present at **M2** conditions have generally been preserved. This preservation, together

with the observed small scale oxygen and carbon isotopic heterogeneity, precludes the possibility of pervasive regional passage of isotopically homogeneous oxygen-bearing fluids at or after M2.

In general, open system behaviour of chemical elements in the Faurefjell Metasediment Formation is related to the possibility of reaction with fluids. This possibility was highest early in the rock history (deposition, diagenesis, early metamorphism), before loss of permeability due to compaction and recrystallization.

REFERENCE

Sauter PCC (1983) Metamorphism of siliceous dolomites in the high-grade Precambrian of Rogaland, SW Norway. PhD Thesis, Geol Ultraiectina 32, 143 pp

CURRICULUM VITAE

Luc C.G.M. Bol is op 12 februari 1958 te Oisterwijk geboren. In juni 1976 behaalde hij het diploma Gymnasium-ß aan de rijksscholengemeenschap Koning Willem II te Tilburg. In september van dat jaar begon hij met de studie Geologie (G1) aan de Rijksuniversiteit te Utrecht. In juni 1981 werd het kandidaatsexamen (G5) afgelegd en in mei 1985 het doctoraal examen Geochemie, met als bijvakken Isotopen Geochemie en Exploratie Geofysica. Na de militaire dienst was de hij, vanaf september 1986 tot september 1989, in dienst van de Nederlandse Organisatie voor Wetenschappelijk Onderzoek. In die periode was hij werkzaam als onderzoeks-medewerker bij de afdeling Chemische Geologie van het Instituut voor Aardwetenschappen van de Rijksuniversiteit te Utrecht. Daar werd het onderzoek verricht dat aan dit proefschrift ten grondslag ligt. Thans is de auteur als onderzoeker verbonden aan het Research- en Bedrijfslaboratorium van Hoogovens Groep BV, te IJmuiden.